Realistic Cochlear Implant Simulations to Capture Sound Quality

DISSERTATION

zur Erlangung des Doktorgrades der Naturwissenschaften (Dr. rer. nat.)

der

Naturwissenschaftlichen Fakultät II
Chemie, Physik und Mathematik

der Martin-Luther-Universität
Halle-Wittenberg

vorgelegt von

Frau Anna Christina Kopsch

Erstgutachter:	apl. Prof. Dr. rer. nat. Detlef Reichert
Zweitgutachter:	apl. Prof. Dr. rer. nat. Torsten Rahne
Drittgutachter:	Prof. Dr.-Ing. Dr. rer. med. Ulrich Hoppe
Tag der öffentlichen Verteidigung:	08.12.2025

Abstract

Cochlear implants (CIs) are inner ear prostheses that enable people with profound hearing loss or deafness to perceive acoustic stimuli. An electrode array inserted into the cochlea stimulates the auditory nerve using electrical impulses via a defined number of electrode contacts. Various factors, such as signal processing losses, result in a change in sound perception with a CI compared with that of acoustic hearing. The aim of this study was to create German-language CI simulations for CI users at different stages of rehabilitation. These simulations were used to determine perceived sound quality and investigate potential influencing factors.

A software sound tool developed specifically for this thesis was programmed to create CI simulations. The sound tool involved several signal processing techniques, such as filtering, vocoding or pitch shifting, to match an acoustic signal to that perceived by a CI. It was used in a prospective, experimental study consisting of two parts. In the first part, 15 single-sided deafened CI users with at least 2 years of CI experience participated. In the second part, five CI users with a maximum of 5 days of CI experience participated. The latter returned for a second study visit after 6 months of CI experience. CI speech simulations were generated by altering acoustic signals with the software sound tool, according to the reference signal of each participant's CI ear. The similarity of the CI simulations was scored on a scale from 1.0 (no similarity) to 10.0 (signals are identical). On average, the simulations were rated with a similarity of 9.7 ± 0.5 by experienced and 8.9 ± 0.8 by unexperienced CI participants. This indicates a large similarity between the simulations and CI sound perception. At the same time, substantial interindividual variability was observed.

To quantify this variability, psychoacoustic experiments were conducted with normal hearing participants to measure CI sound quality. Additionally, an objective measure of spectral deviation between the simulation and the reference signal was introduced and correlated with subjective ratings. On average, a fair sound quality of the CI simulations was found, with ratings ranging from 'bad' to 'excellent'. Spearman's correlation revealed a significant negative relationship between sound quality and spectral deviation ($r_s(15) = -0.80$, $p < 0.05$).

On the basis of these findings, potential factors influencing sound quality were investigated. CI experience showed a moderate linear and logistic correlation with sound quality ($R^2_{linear} = R^2_{logistic} = 0.41$). The sound quality saturates to excellent sound quality for large CI experiences (> 6 years), suggesting that CI sound perception can approximate that of a normal hearing ear over time. This observation highlights the relevance of neuronal plasticity in the rehabilitation process following cochlear implantation.

The CI simulations showed their potential for investigating CI sound quality in this thesis. In addition, owing to their large similarity to CI sound, they are valuable for educational purposes, as they allow a realistic assessment of the sound perception of CI users.

Kurzfassung

Cochlea-Implantate (CIs) sind Innenohrprothesen für Menschen mit hochgradigem oder vollständigem Hörverlust und ermöglichen die Wahrnehmung akustischer Reize. Ein in die Cochlea eingeführter Elektrodenträger stimuliert den Hörnerv mittels elektrischer Impulse. Verschiedene Faktoren, wie Signalverarbeitungsverluste, führen dazu, dass sich die Klangwahrnehmung mit CI im Vergleich zum akustischen Hören verändert. Ziel dieser Arbeit war es, die Klangwahrnehmung von CI-Tragenden in unterschiedlichen Rehabilitationsphasen anhand von Klangbeispielen („CI-Simulationen“) zu erfassen. Anschließend sollte die Klangqualität und deren Einflussfaktoren aus den CI-Simulationen ermittelt werden.

Zur Erstellung der CI-Simulationen wurde ein für diese Arbeit entwickeltes Software-Mischpult programmiert. Verschiedene Signalverarbeitungstechniken wie Filterung, Vokoding oder Tonhöhenverschiebung wurden implementiert um ein akustisches Signal an das mit einem CI wahrgenommene anzupassen. Das Mischpult wurde in einer zweiteiligen, prospektiven, experimentellen Studie verwendet. Im ersten Teil nahmen 15 einseitig ertaubte CI-Tragende mit mindestens 2 Jahren CI-Erfahrung teil. Im zweiten Teil wurden fünf Personen mit maximal 5 Tagen CI-Erfahrung befragt. Letztere nahmen nach 6 Monaten erneut an der Studie teil. Die CI-Simulationen wurden erzeugt, indem Sprachsignale durch das Mischpult an den CI-Klang angepasst wurden. Die Ähnlichkeit der CI-Simulationen im Vergleich zum CI-Klang wurde abschließend auf einer Skala von 1,0 (keine Ähnlichkeit) bis 10,0 (Signale sind identisch) bewertet. Die erzeugten CI-Simulationen wurden im Mittel mit einer Ähnlichkeit von 9,7 $\pm$ 0,5 durch die erfahrenen beziehungsweise 8,9 $\pm$ 0,8 durch die unerfahrenen CI-Tragenden bewertet. Die Mittelwerte weisen auf eine hohe Übereinstimmung zwischen Simulation und tatsächlicher CI-Klangwahrnehmung hin. Gleichzeitig zeigte diese eine erhebliche interindividuelle Variabilität.

Zur Quantifizierung dieser Variabilität wurden psychoakustische Experimente mit normalhörenden Studienteilnehmenden durchgeführt um die Klangqualität zu bewerten. Ergänzend wurde ein objektives Maß zur spektralen Abweichung zwischen Simulation und Referenzsignal eingeführt und mit den subjektiven Bewertungen korreliert. Im Mittel zeigten die CI-Simulationen eine moderate Klangqualität, wobei diese zwischen den Simulationen stark variierte. Die Spearman-Korrelation ergab einen signifikanten negativen Zusammenhang zwischen Klangqualität und spektraler Abweichung ($r_s(15) = -0{,}80$, $p < 0{,}05$).

Basierend auf diesen Ergebnissen wurden potentielle Einflussfaktoren auf die Klangqualität untersucht. Die CI-Erfahrung wies eine moderate Korrelation mit der Klangqualität auf ($R^2 = 0{,}41$). Insbesondere bei CI-Tragenden mit einer CI-Erfahrung von mehr als sechs Jahren wurden exzellente Klangqualitäten gefunden. Dies deutet auf eine Annäherung der CI-Klangwahrnehmung an das Hören eines normalhörenden Ohres hin und unterstreicht die Bedeutung der neuronalen Plastizität im CI-Rehabilitationsprozess.

Die CI-Simulationen zeigten das Potential zur Untersuchung der CI-Klangqualität. Darüber hinaus eignen sie sich zu Aufklärungszwecken, um eine realistische Erwartungshaltung zu vermitteln.

Table of Contents

1 Introduction

1.1 Motivation

The world report on hearing estimated that 430 million people worldwide have a moderate to total hearing loss (World Health Organization 2021). Untreated hearing loss is often related to reduced quality of life, social isolation and loss of cognitive functions up to dementia (Arlinger 2003; Dalton et al. 2003; Livingston et al. 2024; Thomson et al. 2017). In cases of moderate to profound hearing loss, conventional hearing aids may not lead to sufficient benefits, and a cochlear implant (CI) is used for hearing rehabilitation. Between 2005 and 2016, more than 32,000 CI implantations were performed in Germany (Wissenschaftliche Dienste des Deutschen Bundestages 2022).

CIs are neural prostheses that convert an acoustic signal in electric pulses (coding strategy) and stimulate the cochlear nerve to generate auditory perception. An acoustic signal is characterized by an envelope and a temporal fine structure (Wouters et al. 2015). For speech recognition, the envelope is especially important so that most coding strategies focus on the envelope to optimize the transmission of speech signals (Hochmair et al. 2015; Smith et al. 2002; Xu et al. 2003). The envelope is sampled and spectrally decomposed in frequency bands. This information is used to stimulate the auditory nerve with electric current pulses via an electrode array. The CIs used today have electrode arrays with 12 to 24 intracochlear electrode contacts (Dhanasingh et al. 2024). Due to technical progress in the last 60 years, CIs can contribute to open speech recognition in quiet (Ma et al. 2023; Zeng et al. 2008). In particular, the fine structure information is important for tonal components, e.g., prosody, sound and music perception (Hochmair et al. 2015). Signal processing, the limited number of electrode contacts, and the spread of electric fields reduce the spectral resolution of CI transmitted signals (Bingabr et al. 2008). As a result, CI users often describe the sound perceived with their CI (= CI sound) as unnatural, tinny, squeaky, robotic and high-frequency-voiced (Caldwell et al. 2017; Peters et al. 2018; Dorman et al. 2019a; 2022).

Extensive consulting is necessary to ensure patients' acceptance to the unfamiliar sound impressions, to improve family members' sympathy for the patients' situations and to strengthen family support. The presentation of sound samples to patients and their family members could assist in technical and medical consulting.

In Germany, hearing rehabilitation is divided into different stages. 'Basic therapy' begins the first postoperative day, lasts 6 weeks and continues with 'follow-up therapy', which takes up to 2 years for adults and ends with lifelong 'aftercare' (Präsidium der DGHNO-KHC 2021). The rehabilitants are supported by audioverbal therapy and technical CI processor fitting. Even small technical changes in

the processor settings can lead to a change in CI performance. Many studies have investigated the factors influencing CI performance in terms of speech recognition (Blamey et al. 2013; Canfarotta et al. 2022; Hoppe et al. 2021; Kim et al. 2018; Lazard et al. 2012) and found several factors and prediction models. The strongest improvement in word recognition is in the first 6 months after implantation (Blamey et al. 2013; Buchman et al. 2014). Simultaneously, previous studies have shown, that speech recognition correlates only weakly to moderately with CI sound perception and CI sound quality (Gfeller et al. 2008; Mertens et al. 2015). However, few studies have examined the factors that influence CI sound perception and quality, which highlights the importance of investigating these influencing factors (Bessen et al. 2021; Gfeller et al. 2008; Mertens et al. 2015; Saki et al. 2023). A possible reason is that CI sound perception and quality are highly subjective measures, without established definitions. Accordingly, only a few methods are currently available for assessing CI sound perception and quality. Most of these methods are based on self-reported sound quality via questionnaires. Owing to the subjective nature of such questionnaires, whose results also include personal, emotional, and psychological factors, investigating other influencing factors is difficult (Amann et al. 2014).

As the brain must learn how to interpret electrical impulses during rehabilitation, sound perception clearly depends on neuronal plasticity and CI experience (e.g., Bernhardi et al. 2017; Bessen et al. 2021; McDermott et al. 2009; Reiss et al. 2007). Factors such as the duration of deafness, time of usage, the health of biological tissue and insertion depth of the electrode array affect CI performance and are therefore also possible factors influencing sound quality (Gfeller et al. 2008; Blamey et al. 2013; Mertens et al. 2015; Bessen et al. 2021; Canfarotta et al. 2022; Dorman et al. 2022; Schvartz-Leyzac et al. 2023; Dorman et al. 2024).

As sound quality also contributes to quality of life (Akbulut et al. 2024; Fuller et al. 2022; Saki et al. 2023), CI manufacturers have developed new coding strategies. These use virtual channels and transmit the fine structure to improve the perception of tonal components (Hochmair et al. 2015; Landsberger et al. 2009). To improve CI sound perception, a better understanding of sound perception itself is essential. However, methods that measure the sound perception and sound quality perceived by CI users are needed.

1.2 Thesis Aim and Objectives

The aim of this thesis is to investigate CI sound perception and the CI sound quality of speech signals. In the first step, a fundamental understanding of human hearing and sound perception with CI was established (Chapter 2). Afterwards, German-language sound samples were created that make the CI sound audible to normal hearing people (Chapter 3). These 'CI simulations' focus on sound perception, not on the functionality or processing mechanisms of electrical stimulation with CIs. For this purpose, a software sound tool was designed that is able to create CI simulations in approximation of the CI sound. The simulations were compared with the CI sound and evaluated by single-sided deafened (SSD) CI users. CI simulations were generated for CI users at different stages of rehabilitation (basic therapy, follow-up therapy, and aftercare). On the basis of the new CI simulation models of the rehabilitated participants (aftercare), the CI sound was quantified in terms of CI sound quality. Two methods of quantification, one based on psychoacoustic experiments and one more objective, were evaluated (Chapter 4). In the last step, possible factors influencing CI sound quality were investigated and determined from patient-related data (Chapter 5). Consequently, this thesis examines three objectives:

1. To create German-language CI simulations for CI users at different stages of rehabilitation.
2. To develop a new method for measuring CI sound quality from CI simulations.
3. To determine factors influencing CI sound quality.

2 Theoretical Background

2.1 Physics of Sound

If particles of an elastic medium are deflected from equilibrium, an oscillation is triggered by the elastic and inertial properties of the medium. Pressure and density fluctuations result. The propagation of mechanical oscillation through a medium is called a sound wave (Photinos 2021). Mathematically, the spatial and temporal propagation of a sound wave is described by the wave equation and its solution. Sound is often associated with sound waves that are auditory perceivable by humans and have frequency ranges from approximately 16 Hz to 20 kHz (Bille et al. 2013).

The frequency f is the number of oscillations per unit of time and is inversely proportional to the wavelength that describes the length between two states of equilibrium. The proportional factor between the frequency and the inverse wavelength is the speed of the sound. The amplitude of the sound signal, called the sound pressure, is another important parameter for characterizing a sound wave and modulates the perceived volume of a sound signal (Bille et al. 2013).

The most elementary sound signal is a pure tone, which is a sinusoidal oscillation of a single frequency (Bille et al. 2013). As Fourier recognized, 'series formed of sines or cosines of multiple arcs are therefore adapted to represent, between definite limits, all possible Functions' (Fourier et al. 2009). This means that a periodic time signal (functions of the Hilbert (Lebesque) space $L_2([-\pi, \pi])$) is a composition of various signals of singular frequency. This is expressed by the convergence of the Fourier series to the time-dependent function $x(t)$ (Equation 2.1, Kerner et al. 2013).

$$x(t) = \frac{a_0}{2} + \sum_{n=1}^{\infty} a_n \cos(2\pi f n t) + \sum_{n=1}^{\infty} b_n \sin(2\pi f n t) \tag{2.1}$$

Here, a_0, a_n and b_n are the Fourier coefficients resulting from the integration over $x(t)$. These can be interpreted as the discrete frequency spectrum of $x(t)$ (Meyer 2021).

For aperiodic, integrable functions, the Fourier transform 2.2 of $x(t)$ is used to calculate the continuous frequency spectrum (Fourier spectrum) $X(f)$. This is obtained by using Euler's formula in equation 2.1 and considering the limiting case of an infinite period of the signal (Maurits et al. 2024; Möser 2015).

$$X(f) = \int_{-\infty}^{\infty} x(t) \mathrm{e}^{-2\pi i f t}\, dt \tag{2.2}$$

2.1.1 Principles of Sound Signal Processing

One of the most common audio file formats for sound signals is the WAVE file format, which stores a discrete-time and discrete-amplitude representation of an audio signal via pulse-code modulation (PCM, Nadir et al. 2016; Whibley et al. 2015). The analog audio signal is sampled at a sampling rate that fulfills the Nygquist theorem 2.3. The Nyquist theorem states that a signal containing a maximum frequency f_{max} can only be reconstructed from its sampled version correctly if the sampling rate f_s is at least twice as large as f_{max} (Nyquist 1928; Shannon et al. 1995, often, e.g., $f_s = 44.1\,\text{kHz}$, Meyer 2021). In PCM, quantization is performed by assigning each digitized, continuous value to the closest value in a set of discrete values (Siniša Tomić et al. 2023; Waggener et al. 1995).

$$f_s > 2f_{max} \tag{2.3}$$

Since the Fourier transform 2.2 is defined for functions, it cannot be applied to sampled, digital signals. Instead, the discrete Fourier transform (DFT) yields a discrete frequency spectrum (spectral lines) from a discrete time-dependent sequence $x[n]$ of length N. The DFT and its inverse are calculated via Equations 2.4 and 2.5 .

$$X[m] = \sum_{n=0}^{N-1} x[n]\, \mathrm{e}^{-2\pi i \frac{mn}{N}} \tag{2.4}$$

$$x[n] = \sum_{m=0}^{N-1} X[m]\, \mathrm{e}^{-2\pi i \frac{mn}{N}} \tag{2.5}$$

m is the ordinal number of each spectral line (Meyer 2021). The algorithm that performs a DFT is called fast Fourier transform (FFT) and assumes that N is a power of 2 (Maurits et al. 2024). The short-time Fourier transform (STFT) is used to calculate the temporal changes in a spectrum (spectrogram), which first windows the signal into time segments before the spectrum is calculated (Meyer 2021).

In sound processing, filters are used to attenuate certain frequencies in a signal. The most common filter types are low-pass, high-pass and band-pass filter. Filters have frequency-dependent passbands, in which the signal components are passed without attenuation, stopbands, in which the signal components are completely attenuated and transition bands, in which signal components are attenuated to a certain value (Meyer 2021). The 3 dB-cutoff frequency f_c, at which the amplitude response is reduced by 3 dB, are used to characterize filters (Meyer 2021). The slope of the attenuation in the transition band is described by the order of the filter (Meyer 2021). Figure 2.1 shows examples of amplitude-frequency responses for a low-pass, high-pass and band-pass filter.

A superposition of a signal with its time-delayed version (e.g., due to reflection) results in a comb filtered signal. The amplitude-frequency response shows a periodic attenuation of frequencies with the same spacing f_0 (fundamental frequency, Figure 2.1d). As digital filters, comb filters are often used in music production (also

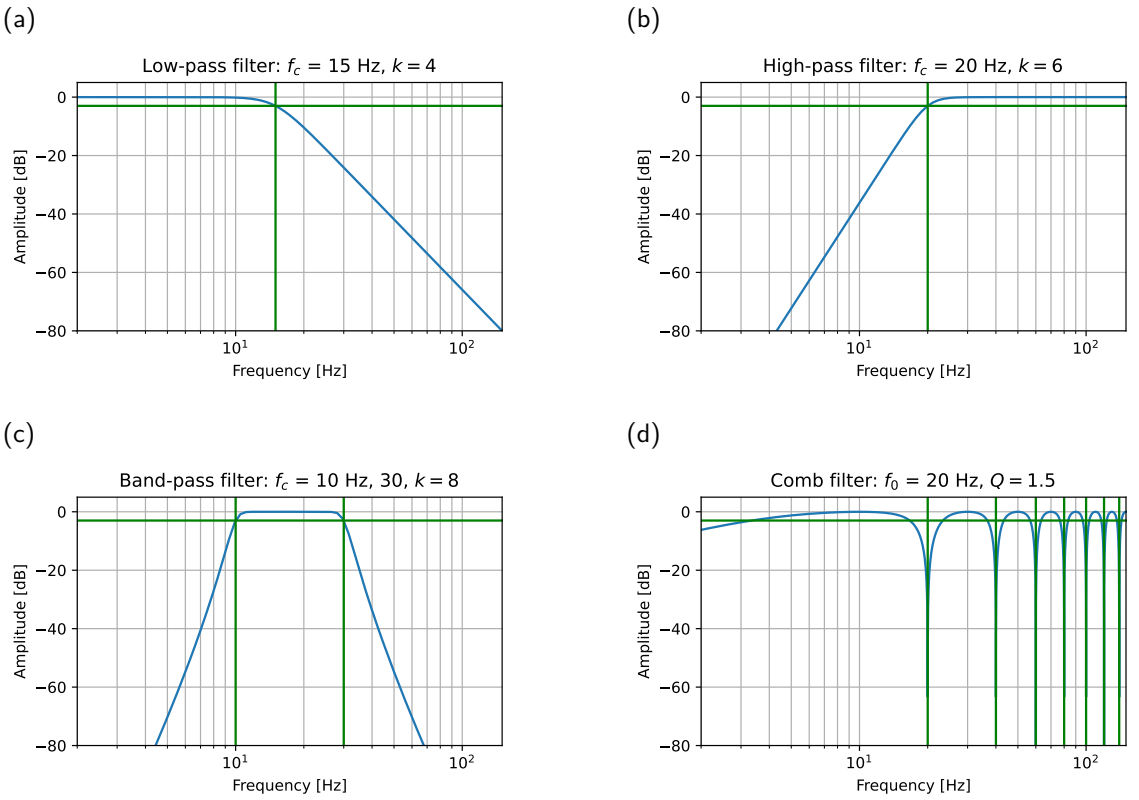

Figure 2.1: Amplitude-frequency responses for various filters. The green lines mark the cutoff or the peaking frequency, respectively.(a) Butterworth low-pass filter with cutoff frequency $f_c = 15\,\mathrm{Hz}$ and order $k = 4$. (b) Butterworth high-pass filter with $f_c = 20\,\mathrm{Hz}$ and order $= 6$. (c) Butterworth high-pass filter with $f_c = 10\,\mathrm{Hz}$ and $30\,\mathrm{Hz}$ and order$= 8$. (d) Comb filter with fundamental frequency $f_0 = 20\,\mathrm{Hz}$ and quality factor $Q = 1.5$.

referred to as flanging, Orfanidis 1996). The parameter that describes the slope of attenuation around the critical frequencies is referred to as the quality factor Q. It is calculated from the ratio of the fundamental frequency and the 3 dB bandwidth (Virtanen et al. 2020).

2.2 Anatomy, Physiology and Pathophysiology of the Auditory System in the Context of Cochlear Implantation

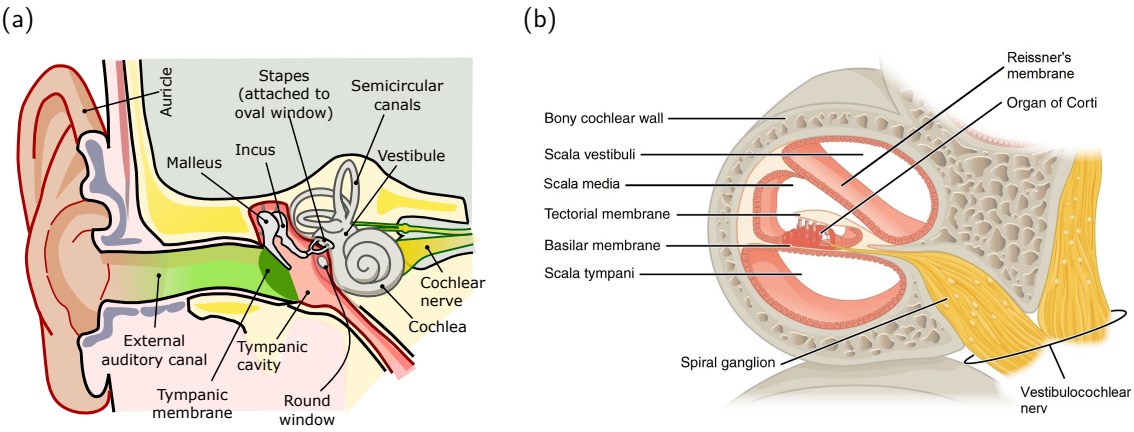

Figure 2.2: (a) Anatomy of the peripheral auditory system. Source: Chittka et al. 2005, modified. (b) Cross section of the cochlea. Source: OpenStax 2016, modified.

The auditory system comprises the peripheral and central parts. The peripheral auditory system receives sound waves and processes them into an electrochemical nerve signal, which is transmitted to the auditory cortex via the central auditory pathways. The peripheral auditory system consists of the outer, middle and inner ear (Brandes et al. 2020).

The auricle and the external auditory canal lead sound waves to the tympanic membrane. It transmits sound waves from the outer ear to the middle ear. The tympanic cavity, which contains three ossicles (malleus, incus, stapes), is behind the tympanic membrane. The ossicles in the middle ear transmit sound energy to the oval window of the inner ear (Figure 2.2a, Brandes et al. 2020).

The inner ear is a bony labyrinth consisting of the cochlea and the vestibular organ (vestibule and semicircular canals, Marsh et al. 1993; Xu et al. 2000). The cochlea is a fluid-filled, tube-like organ that spirals in 2.5 turns around a bony axis, the modiolus (Kral et al. 2021). Reissner's membrane and the basilar membrane divide the cochlea into three tubes: the scala vestibuli, scala media and scala tympani (Figure 2.2b). The scala vestibule starts at the oval window and the scala tympani ends at the round window. Both scalae are connected via the Helicotrema (Brandes et al. 2020).

The transmission of sound energy from the middle ear to the cochlea causes the fluids to vibrate and the basilar membrane to deflect (Brandes et al. 2020). The vibration propagates from the base to the apex of the cochlea on the basilar membrane as a 'traveling wave' (Békésy 1963). The stiffness of the basilar membrane changes along the cochlea, so that different frequencies cause maximum deflection of the basilar membrane at different locations (Békésy 1963).

The $3,500$ inner and $12,000$ outer hair cells are the electromechanic receptor cells of

the cochlea and are located in the organ of Corti on the basilar membrane (Hall et al. 2021). The deflection of the basilar membrane relative to the tectorial membrane, which is located above the hair cells, results in the bending and depolarization of hair cells. Receptor potentials are formed (Brandes et al. 2020).

Different frequencies therefore stimulate hair cells at different locations in the cochlea. This spatial coding of frequencies is called tonotopy (Stakhovskaya et al. 2007). The cochlea can therefore be considered as a mechanical Fourier transformer, in which low frequencies are processed apically and high frequencies basal (Chapter 2.1, Bille et al. 2013). Normal hearing people can perceive frequency differences of 0.3 % at 1 kHz (Brandes et al. 2020). Since the cochlea has a less specific frequency resolution than a Fourier transform (e.g., DFT, Section 2.1.1), the analogy to a bandpass filter-bank is often used in the literature (Schnupp et al. 2012). Each section of the basilar membrane has a characteristic resonance frequency, so that each of these sections can be understood as a single mechanical filter with a bandwidth specific to the resonance frequency (equivalent rectangular bandwidth, critical bands). In contrast to the DFT, nonlinear, approximately logarithmic frequency ranges are considered, as the bandwidth of the auditory filters increases toward high frequencies (Schnupp et al. 2012).

The receptor potential triggers a release of glutamate at the basal pole of hair cells so that spiral ganglion neurons generate action potentials. In addition to the tonotopy, the rate of excitation also enables frequency selectivity. This temporal coding of frequencies is called periodotopy. The spiral ganglions leave the cochlea via the modiolus. The action potentials are transmitted to the auditory cortex via the auditory pathway, which runs through the brain stem, midbrain and diencephalon. At these different stages of the auditory pathway, the sound information is processed (e.g., sound localization) and compared with experiences (Brandes et al. 2020). Further information on the physiology of hearing can be found, e.g., in Brandes et al. (2020).

The cognitive processing and perception of acoustic stimuli are highly complex. The relationship between the physical sound stimulus and the resulting psychological (subjective) auditory perception is examined and described through psychoacoustics (Section 2.5, Zwicker et al. 2007). Neuronal plasticity describes the ability of the human nervous system to reorganize itself in response to new or lost stimuli (Bernhardi et al. 2017; Gazerani 2025). This is the principle of learning and is important in auditory perception, as the brain is capable of adapting to changes in the auditory environment (Bernhardi et al. 2017).

There are various ways that lead to hearing loss. Hearing loss is categorized by its place of origin and can occur in one (single-sided deafness, SSD, unilateral) or both ears (bilateral). Sensory hearing loss originates from impairments of the cochlea. It is caused by, e.g., loud noise, ototoxic medicaments, or genetic defects and ranges from mild hearing loss to deafness (Zahnert 2011). Sensory hearing loss is typically treated with hearing aids or in cases of severe hearing loss with CIs (Boenninghaus et al. 2007). The treatment of hearing loss depends on several factors, such as anamnesis and differential diagnosis (Bruschini et al. 2024).

2.3 Design and Functionality of Cochlear Implants

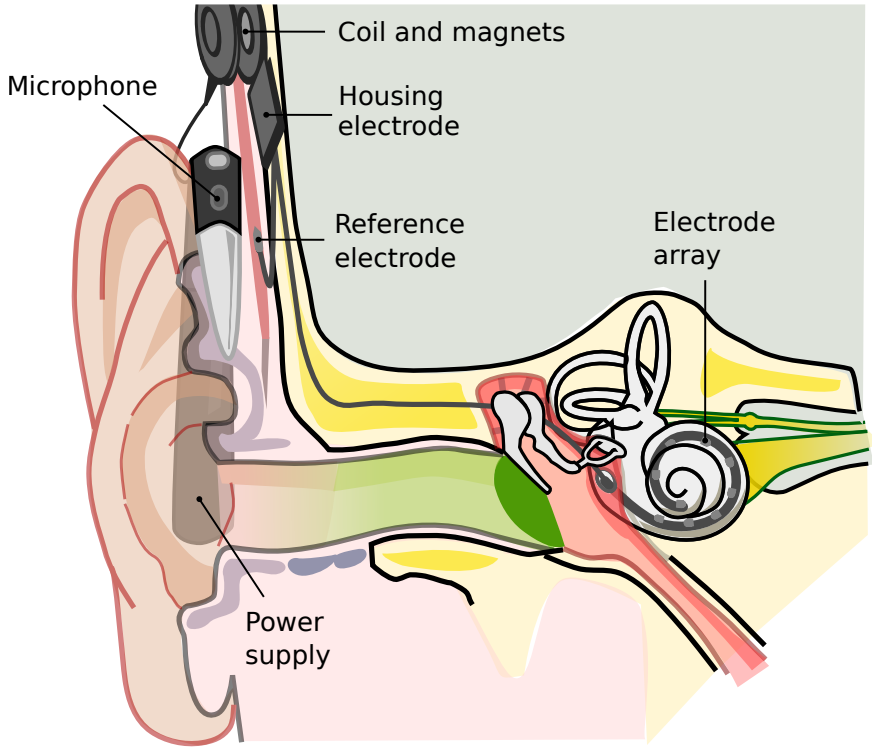

Figure 2.3: Schematic drawing of an implanted cochlear implant (CI) and a behind-the-ear processor. Source: Chittka et al. (2005), modified.

CIs are electronic devices that evoke auditory perception by stimulating the cochlear nerve. The systems commonly used today are partially implantable and consist of two components: the internal and the external component (Figure 2.3). The internal component consists of a housing with reference electrode contact, an induction coil, a permanent magnet and electronics such as current sources, and an electrode array. It is implanted during surgery. Therefore, the housing of the implant is placed beneath the skin in a bone recess and the linear electrode array is inserted into the scala tympani of the cochlea (Dazert et al. 2020). The external component consists of an induction coil, a permanent magnet, microphones, a sound processor and a power supply. The patient wears the audio processor external behind the ear, in the case of behind-the-ear processors (Figure 2.3), or above the induction coil, in the case of single-unit processors (Kral et al. 2021; Hoth et al. 2017).

The processor is fixed on the implant by permanent magnets. The microphones record audio signals. An amplifier and an analog-to-digital converter edit the signal. Afterwards the signal is encoded by a coding strategy to filter the relevant information for speech recognition. The external coil transmits the encoded signal to the internal receiver coil. The implant decodes the signal and applies charge-balanced bi- or triphasic (two or three) current pulses consisting of negative and positive phases to intracochlear electrode contacts. The current flows from a stimulation electrode (intracochlear) to a reference electrode contact (intracochlear: bipolar stimulation

mode, BP, or extracochlear: monopolar stimulation mode, MP1 or MP2) to stimulate the spiral ganglion neurons of the auditory nerve (Kral et al. 2021; Wouters et al. 2015).

Since the electrode array stimulates longitudinally along the scala tympany, the tonotopic organization of the cochlear is used (see section 2.2), and different frequencies are perceivable (Kral et al. 2021). The periodotopy of the cochlea is mimicked by different stimulation rates along the electrode array (Hochmair 2021; Rader et al. 2016a).

In addition to stimulation, voltage measurements and transmissions to the external parts (telemetry) are possible. Intracochlear impedances, voltage drops (Stimulation-Current-Induced Non-Stimulating Electrode Voltage recordings, SCINSEVs, Rijk et al. 2020) and nerve responses (electrically evoked compound action potentials, He et al. 2017) are measurable. These data provide information about the integrity of the implant but can also be used for electrophysiological monitoring. For example, fluctuating impedances can indicate intracochlear inflammatory processes (Shaul et al. 2019). For this reason, telemetry data are part of routine control and should be measured and analyzed at regular intervals (Präsidium der DGHNO-KHC 2021).

SCINSEVs are a highly relevant field of research since they provide information on the intracochlear position, which previously could only be obtained by radiological imaging. Several research groups have shown that SCINSEVs reliably detect a foldover of the electrode array tip, which corresponds to an implant malposition (Franke-Trieger et al. 2024; Hans et al. 2021; Hoppe et al. 2022; Kay-Rivest et al. 2022; Klabbers et al. 2021; Zuniga et al. 2017). During SCINSEV recordings, one intracochlear electrode contact stimulates and the voltages at all nonstimulated electrode contacts are measured so that SCINSEVs are a measure of intracochlear spread of the electric field (Kopsch et al. 2022; Kopsch et al. 2024a; Rijk et al. 2020; Wagner et al. 2023). Incomplete insertion or a scalar dislocation of the electrode array can also be detected via SCINSEVs (Dong et al. 2021; Kopsch et al. 2024b; Rijk et al. 2020; Rijk et al. 2022). The algorithms for detection of tip-foldover, extracochlear electrode contacts or scalar dislocation are based on the fundamental assumption that the voltage decreases with increasing distance from the stimulation electrode contact. A change in voltage drop, e.g., an increase instead of a decrease, indicates one of the above-mentioned malpositions (Dong et al. 2021; Hoppe et al. 2022; Rijk et al. 2020). Initial studies even indicate that the insertion depth of the electrode array can be estimated with SCINSEVs (Aebischer et al. 2021; Schraivogel et al. 2023b; Zhang et al. 2024), so that the examination of SCINSEVs remains a promising field of research.

In Germany, three manufactures produce CIs as approved medical devices: Advanced Bionics[1], Cochlear Ltd.[2] and MED-EL[3]. The fundamental design and functionality of the CIs of all the mentioned manufacturers are the same and correspond to those described above. Differences between the CIs result from the design of electrode contacts (e.g., pairwise arrangement or single), the number of reference electrode contacts, the number of intracochlear electrode contacts (12 to 24), the

[1]Advanced Bionics AG, Stäfa, Switzerland
[2]Cochlear Ltd., Sydney, Australia
[3]MED-EL, Innsbruck, Austria

stiffness of the electrode array, the length, the shape (precurved or straight) and thus the intracochlear position (e.g., perimodiolar, mid scalar or at the lateral wall, Dhanasingh et al. 2024), the optical designs of the external components and the technical properties (e.g., stimulation options and noise suppression mechanisms, Tzvi-Minker et al. 2023). The length of the electrode array can be specified in two ways: active length (length from the first to the last electrode contact) and total length (marking ring for implantation to the electrode array tip). For additional manufacturer-specific properties, please refer to the manufacturer's homepages and manuals[4][5][6].

2.3.1 Signal Processing in Cochlear Implants

The signal processing is split into signal pre-processing and coding. Signal pre-processing is used to improve the signal quality and includes automatic gain control, adjustment of the direction-dependent sound sensitivity (e.g., beamforming) and various noise reduction algorithms. The automatic gain control regulates the input sensitivity depending on the sound pressure level so that soft signals are perceivable and loud signals are not too loud (Kral et al. 2021). The order of processing differs between the manufacturers[4][5][6].

After pre-processing, a coding strategy defines the transformation rule from the acoustic signal to an electrical stimulation pattern (Figure 2.4) and replaces peripheral auditory processing (Kral et al. 2021; Wouters et al. 2015). Over the last 60 years of CI development, various coding strategies have been developed (Zeng et al. 2008). Due to the large number and complexity of coding strategies, only the coding strategy relevant to this thesis, an n-of-m coding strategy, particularly the Advanced Combination Encoder (ACE[7]), will be explained (Figure 2.4). Further information on various coding strategies can be found, e.g., in Wouters et al. (2015).

The digital signal is divided into $m = 22$ logarithmically spaced frequency bands by an FFT- or a bandpass filter-bank comprising cutoff frequencies between 188 and 7938 Hz (Appendix: Table A1, Cochlear Ltd. 2022b). Each filter band is spatialized to one electrode contact according to the tonotopic organization of the cochlea. The temporal envelope (amplitude contour) of each frequency band is calculated via Hilbert transformation (Cychosz et al. 2024; Wouters et al. 2015). The number n ($n \in \mathbb{N}$ and $n < 16$, typically $n = 8$) of electrode contacts with the largest energy in the frequency band (magnitude of the envelope) is used to modulate stimulation pulse amplitudes (Figure 2.4, Cochlear Ltd. 2022b).

The minimum and maximum pulse amplitudes which correlate to the minimum and comfortable loudness must be adjusted for each individual patient and electrode contact ('processor programming', Wouters et al. 2015). The loudness perception depends on the temporal integral of the current, i.e., the pulse width and the current amplitude (Hoth et al. 2017). A variety of parameters can be adjusted to enable individual, optimal hearing. The adjustable parameters (mapping parameters) in

[4]Advanced Bionics AG, Stäfa, Switzerland
[5]Cochlear Ltd., Sydney, Australia
[6]MED-EL, Innsbruck, Austria
[7]Custom Sound Pro Software, Cochlear Ltd. (2022b), Sydney, Australia, version 7.0

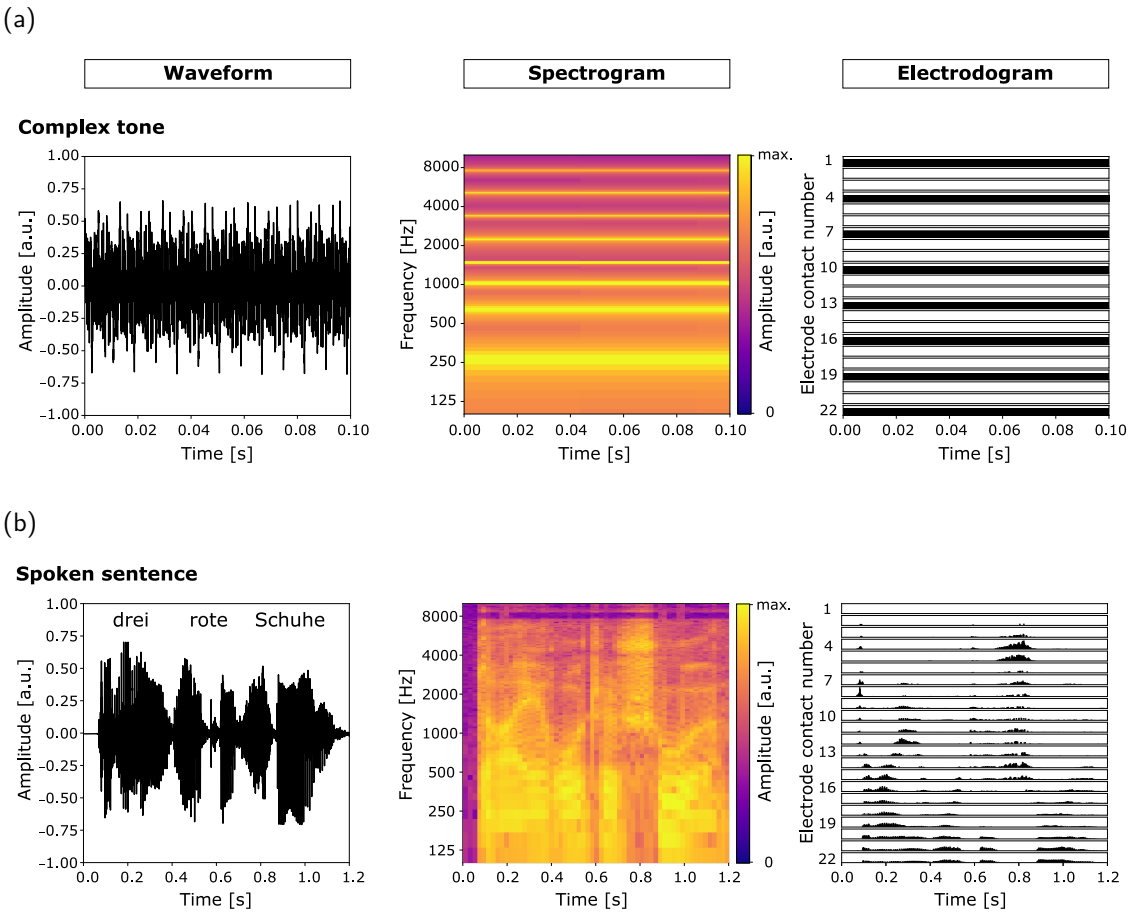

Figure 2.4: Waveforms, spectrograms and pulsatile stimulation patterns (electrodogram) of two acoustic signals. Electrodogram was created on the basis of an n-of-m coding strategy (Wouters et al. 2015) with $n = 8$ and $m = 22$ (number of electrode contacts). Notably: The frequency axis in the spectrogram is logarithmic, whereas the electrode contact axis in the electrodogram is linear. (a) Complex tone created by the summation of eight sine-functions with center-frequencies of electrode contacts 1, 4, 7, 10, 13, 16, 19 and 22 in Table A1 in the Appendix ($f_c = 250.5, 625.5, 1000.5, 1438.0, 2188.0, 3313.0, 5000.5, 7438.0\,\text{Hz}$). (b) Spoken German sentence of the Oldenburg children's sentence test spoken by a male voice ('drei rote Schuhe' ['three red shoes'], Wagener et al. 2005)

the ACE strategy include, e.g., threshold current levels (T-levels), comfortable current levels (C-levels), pulse widths, number of maxima n and stimulation rate. The default stimulation rate is 900 pulses per second (Cochlear Ltd. 2022b).

2.4 Sound of Cochlear Implants

The perception of complex sound signals with CIs is restricted by several factors. To transform the analog complex sound signal into a pulsatile stimulation pattern that can be used by a discrete number of electrode contacts, the sound information

not relevant for speech recognition is neglected (Section 2.3.1, Figure 2.4). In a healthy cochlear, sound signals are transmitted by about 3,500 hair cells to the spiral ganglion neurons (Hall et al. 2021). In an implanted cochlea, the signal is transmitted by 12 to 24 physical intracochlear electrode contacts. Although four electrode contacts are sufficient to achieve speech recognition in quiet, more than 30 electrode contacts may be required to perceive more complex signals (Shannon et al. 2004). The described loss of information is shown graphically in Figure 2.4 by comparing the spectrograms with the electrodograms.

CIs use the physiological tonotopy and periodotopy of the cochlea (Section 2.3.1). However, physiologically, different frequencies are processed over the entire basilar membrane, but the electrode array usually only covers 0.75 to 1.8 of the 2.5 turns (Landsberger et al. 2015; Rader et al. 2024). This is due to the electrode array design, which is related to the decreasing diameter of the scala tympany (Micuda et al. 2024). However, the electrode contacts do not stimulate the basilar membrane, but the spiral ganglion neurons and these only cover 1.6 to 2.0 of the 2.5 turns (Ariyasu et al. 1989; Kawano et al. 1996; Kral et al. 2021; Li et al. 2021). Nevertheless, a frequency-to-place mismatch is possible: the frequency range of an electrode contact and the physiological correct place of processing of that frequency range differ (Baumann et al. 2006; Canfarotta et al. 2022; Dorman et al. 2019b; Landsberger et al. 2015). If the stimulation rate is not adjusted according to the electrode contact position, this leads to a rate-to-place mismatch (Rader et al. 2016a). Furthermore, the physical properties of electrical stimulation lead to a 'spectral smearing'. The current for stimulation evokes an electric field. Depending on the distance between the electrode contact and the neurons, the spread of the electric field has different extents (He et al. 2017; Söderqvist et al. 2023). Thus, the electric field also stimulates more distant neurons, which leads to a spread of spiral ganglion excitation (Kopsch et al. 2022; Söderqvist et al. 2021). The consequence is that spatial precision of stimulation, which is necessary for spectral resolution, is reduced (Bingabr et al. 2008; Tang et al. 2011; van den Honert et al. 1987; Zeng et al. 2014; Zwolan et al. 1997). CI manufacturers try to counteract the frequency-to-place mismatch with variable electrode array lengths, the rate-to-place mismatch with variable stimulation rates along the electrode array and the spectral smearing with, e.g., current steering methods (Berenstein et al. 2008; Hochmair et al. 2015; Rader et al. 2016a).

The loss of information due to electrical signal processing, frequency-to-place mismatch, rate-to-place mismatch and spectral smearing leads to a change in sound perception of CI users (CI sound) compared with that of normal hearing people. CI users with little CI experience often describe their CI as unnatural, tinny, squeaky, robotic and high-frequency-voiced (Caldwell et al. 2017; Peters et al. 2018; Dorman et al. 2019a; 2022).

Changing individual mapping parameters (Section 2.3.1) can lead to a change in CI sound (Dorman et al. 2019b). Neuronal plasticity counteracts these technical features by means of perceptual adaptation (Dorman et al. 2022). As described in Section 2.2, neuronal plasticity describes the ability of the human brain to reorganize itself in response to new or lost stimuli (Bernhardi et al. 2017; Gazerani 2025). Hearing loss or deafness leads to a functional reorganization of the central auditory system. Rehabilitation after cochlear implantation thus depends on the strength of the preoperative reorganization as well as on the ability of the individual's auditory

system to adapt postoperatively (Kral et al. 2016; McKay 2018). The memories and experiences of the individual influence the neuronal plasticity so that the duration of deafness affects postoperative performance (Blamey et al. 2013; Canfarotta et al. 2022; Hoppe et al. 2021; Kim et al. 2018; Lazard et al. 2012). Reiss et al. (2007) and McDermott et al. (2009) showed that pitch perception and perceived frequency-to-place mismatch changes with CI experience. To date, little research has been conducted on the factors influencing CI sound. These findings suggest that the factors that influence speech recognition also influence sound perception. Blamey et al. (2013) reported that CI experience has the greatest influence on postoperative speech recognition. However, age at implantation, electrode array insertion depth, age at onset of deafness, duration and cause of deafness also affect speech recognition with CIs (Blamey et al. 2013; Canfarotta et al. 2022; Hoppe et al. 2021; Kim et al. 2018; Lazard et al. 2012) and may influence CI sound perception.

The knowledge of CI sound is important in consulting patients to ensure patients' acceptance to the unfamiliar sound impressions, to improve family members' sympathy for the patients' situation, to strengthen family support, to educate clinical staff, to identify factors influencing CI sound quality and to develop the hardware and software of CI systems.

2.4.1 Review of Cochlear Implant Sound Perception Measurements

The sound of a CI is a very subjective perception and cannot simply be measured with a microphone and played through a loudspeaker such as an acoustic sound. The CI sound essentially depends on the electro-neural interaction of the individual. Some studies have attempted to reproduce the sound of a CI with so-called vocoders (voice encoders, Peters et al. 2018; Karoui et al. 2019). Vocoders originate from military telephone technology and are intended to encode voice signals into a digital signal that can be resynthesized by a receiver (van Veen 2012). The signal processing in vocoded signals is very similar to signal processing in CIs, so that vocoders are often used to 'simulate' CI signals (Fu et al. 2004; Mesnildrey et al. 2016; Rosen et al. 2015; Steinhauer et al. 2023) and are also widely presented on the internet as 'CI simulations' (Cychosz et al. 2024). However, it must be explicitly noted that vocoders simulate parts of signal processing of a CI and, therefore, the information content transmitted by a CI, but they do not simulate the highly complex cognitive processing. Thus, vocoders do not reflect the sound of a CI as they do not simulate neuronal plasticity (Cychosz et al. 2024; Peters et al. 2018).

Although CIs have been implanted for approximately 60 years (Zeng et al. 2008), the indication criteria (Präsidium der DGHNO-KHC 2021) have changed in recent decades due to technical developments. In 2008, a person with SSD was implanted with a CI for the first time (van de Heyning et al. 2008). The relatively new patient group of SSD patients enables a direct comparison between a normal hearing ear and a CI ear (e.g., Dorman et al. 2017; Peters et al. 2018; Karoui et al. 2019).

In studies by Dorman et al., SSD CI users matched the sound of a spoken sentence on the contralateral ear to the sound of their CI (Dorman et al. 2017; 2019; 2019; 2020; 2022; 2024). The audio signal was modified via a software sound tool corresponding

to the participant's descriptions of the CI sound. If no further approximation of the audio signal to the CI sound was possible, the similarity of the two signals was scored on a scale from 1.0 (no similarity) to 10.0 (signals are identical, Dorman et al. 2017). In this way, sound samples were created, e.g., for 14 CI users, which were scored with an average similarity score of 8.8 ± 0.9 and one full match (similarity score = 10) was found (Dorman et al. 2020). Therefore, the most often needed modification was a high-, low- or band-pass filter (Dorman et al. 2020). The generated sound samples correspond to CI simulations that reflect the sound of a CI with a large degree of similarity. In accordance with this definition (Dorman et al. 2020), the term 'CI simulation' is used throughout this thesis. These replicate the CI sound and do not simulate the functionality or processing mechanisms of a CI.

Dorman et al. conducted several studies on the design described above (Dorman et al. 2017; 2019; 2019; 2020; 2022; 2024). CI users with shorter electrode arrays (active length: 15.0 mm, total length: 18.5 mm, Advanced Bionics AG 2022; Dhanasingh et al. 2024, Section 2.3) and longer electrode arrays (active length: 23.1 mm, total length: 28 mm, Med-El 2012) were tested (2022; 2024). Dorman et al. concluded that the length of the electrode array has an influence on sound perception: CI users with shorter electrode arrays perceive their CI to be higher pitched than CI users with long electrode arrays do (Dorman et al. 2022; 2024). Very short electrode arrays (total length $<$ 18.5 mm) have not yet been investigated in the above-mentioned study design.

In another study, Dorman et al. (2022) investigated the change in CI sound over time. For this purpose, the sound perception of a group of five CI users with shorter, mid scalar electrode arrays (active length: 15.0 mm, total length: 18.5 mm, Advanced Bionics AG 2022; Dhanasingh et al. 2024) was examined at two study visits. The CI experience in the first and second study visits as well as the time difference between visits was variable between the participants. The participants had between 2.7 and 20 months of CI experience at the first study visit, and between 17 and 47 months at the second visit. Even though some sound characteristics changed over time, Dorman et al. (2022) reported that pitch perception did not change over time in the investigated study cohort.

2.4.2 Review of Vocoder Design Considerations

As described above, vocoders alone often do not reflect the sound of a CI (Section 2.4.1, e.g., Peters et al. 2018). Nevertheless, they have been widely used in the literature to 'simulate' CIs, as they mimic certain aspects of the CI's signal processing, such as the impact of the spread of the electric field on speech recognition (Fu et al. 2004; Fu et al. 2005; Mesnildrey et al. 2016; Rosen et al. 2015; Steinhauer et al. 2023; Kopsch et al. 2024a). This enables a study design with large experimental control on normal hearing people to achieve a greater number of participants and to reach a better understanding of hearing with CIs (Cychosz et al. 2024). Furthermore, vocoders are able to provide information about certain sound cues (Dorman et al. 2020).

Vocoding is a broad category of signal processing techniques. In this section, only the vocoder processing steps relevant to this thesis are discussed (Figure 2.5 and 2.7).

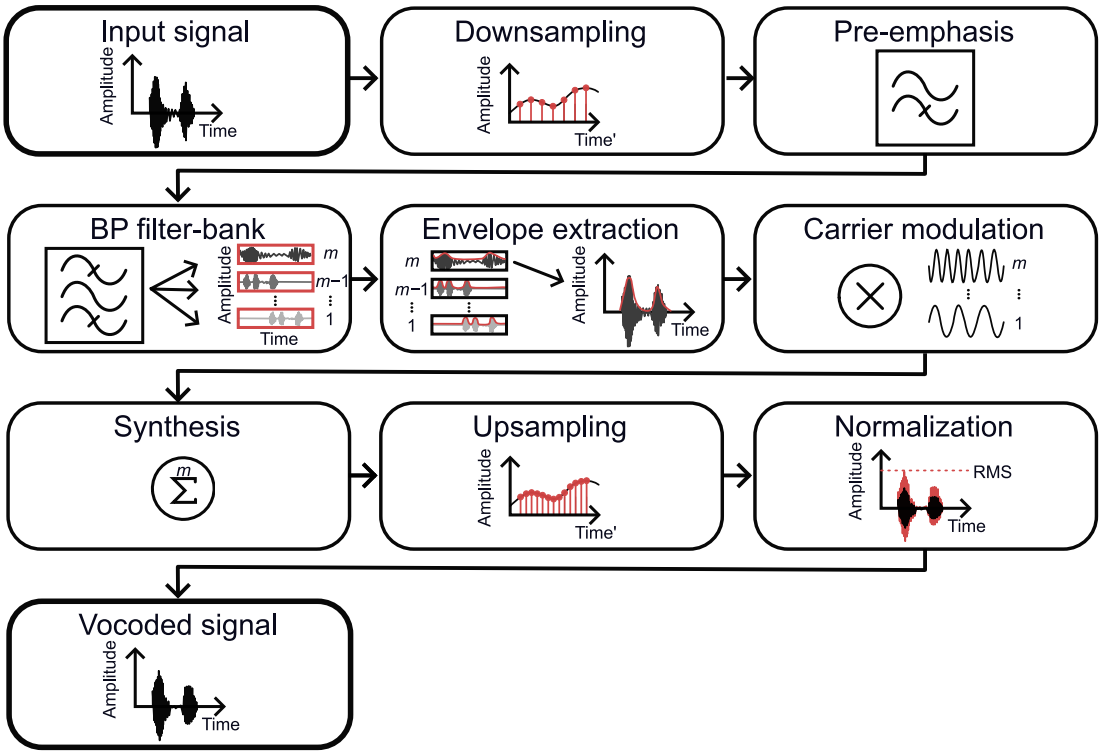

Figure 2.5: Block diagram of a band-pass (BP)-vocoder. m: number of frequency bands, RMS: Root mean square.

For further reading, please refer to Cychosz et al. (2024).

Vocoding can be divided into four processing steps: Pre-processing, analysis, synthesis and post-processing. In pre-processing, a digital signal is sampled at a rate that equates to the sampling rate of a CI coding strategy (e.g., ACE: 16 kHz, Nogueira et al. 2005; Vandali et al. 2000) to mimic CI signal processing. As the magnitude spectrum of a speech signal is characterized by a loss of energy toward larger frequencies, the signal is first filtered to compensate for the loss (pre-emphasis, Cychosz et al. 2024; Sun 2000). To analyze the pre-processed signal, a filter-bank divides the signal into m ($m \in \mathbb{N}$) frequency bands. The number of frequency bands is often oriented on the number of electrode contacts of the CI to be simulated (Cychosz et al. 2024). The cutoff frequencies of frequency bands are typically logarithmically spaced such as in CIs (Section 2.3.1 and Appendix: Table A1). As different CI manufacturers implement the filter-bank differently (e.g., Nogueira et al. 2005 versus Hochmair et al. 2015) various filter-banks are also used in vocoder research (Cosentino et al. 2014). Therefore, the choice of filter-bank depends on the research question. The most common filter-banks are based on band-pass filters (e.g., Peters et al. 2018) or FFTs (e.g., Cucis et al. 2021, Section 2.1.1). The processing steps of analysis differ slightly between band-pass (BP)-vocoders and FFT-vocoders and are shown in Figures 2.5 and 2.7.

BP-vocoders (Figure 2.5) use m bell-shaped band-pass filters (Hochmair et al. 2015), e.g., Butterworth filters (e.g. Figure 2.1c, Fu et al. 2005; Peters et al. 2018). To determine the temporal envelope from the frequency bands, half-wave rectification with low-pass filtering or Hilbert transformation is often used (Cychosz et al. 2024; Fu et al. 2005). At this processing step, an n-of-m selection method could be

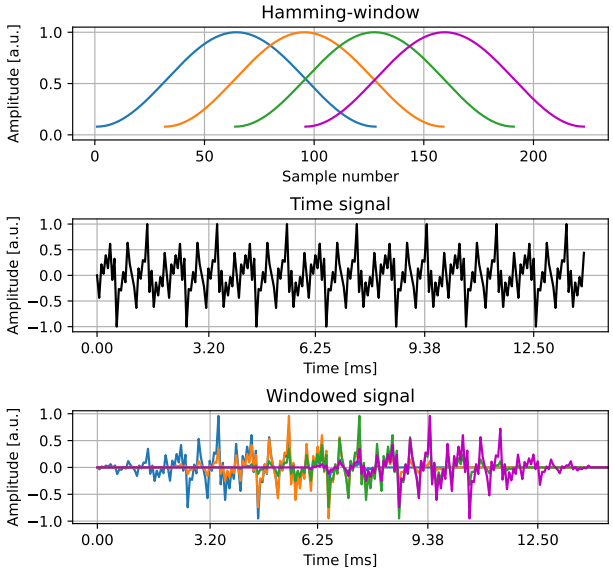

Figure 2.6: Exemplary signal windowing with Hamming-windows for a complex tone.

applied. Since the BP-vocoder used in this thesis was implemented without an n-of-m selection method, the block diagram in Figure 2.5 neglects it.

The FFT-vocoder (Figure 2.7) windows the signal into frames of a specific length, e.g., 128 samples via Hamming-windowing (Figure 2.6, Cucis et al. 2021). Each frame has a temporal overlap with the neighboring frame, e.g., 75 % which corresponds to 96 samples. The FFTs (absolute values) of each frame result in 64 frequency bins. The bins are combined into m frequency bands by calculating the means of the FFT coefficients. The upper and lower cutoff frequencies of the frequency bands are set by the filter-bank. An average FFT value is now assigned to each temporal frame of each frequency band. At this processing step, an n-of-m selection method, as described in Section 2.3.1, can be applied to choose the n frequency bands with the largest amplitudes in each temporal frame. The remaining channels are set equal to zero (Cucis et al. 2021). For temporal envelope reconstruction, Hamming windows are modulated with the mean FFT values. The modulated Hamming functions are overlapped (e.g., 75 %) and summed so that temporal envelopes are calculated for the n selected frequency bands. Marginally, vocoders can also be used for other signal processing, such as time stretching, if the extent of overlap in reconstruction is changed (for further reading, see Driedger et al. 2016).

Up to this processing step, the signal processing corresponds to that of a CI. The difference between the CI and vocoder is that a CI stimulates electrically, and a vocoder needs an acoustic output. Therefore, a basic signal (carrier) is modulated with the envelope of each frequency band by multiplying the carrier signal and envelopes (Cychosz et al. 2024). The most often used carriers are sine-waves or noise carriers. Sine functions with frequencies that correspond to the center frequencies of the frequency bands of envelopes are used as sine-wave carriers. A narrow band noise bank can be used as a noise carrier. For this purpose, a filter-bank is applied to broadband Gaussian noise. By varying the filter-slope in the noise-filter-bank, the spread of the electric field is simulated. A steep, moderate or flat slope corresponds

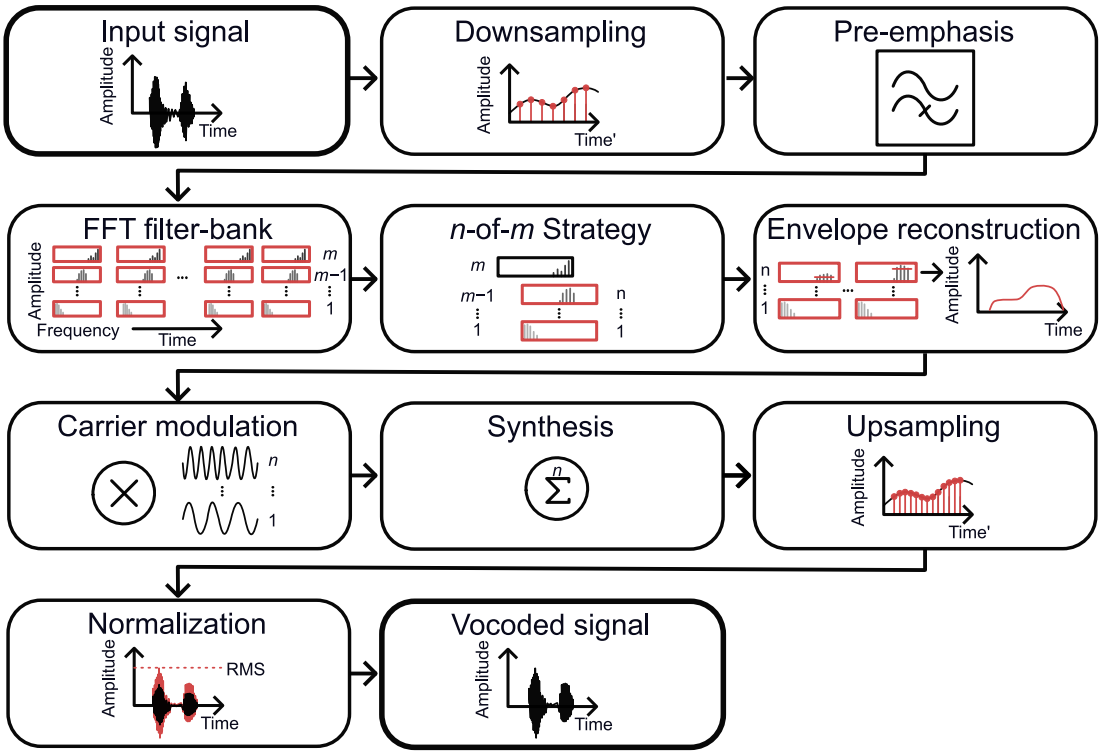

Figure 2.7: Block diagram of a fast Fourier transform (FFT)-vocoder. m: number of frequency bands, n: number of selected frequency bands with the largest energy, RMS: Root mean square.

to a weak, moderate or broad spread of excitation (Cucis et al. 2021; Cychosz et al. 2024; Fu et al. 2005; Mehta et al. 2017).

In conclusion, the vocoded signal is created by summing the modulated carriers. As a final step, resampling to the input sampling rate (Cucis et al. 2021) and root-mean-square (RMS) normalization of energy to obtain a stable amplitude of output compared with the input signal are performable (Cychosz et al. 2024). Therefore, the RMS of the complete audio signal is calculated (Equation 2.6),

$$\mathrm{RMS} = \sqrt{\frac{1}{N}\sum_{n=0}^{N-1} x^2[n]} \tag{2.6}$$

where $x[n]$ is the amplitude of the discrete time signal of the audio signal of length N. The scaling factor is set to the maximum factor by which the audio signal can be scaled without inducing clipping (Cychosz et al. 2024).

2.5 Review of Sound Quality Measurements

Sound quality is not a purely physical or acoustic quantity, as it essentially depends on the subjective hearing perception of the human auditory system. It is a psychoacoustic parameter, and there is no consistent definition of sound quality. In

product engineering, a quality evaluation based on the sounds of certain products is used, e.g., the closing sound of a car door can have high or low sound quality. Blauert et al. (1997) defined '[...] sound quality is a descriptor of the adequacy of the sound attached to a product [...]'. In contrast, in the treatment of hearing loss, sound quality is the perceived richness of the hearing aid (Caldwell et al. 2017). In addition, sound appraisal is differentiated from sound quality, which describes the subjective melodiousness of a sound (Caldwell et al. 2017).

However, sound quality is a multidimensional quantity and depends on, e.g., loudness, sharpness and roughness (Fastl et al. 2007). Due to the dependency on human perception, there is no measuring tool to record sound quality, appropriately. Certain models attempt to capture psychoacoustic quantities such as loudness, roughness and sharpness and combine them into a new quantity, psychoacoustic annoyance, as a measure of sound quality (Ma et al. 2020; Zhang et al. 2019; Zwicker et al. 2007). However, these models are derived from subjective data and are not validated for all types of acoustic stimuli (Schell-Majoor et al. 2016). The sound quality of an acoustic signal is most frequently measured via subjective rating methods (Roy et al. 2012b).

Fastl (2005) described four methods to assess sound quality and its dimensions: random access, semantic differential, category scaling and magnitude estimation. In a random access task, several acoustic signals have to be sorted according to their sound quality so that a ranking is created. The acoustic signals can be listened to in any order and as often as desired. This method provides information on whether the sound quality of one signal is better than that of another. In a semantic differential task, it is decided which adjective of opposing adjectives (e.g., loud - quiet) describes the acoustic signal better. A visual analog scale is sometimes used to quantify the degree of appropriateness of an adjective. The semantic differential can provide information about why a sound quality is bad or good. Category scaling and magnitude estimation indicate the extent to which sound qualities differ between several acoustic signals. In a category scaling task, the sound quality is assessed via a scale (e.g., bad - poor - fair - good - excellent). The magnitude estimation task is a pairwise comparison between a reference acoustic signal and an acoustic signal to be evaluated. The signals are then assigned a numerical value relative to each other depending on the sound quality. In addition to sound quality, other psychoacoustic quantities (e.g., roughness) can be queried via random access, category scaling and magnitude estimation (Fastl 2005).

As described above, each of the four methods provides information on a specific question ('which signal is better?', 'how much better is a signal?', 'why is a signal better?', Fastl 2005). If several questions are to be answered in the same experiment, combinations of different methods are also possible.

Chung et al. (2006) used a combination of pairwise comparison and category scaling. In the pairwise comparison, no anchor signal is used, but all the acoustic signals are permuted and compared in pairs. For each signal pair, the preferred signal is chosen, and the strength of the preference is given on a scale. The pairwise comparison enables the detection of small differences in sound, and by counting the number of preferences of each signal, a ranking is given. In contrast to, e.g., random access, pairwise comparisons are carried out in a structured manner, and each acoustic

signal is heard once in comparison to every other signal (Anderson 1994).

The International Telecommunication Union (ITU) published the recommendation ITU-R BS.1534-3 (ITU-R 2015) to assess the average sound quality of audio systems. The recommendation includes a method called the Multi-Stimulus Test with Hidden Reference and Anchor (MUSHRA, ITU-R 2015). The sound quality of acoustic signals is rated on a MUSHRA scale from 0 (poor sound quality) to 100 (excellent sound quality) via sliders. The rating scale has five sections (poor: 0 to 20, fair: 21 to 40, good: 41 to 60, excellent: 61 to 100). The sound quality is evaluated in comparison with an unaltered, reference signal (MUSHRA sound quality = 100). The acoustic signals can be listened to in any order and as often as desired. The signals to be evaluated include a 'hidden reference' and one or more 'anchor signals' (e.g., typically low-pass filtered reference signals). The evaluation of the 'hidden reference' is used to detect untrained listeners who do not recognize the hidden reference as such. The 'anchor signal' is used to compare the audio signals to be evaluated with known audio qualities (comparability between experiments) and enables reproducible use of the entire MUSHRA scale. The ITU-R BS.1534-3 recommendation contains fixed specifications, such as a maximum number of nine audio systems to be evaluated (ITU-R 2015).

The MUSHRA has been used frequently and has adaptations that are discussed in the literature (CI-MUSHRA: Roy et al. 2012b, 'MUSHRA-simple' and 'MUSHRA-drag&drop': Völker et al. 2015). In the 'MUSHRA-drag&drop', the acoustic signals are displayed as boxes on a graphical user interface (GUI). The boxes are moveable along the horizontal MUSHRA scale (left: 0, right: 100). The reference signal is fixed on the scale at the value 100. The 'drag&drop' variant allows presorting of the acoustic signals in a ranking according to the sound quality and determining the exact value on the MUSHRA scale in a second step during fine adjustment. 'MUSHRA-drag&drop' is a combination of random access, categorical scaling and magnitude estimation (Völker et al. 2015).

2.5.1 Review of Cochlear Implant Sound Quality Measurements

As described in Section 2.5, sound quality is a subjective, multidimensional quantity (Zwicker et al. 2007). It describes the richness (Caldwell et al. 2017) or pleasantness of the sound (sound appraisal, Caldwell et al. 2017) of a CI as well as the deviation of the sound (Blauert et al. 1997) of a CI from that of a normal hearing ear. The sound quality of CIs depends on the electro-neural interface and is influenced by neural plasticity, as well as the memories and experiences of the individual (Section 2.4, Bernhardi et al. 2017; Dorman et al. 2022; Kral et al. 2016; McKay 2018). The ability to discriminate sounds (e.g., identification of musical instruments, identification of rhythm, pitch discrimination) with CIs could not be correlated with sound quality in previous studies (especially in music perception) and therefore does not serve as a measure of sound quality (Wright et al. 2012).

For this reason, questioning CI users themselves is the most commonly used method for recording sound quality (Roy et al. 2012b). Roy et al. (2012a) developed an adaptation of the MUSHRA, the 'CI-MUSHRA'. They used 5 seconds long musical

stimuli, of which seven versions with varying sound quality (high- and band-pass filtered) were created. The sound quality of the stimuli was rated via sliders on a MUSHRA scale from 0 (poor sound quality) to 100 (excellent sound quality) in comparison to the unaltered, reference stimuli. The procedures were performed with a CI group and a normal hearing control group to assess the ability to detect differences in sound quality. As a result, Roy et al. (2012a) reported that CI users reported significantly better sound quality on average than those with normal hearing did. However, caution should be exercised when interpreting these results. As the reference signal is fixed at 100 (excellent sound quality), this method captures the ability to detect small differences in sound quality rather than the sound quality perceived by CI users itself(Roy et al. 2012a).

In contrast questionnaires measure self-reported CI sound quality. The Hearing Implant Sound Quality Index (HISQUI_{19}) is a questionnaire validated on a large cohort ($n = 75$) to record sound quality in everyday situations (Amann et al. 2014). However, some of the HISQUI_{19} questions also ask for the ability to discriminate. (e.g., HISQUI_{19}: 'Can you effortlessly hear the ringing of the phone?', Amann et al. 2014).

In addition to questionnaires, methods from psychoacoustics, described in Section 2.5, are also used in CI research. For example, Gfeller et al. (2003) used a type of semantic differential with a visual analog scale to assess the likeability of sound samples by CI users. Questionnaires and measurements of the discrimination ability of CI users are well suited to record the auditory benefit of the CI. However, as summarized by Caldwell et al. (2017) in his nonsystematic review on sound quality, 'measures like these [...] do not offer an [...] insight into the richness of sounds heard through a CI relative to acoustic hearing'.

Some studies have investigated factors influencing self-reported CI sound quality via the HISQUI_{19} (Amann et al. 2014) questionnaire (Bessen et al. 2021; Mertens et al. 2020). Bessen et al. (2021) evaluated the self-reported CI sound quality of 60 CI users and reported on average, fair self-reported CI sound quality. The results showed that age at implantation has a slightly negative effect on self-reported CI sound quality and that CI experience has a slightly positive effect (Bessen et al. 2021). Although the importance of such questionnaires should not be doubted, it should be explicitly noted that self-reported CI sound quality is very subjective. Personal, emotional and psychological factors such as previous hearing experience, cognitive abilities or expectations may affect self-perceived CI sound quality (Amann et al. 2014). This means that an interindividual comparison to determine factors influencing sound quality via questionnaires or psychoacoustic methods is meaningful only to a limited extent.

Since people with SSD are also implanted with CIs, it is possible to make the CI sound audible for people with normal hearing (Section 2.4, e.g., Dorman et al. 2019a). Dorman et al. (2022) used questionnaires in addition to recording sound perception. The results showed that some CI users described the sound quality of their CIs with oppositional adjectives such as 'normal' and 'computer-like'. A comparison of the description of the CI sound with the generated sound samples also revealed major mismatches: some of the participants who described their CI sound as 'normal' required large modifications in the simulation to match the CI sound.

The mismatch between perception and description may be related to the subjective experience that 'normal' tends to mean 'well-known' (Dorman et al. 2022). This mismatch should be investigated further so that new methods for CI sound quality measurements that are not based on the subjective experiences and memories of CI users are reasonable.

One way to realize this would be an approach based on CI simulations (e.g., Dorman et al. 2019a). Assuming that CI simulations that are identical to the CI sound could be generated, the subjectivity of the CI user is greatly reduced. These sound samples could then be used to determine the CI sound quality perceived by normal hearing people using psychoacoustic methods (Section 2.5). Sound quality evaluations by normal hearing people also lead to variability in sound quality measurement by subjectivity (Roy et al. 2012b). However, this can be compensated with a suitable sample size (several study participants would rate the same sound sample) and study design (Das et al. 2016).

2.6 Radiological Evaluation of Cochlear Size and Electrode Array Placement

For postoperative success, correct intracochlear electrode array placement is essential (Mewes 2024). For quality assurance, most German clinics perform X-ray-based imaging (Vogl et al. 2015). These include, for example, planar X-ray images, computed tomography (CT) or cone-beam CT (CBCT, Vogl et al., 2015). The knowledge of incorrect electrode array placement (e.g., tip-foldover, scalar dislocations, incomplete insertion) influences processor programming (Section 2.3.1). Exemplary, a scalar dislocation often leads to increased charge consumption to generate an auditory perception (Trudel et al. 2018) and a tip-foldover can result in deactivation of single electrode contacts (Rader et al. 2016b; Zuniga et al. 2017).

With complication-free electrode array insertion and regular electrophysiological, intraoperative measurements, a planar X-ray image is typically sufficient to assess electrode array projection onto the cochlea (Cohen et al. 1996). However, scalar dislocations cannot be recognized from planar X-ray images. If intraoperative abnormalities are present, tomographic imaging is used to detect incorrect electrode array placement such as scalar dislocation (Alzhrani et al. 2024; Kopsch et al. 2024b). Tomographic imaging reconstructs cross-sectional images by combining planar X-ray projections from multiple angles through advanced computer algorithms (Buzug 2004). As CBCT involves less radiation exposure, fewer metal artifacts and better resolution than conventional CT does, CBCT is preferable to CT (Alzhrani et al. 2024; Knörgen et al. 2012).

In addition to monitoring correct intracochlear placement and quality assurance (determining the actual position to identify any subsequent electrode array migration), postoperative imaging is to determine the insertion depth of the electrode array (Aebischer et al. 2021; Mewes 2024). The insertion depth can be used for frequency electrode contact mapping in the individual to minimize the frequency-to-place mismatch (Section 2.4, e.g., Di Maro et al. 2022; Müller-Graff et al. 2024).

For this purpose, the software Otoplan[8] is used in current studies, which measures the size of the cochlea preoperatively, measures the insertion depth postoperatively and outputs an individual frequency map (anatomy-based fitting, e.g., Müller-Graff et al. 2024; Kurz et al. 2025).

In addition, initial work has shown that the insertion depth and various SCINSEV methods for recording the spread of electric fields are related (Aebischer et al. 2021; Schraivogel et al. 2023a; Schraivogel et al. 2023b; Schraivogel et al. 2024; Sehlmeyer et al. 2024). Dorman et al. hypothesized that the length of the electrode array, and thus the insertion depth, influences sound perception (Dorman et al. 2022; 2024). The authors examined CI users with shorter (active length: 15.0 mm, full length: 18.5 mm, Advanced Bionics AG 2022; Dhanasingh et al. 2024) and longer electrode arrays (active length: 23.1 mm, total length: 28 mm, Med-El 2012). They reported that CI users with shorter electrode arrays perceive their CI higher pitched than CI users with longer electrode arrays (Section 2.4.1, Dorman et al. 2022; 2024).

The insertion depth depends on the electrode array design (e.g., mechanical properties), the surgical technique and the size of the cochlea (Franke-Trieger et al. 2014). As briefly mentioned in Section 2.3, CI manufacturers offer electrode arrays with different lengths. The lengths of currently available electrode arrays are between 15 mm and 34 mm (total length, Med-El 2012). The elastic properties of electrode arrays also vary. Pre-curved, stiffer electrode arrays lie close to the cochlear axis, and the modiolus (perimodiolar electrode arrays) and straight electrode arrays lie close to the outer wall of the cochlea (lateral wall electrode arrays, Dhanasingh et al. 2024). Both the length of the electrode array and the curvature, and thus the intracochlear trajectory that the electrode array follows, influence the insertion depth.

2.6.1 Cochlear Size

Various parameters can be used to describe cochlear size, e.g., diameter, width, height or cochlear duct length (CDL). These parameters can either be recorded ex vivo using a histology section or in vivo via radiological imaging techniques (Müller-Graff et al. 2024). Either a 3D reconstruction or reconstructions of the axial, coronal and sagittal view of the cochlea can be used to measure the cochlea from routine, preoperatively recorded tomographic images (Figure 2.8, Müller-Graff et al. 2024). The diameter, width and height are assigned capital letters A, B and H (Escudé et al. 2006; Müller-Graff et al. 2024).

Figure 2.8 shows exemplary measurements of A, B and H in the software Otoplan[8]. To determine these quantities with the smallest possible systematic measurement error, the correct view is necessary. In the 'cochlear view', the view is directed parallel to the modiolus and the full, basal turn is shown (Marsh et al. 1993; Xu et al. 2000). The diameter of the basal turn A corresponds to the largest distance between the center of the round window and the lateral wall measured in the cochlear view (Marsh et al. 1993; Xu et al. 2000). The width of the basal turn B is measured perpendicular to the diameter A and corresponds to the distance from the inferior to the superior point of the cochlea in the sagittal view (Escudé et al. 2006). The

[8]Otoplan, Cascination AG, Bern, Switzerland in cooperation with MED-EL, Innsbruck, Austria

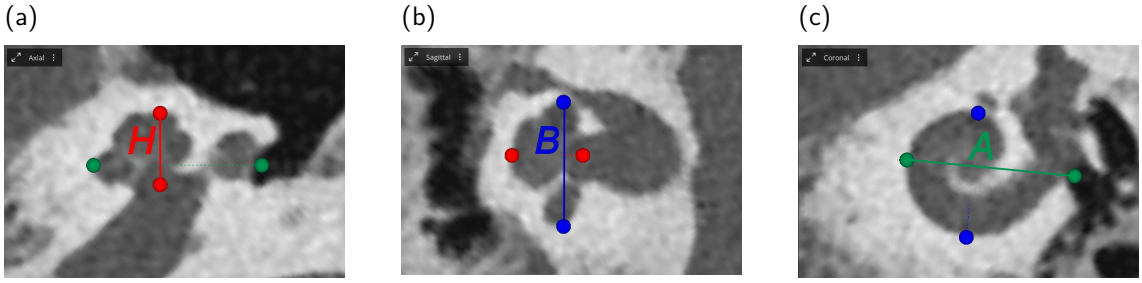

Figure 2.8: Cochlear size measurement. Screenshots from the software Otoplan (Cascination AG 2024, Bern, Switzerland in cooperation with MED-EL, Innsbruck, Austria, version 3.0.0). Red markers indicate height (H), blue markers indicate width (B), and green markers indicate diameter (A). (a) Computed tomography (CT), axial multiplanar reconstruction. (b) CT, sagittal multiplanar reconstruction. (c) CT, coronal multiplanar reconstruction ('cochlear view').
Radiological data were made available with the kind permission of Prof. Kösling (Department of Radiology, Martin Luther University Halle-Wittenberg, University Medicine Halle, Halle, Germany).

height H measures the distance from the base to the apex of the cochlea in the axial view (Mertens et al. 2020).

The CDL generally describes the length of the scala media or the organ of Corti. As seen in the review by Koch et al. (2017), the definitions of the CDL differ in the literature. For example, Alexiades et al. (2015) defined the CDL starting at the round window, whereas Hardy (1938) considered the full length of the organ of Corti. Different equations for the CDL based on spiral or elliptical models are derived in earlier studies (e.g., Escudé et al. 2006; Mertens et al. 2020). For example, the CDL is calculated via Equation 2.7 in the software Otoplan[9]. It considers the full length of the organ of Corti and is calculated from the diameter A and the width B in mm.

$$\mathrm{CDL} = 2.02 \cdot A + 4.60 \cdot B - \sqrt{2.11 \cdot (A - 1\,\mathrm{mm}) \cdot (B - 1\,\mathrm{mm})} - 3.94\,\mathrm{mm} \quad (2.7)$$

CDLs between 25.3 mm (Hardy 1938) and 46.8 mm (Di Maro et al. 2022) have been reported in previous studies (Müller-Graff et al. 2024). This large variability is partly due to the variation in size between individuals, but also, as described above, caused by different measurement and calculation methods (Hardy 1938; Müller-Graff et al. 2024).

2.6.2 Electrode Array Insertion Depth

The insertion depth can be specified as a linear length or angle value in mm or °, respectively (Aebischer et al. 2021; Franke-Trieger et al. 2014). The insertion angle can be determined both from tomographic images and from planar X-ray images (Kong et al. 2012). The cochlea should be shown in both variants in the 'cochlear

[9] Otoplan, Cascination AG, Bern, Switzerland in cooperation with MED-EL, Innsbruck, Austria, version 3.0.0

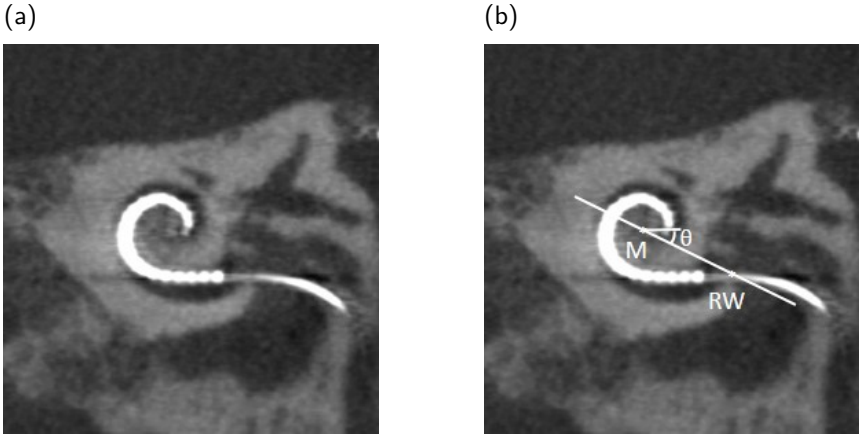

Figure 2.9: Cochlear implant electrode array insertion angle measurement via cone-beam computed tomography (CBCT) coronal thick-sliced maximum intensity projection (MIP) (a) without and (b) with markers and reference lines for insertion angle measurement. M: modiolus, RW: round window, Θ: insertion angle
Radiological data were made available with the kind permission of Prof. Kösling (Department of Radiology, Martin Luther University Halle-Wittenberg, University Medicine Halle, Halle, Germany).

view' (Figure 2.8c). A coordinate system is constructed with anatomical structures as markers. The reference line (0 °, multiples of 360 °) corresponds to the connecting line between the round window and the modiolus. The angle is measured relative to this reference line up to the tip of the electrode array. As the tip of the electrode array is often difficult to visualize in imaging, the insertion angle is measured at the most apical electrode contact (Cohen et al. 1996; Mertens et al. 2020; Xu et al. 2000). Figure 2.9 shows an example of the reconstruction of the 'cochlear view' and the measurement of the insertion angle via a CBCT dataset.

In contrast, the round window and the modiolus cannot be imaged in planar X-ray images (Figure 2.11a). Marsh et al. (1993), Cohen et al. (1996), and Xu et al. (2000) developed a method to determine the insertion angle from planar X-ray images. The associated X-ray technique is called 'modified Stenver view' and is used to obtain the cochlea in the 'cochlear view' (Figure 2.10). The patient rotates the head so that the head (midsagittal plane) and the X-ray detector enclose an angle of 50 ° (for further information, see Xu et al. 2000, Figures 2.10 and 2.11). The round window is approximated by the intersection of the line connecting the apex of the superior semicircular canal and the centrum of the vestibule with the electrode array. The modiolus is approximated as the center of the electrode array trajectory (Figure 2.11b, Mewes 2024; Svrakic et al. 2015; Xu et al. 2000).

The measurement of insertion angles is influenced by various factors, such as image resolution, metal or motion artifacts and contrast (e.g., Figure 2.13a, Ishiyama et al. 2020; Wang et al. 2019). For planar X-ray images, the projection angle/technique influences the measurement of insertion angles (e.g., Figures 2.10, 2.13b and 2.12, Svrakic et al. 2015).

According to Xu et al. (2000), a fixed projection angle of 50 ° between the head

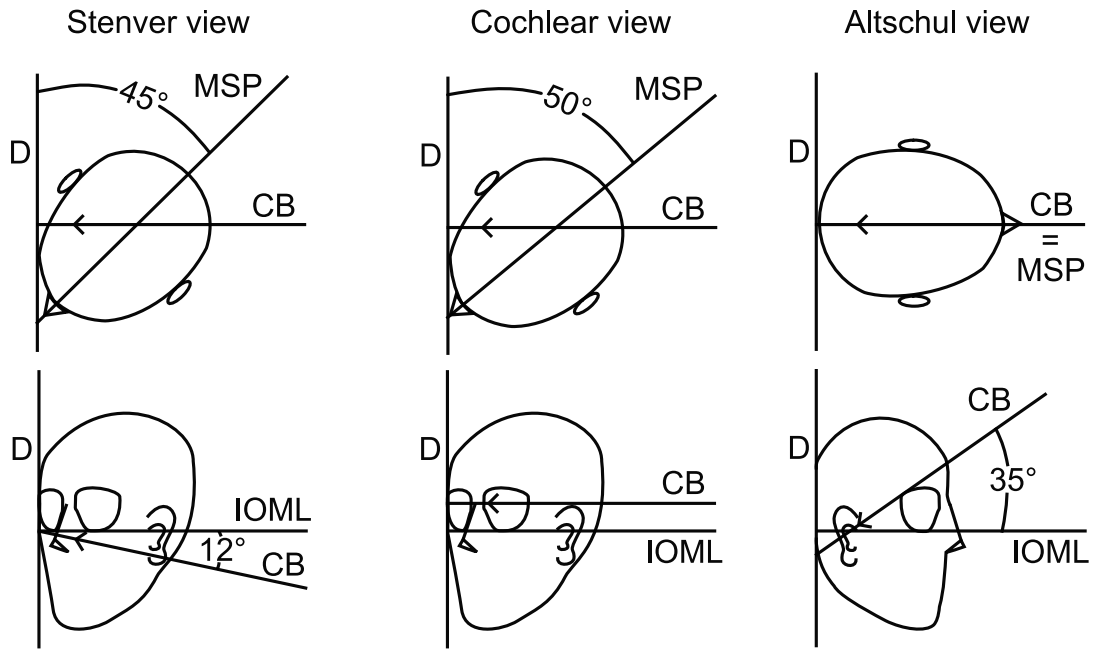

Figure 2.10: Schematic representation of acquisition angles for planar X-ray imaging techniques in Stenver, cochlear and Altschul view (Xu et al. 2000; Brusis et al. 1984).
D: detector, MSP: midsagittal plane, CB: central beam, IOML: infraorbitomeatal line (connecting line of the inferior margin of the orbit to the superior margin of the external auditory canal, Brusis et al. (1984)).

(midsagittal plane) and the X-ray detector is required for the cochlear view (Figure 2.10). Deviations from this angle are possible due to patient-related positioning problems (e.g., non-compliant people, patients cannot hold the head in the desired position) or measurement errors (e.g., random errors, less experienced radiographers). In addition, some clinics use different or non-standardized imaging techniques (Harris et al. 2011; Svrakic et al. 2015), which results in variable radiographic projection angles between the midsagital plane and the X-ray detector (e.g., Stenver view: 45 °, Figure 2.10) or the infraorbitomeatal line (IOML, connecting line of the inferior margin of the orbit to the superior margin of the external auditory canal, Brusis et al. (1984)) and the central beam (e.g., Stenver view: 12 °, Altschul view: 35 °, Figures 2.12 and 2.10, Brusis et al. 1984). Deviations in the projection angle from the cochlear view are evident, for example, in the representation of the superior semicircular canal. When X-rayed in the cochlear view, the superior semicircular canal appears only as a striped shadow, and deviations in the projection angles lead to a projection as a looped shadow (Figure 2.11 or 2.12, Marsh et al. 1993).

The effect of variable angles between the central beam and the midsagittal plane was investigated by Svrakic et al. (2015). A high-resolution CT image of an implanted temporal bone was recorded. From this, planar (2D) images were reconstructed from different angles to simulate different angles between the central beam and the midsagittal plane. The authors reported that systematic errors of up to 8 % are caused by the projection angle, which is, however, on the order of magnitude of the interrater variability (Svrakic et al. 2015).

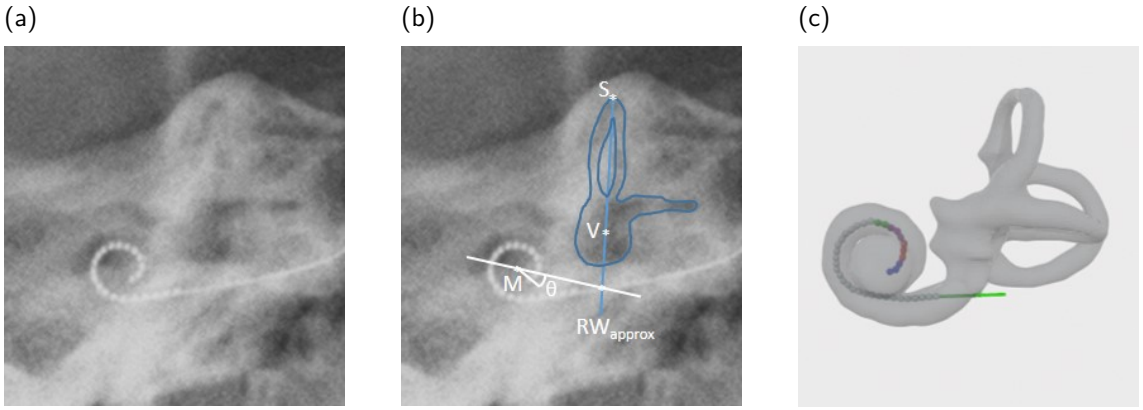

Figure 2.11: Cochlear implant electrode array insertion angle measurement in planar X-ray image in Stenver view (a) without and (b) with markers and reference lines for insertion angle measurement. The vestibular organ is contoured in blue. (c) 3D reconstruction of an inner ear, approximately at projection angles of (a) and (b) for visual assistance in interpreting (a) and (b). Not all three semicircular canals are visible in (a) and (b). M: modiolus, S: superior semicircular canal, V: vestibule, $\mathrm{RW}_{\mathrm{approx}}$: round window approximation according to Marsh et al. (1993), Cohen et al. (1996), and Xu et al. (2000), Θ: insertion angle
Radiological data were made available with the kind permission of Prof. Kösling (Department of Radiology, Martin Luther University Halle-Wittenberg, University Medicine Halle, Halle, Germany).

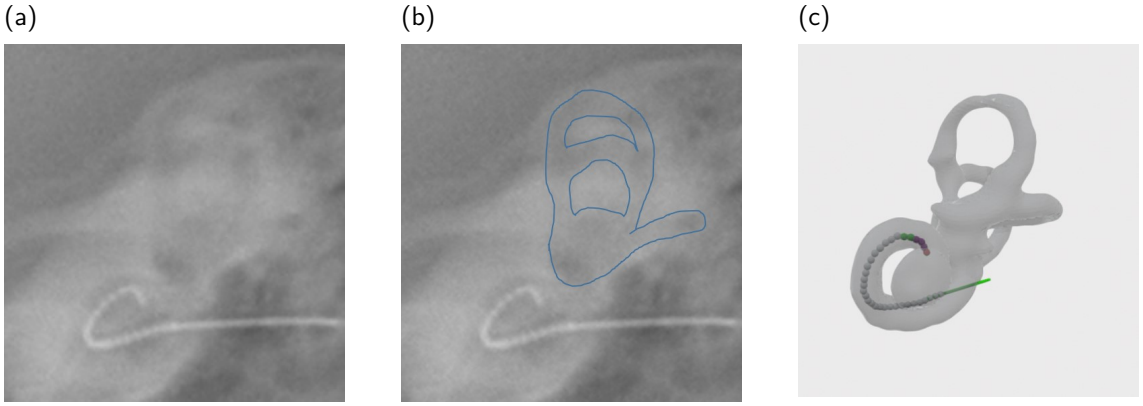

Figure 2.12: X-ray image in Altschul view (a) without and (b) with markers. The vestibular organ is contoured in blue. (c) 3D reconstruction of an inner ear, approximately at projection angles of (a) and (b) for visual assistance in interpreting (a) and (b).
Radiological data were made available with the kind permission of Prof. Kösling (Department of Radiology, Martin Luther University Halle-Wittenberg, University Medicine Halle, Halle, Germany).

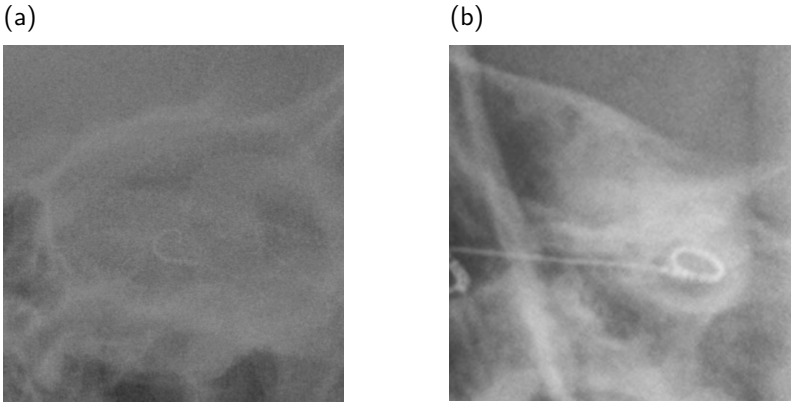

Figure 2.13: Examples of planar X-ray images not suitable for insertion angle measurement according to Marsh et al. (1993), Cohen et al. (1996), and Xu et al. (2000), Figure 2.11. (a) A coordinate system constructed with the anatomical structures as markers is not possible: Vestibular organ not viewable. (b) Last electrode contact not viewable due to deviating X-ray exposure angle.
Radiological data were made available with the kind permission of Prof. Kösling (Department of Radiology, Martin Luther University Halle-Wittenberg, University Medicine Halle, Halle, Germany).

3 Experimental Validation and Optimization of Cochlear Implant Simulations

3.1 Background Information

As introduced in Section 2.4, the sound of a CI can differ greatly from that of a normal hearing ear. Thus, extensive consultation is important to ensure the patients' acceptance to the unfamiliar sound impressions, to improve family members' sympathy for the patients' situation and to strengthen family support. In addition, CI candidates often ask for the sound of a CI and fear an unfamiliar sound, which can make them hesitant about important hearing restoration. Presenting CI simulations to patients and their family members could assist with technical and medical consulting.

To date, as described in Section 2.4.1, only English-language CI simulations for devices with 12 and 16 electrode contacts with longer (active length: 23.1 mm, total length: 28 mm, Med-El 2012) and shorter (active length: 15.0 mm, full length: 18.5 mm, Advanced Bionics AG 2022; Dhanasingh et al. 2024) electrode array lengths have been reported (Dorman et al. 2017; 2019; 2020; 2022). Dorman et al. (2019b) concluded that CI users with longer electrode arrays required fewer or less modifications in simulations to replicate the CI sound than CI users with shorter electrode arrays did. The participants with shorter electrode arrays showed a greater upward shift in pitch perception than those with longer electrode arrays did. The authors explained this by a larger frequency-to-place mismatch in the participants with shorter electrode arrays (Section 2.4).

Several studies have shown that CI sound can change with CI experience (Bessen et al. 2021; McDermott et al. 2009; Reiss et al. 2007). For example, McDermott et al. (2009) reported a decreasing pitch with increasing CI experience. However, as introduced in Section 2.4.1, Dorman et al. (2022) reported that pitch perception did not change in the first 3 years of CI experience for CI users with shorter (active length: 15.0 mm, full length: 18.5 mm, Advanced Bionics AG 2022; Dhanasingh et al. 2024) electrode arrays. This could be due to inhomogeneity in CI experiences during study visits (first visit between 3 and 20 months, second visit between 17 and 47 months, Dorman et al. 2022, Section 2.4.1).

A homogenization of the CI experience across study visits could lead to a measurable effect of the CI experience on the CI sound. For example, in Germany, rehabilitation lasts approximately 2 years (Präsidium der DGHNO-KHC 2021), during which CI users learn to interpret and understand the signals transmitted by the CI (neuronal

plasticity, Section 2.4). The rehabilitation period is divided into two phases on the basis of CI experience: 'basic therapy' (from the first postoperative day until the sixth week) and 'follow-up therapy' (from the sixth week up to 2 years). These involve routine control visits at fixed times (usually: 1, 3, 6, 12 and 24 months after initial activation) in the implantation and rehabilitation clinic. After the completion of rehabilitation, lifelong 'aftercare' ($>$ 2 years) follows (Präsidium der DGHNO-KHC 2021).

This chapter presents the first approach to create German-language CI simulations for devices with 22 electrode contacts. In addition, the CI sound in the three phases of rehabilitation (basic therapy, follow-up therapy and aftercare) are recorded via CI simulations. The simulations are created on the basis of one sentence. A further aim was to investigate whether the application of the CI simulation parameters to two other sentences still approximates the CI sound.

3.2 Materials and Methods

A prospective, non-interventional, experimental study consisting of two study parts was conducted with adult SSD CI users. All study measurements were performed at the Department of Otorhinolaryngology, Head and Neck Surgery at the University Hospital Halle (Saale), Germany, between August 2022 and January 2024. The ethical review board of University Medicine Halle approved the study protocol and the informed consent forms according to the Declaration of Helsinki with approval number 2022-048. Informed consent forms for participation were obtained from all study participants.

All study participants were adult CI users with Nucleus[10] devices (CIx22, CIx12, CIx32 or CI24RE(CA)) in which at least 19 electrode contacts were activated. A further inclusion criterion was contralateral pure-tone hearing thresholds for air-conduction, averaged over 0.5, 1, 2, and 4 kHz (four frequency pure tone average, 4PTA) not worse than the age- and sex-related 95th percentiles according to DIN EN ISO 7029 (2017). In addition, the study participants were native German speakers and their CI indication was acquired postlingually. Pregnant persons and persons who were unable to understand the study procedure or who did not consent to participate in the study were excluded from the study.

3.2.1 Longitudinal Study during the First 6 Months of CI Experience

The first part of the study was a longitudinal, hypothesis-generating multiple case study. For this purpose, a case series with five participants was planned. This part of the study comprised two study visits. At the first visit, the participants had a maximum CI experience of 5 days. The second visit was at the routine 6 month follow-up, 5 to 7 months after the first visit.

[10] Cochlear Ltd., Sydney, Australia

3.2.2 Cross-Sectional Study After at Least 2 Years of CI Experience

The second part of the study had a cross-sectional study design, consisting of one study visit at which the participants had at least 2 years of CI experience. An additional inclusion criterion was that participants had a word recognition score of at least 50 % in the Freiburg monosyllable test (Hahlbrock 1953) in open sound field with frontal presentation at 65 dB SPL (sound pressure level, SPL) in previous tests. The sample size calculation is based on the results of earlier studies (Dorman et al. 2020) and an assumption of a standard deviation (SD) of the primary endpoint of 1.5 (similarity score). Including a drop out of three participants, this results in a sample size of 15 participants under the requirement of determining the mean value with a 95 % confidence interval and a confidence interval length of 2.0 (Dhand et al. 2014).

3.2.3 Procedures

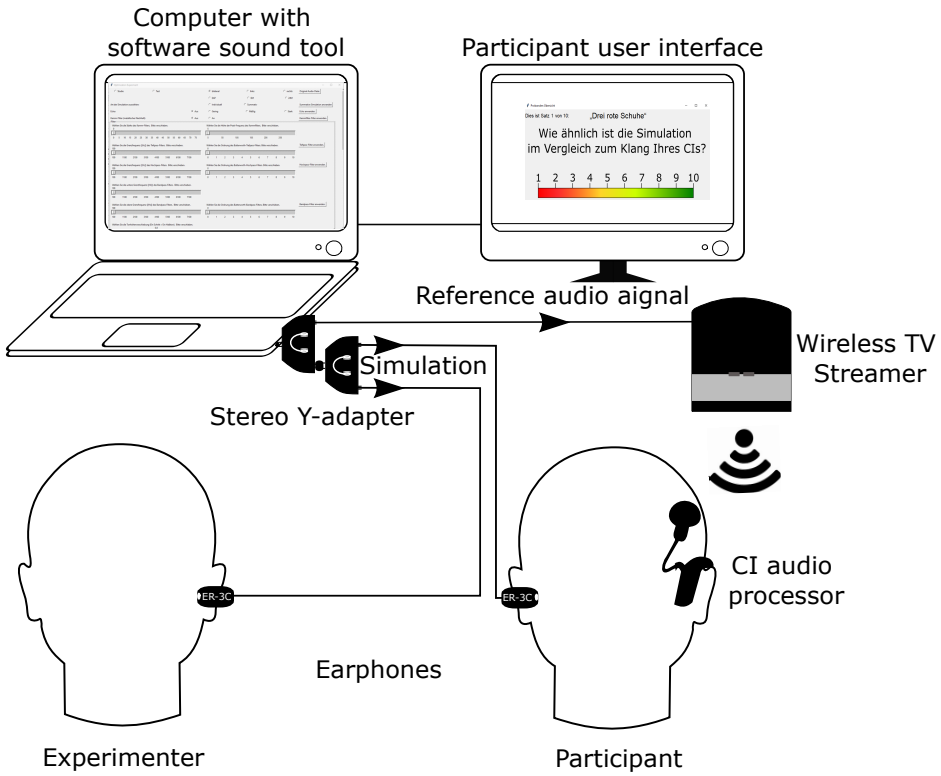

Figure 3.1: Experimental set-up to create CI simulations.

The experimental set-up for creating the CI simulations is illustrated in Figure 3.1. The study measurements were performed in a quiet room. The participants heard an unprocessed speech signal ('reference') via their CI. Therefore, a wireless TV streamer[11], which transmits a stereo signal, was connected to the computer and to the participants' CI. A modified version of the reference signal was presented on the contralateral, age-appropriate normal hearing ear via an insert earphone[12]. In

[11] Cochlear Ltd., Sydney, Australia
[12] ER-3C, Etymotic Research Inc., Elk Grove Village, USA

the following, the modified version is referred to as 'simulation'. The participants' task was to rate the similarity of both signals (simulation vs. reference) on a visual analogue scale from 1.0 (= no similarity) to 10.0 (= signals are identical) in steps of 0.5. The experimenter heard the simulation via a second insert earphone[13] and led through the study. The participants watched supporting materials (the visual analogue scale, an adjective list, written sentences to read along) on a display.

The Oldenburg children's sentence test (['Oldenburger Kinder-Satztest'], OlKiSa, 1st test list: the first 10 sentences, Wagener et al. 2005), whose sentences consist of three words (number, adjective, object), was used as speech material. The sentences used are listed in Table A2 in the Appendix. The study procedure was performed with the processor-setting of the everyday use.

In a preliminary talk, the study tasks and study consent were explained to the participants. Social activity level ('How many times in the last 7 days have you met friends or talked to friends on the phone for more than 5 minutes?'), and the occupation was queried for later characterization of the study cohort (Li et al. 2016). The participants were also asked for a subjective description of the sound of their CI.

Training Task

Before starting the study tasks, the participants completed a training task. The training task consisted of a short version of the first study task. During this task, the sound volume of both signals was individually set to a subjectively comfortable level and it was ensured that the participant understood the study task and was able to perform it. Furthermore, it introduces the participants to the simulations and the use of the similarity score scale. Afterwards, three study tasks were performed.

Ranking Experiment

In the first task, the ranking experiment, participants alternately heard a reference speech signal on the CI ear and one of 100 simulations on the contralateral ear. After each pair of signals, the participant rated the similarity of both signals on the scale ranged from 1.0 to 10.0. Each of the ten sentences of the OlKiSa (Table A2, Wagener et al. 2005) was simulated with each of the ten parameter sets from Table 3.1. The parameter sets were created on the basis of previous studies (Dorman et al. 2020; Peters et al. 2018). Participants could listen to the signal pairs as often as desired. The simulations for each sentence were presented in a randomized order. The participants could read the sentences on the participant user interface (Figure 3.1) to avoid evaluating speech recognition instead of sound similarity. The presentation of the speech signals and the documentation of the similarity scores were controlled via a GUI developed for this purpose (Figure 3.2). The GUI exported the acquired data automatically to Microsoft Excel[14] for data storage. After rating all 100 simulations, the software generated a boxplot representing the similarity scores as a function of the parameter set. The parameter set with the largest median similarity score was used for the second study task.

[13] ER-3C, Etymotic Research Inc., Elk Grove Village, USA
[14] Excel, Microsoft Corporation, Mircosoft Office Professional Plus 16

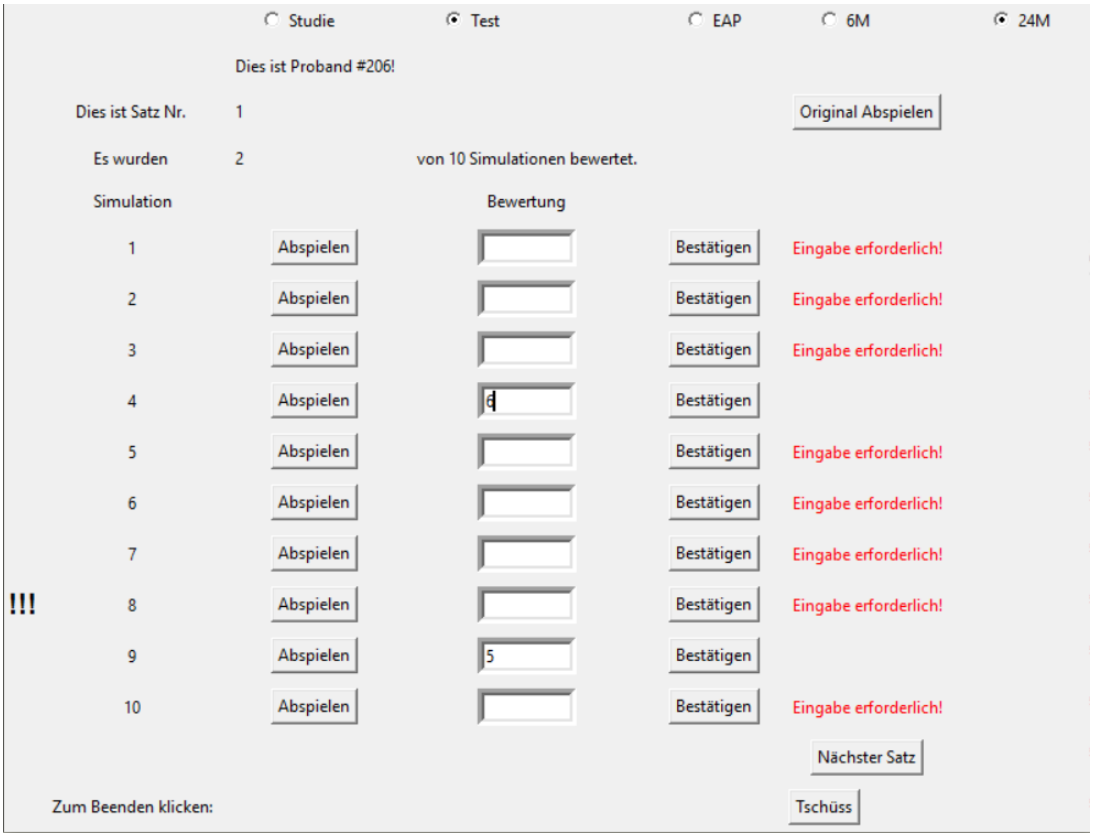

Figure 3.2: Screenshot of the graphical user interface (GUI) for the ranking experiment. The three exclamation points mark the next simulation to be played for randomized presentation.

Table 3.1: Simulation parameter sets for the ranking experiment. Each parameter set was applied to each of the ten test sentences (Table A2).

No.	Parameter
1.	Band-pass filter: 4th order, $f_c = 188\,\mathrm{Hz}$ and $7938\,\mathrm{Hz}$
2.	High-pass filter: 4th order, $f_c = 1000\,\mathrm{Hz}$
3.	Low-pass filter: 4th order, $f_c = 1000\,\mathrm{Hz}$
4.	Comb filter: $Q = 30$, $f_0 = 60\,\mathrm{Hz}$
5.	Frequency/pitch shift: $f_s = 300\,\mathrm{Hz}/4$ semitones; overmodulation: factor $= 2.5$
6.	BP-vocoder: carrier = sine, $m = 8$, SOE-order = 4
7.	BP-vocoder: carrier = noise, $m = 8$, SOE-order = 4
8.	FFT-vocoder: carrier = sine, $n = 8$, SOE-order = 4
9.	FFT-vocoder: carrier = noise, $n = 8$, SOE-order = 4
10.	BP-vocoder: carrier = sine, $m = 8$, SOE-order = 4; pitch shift: $f_s = 10$ semitones

BP: band-pass, FFT: fast Fourier transform, SOE: spread of excitation, f_c: cutoff filter frequency, Q: quality factor, f_0: fundamental frequency, f_s frequency shift, m: number of frequency bands, n: number of selected frequency bands with the largest energy.

Opimization Experiment

Figure 3.3: Screenshot of the graphical user interface (GUI) for the optimization experiment.

In the second task, the optimization experiment, the simulation, which had the largest median similarity score over all sentences from the ranking experiment, served as a starting point for an optimization procedure similar to that described by Dorman et al. (2020). The optimization was performed for the sentence 'drei rote Schuhe' ['three red shoes'] (Wagener et al. 2005). The experimenter asked the participants how the simulation should be changed to make it sound more similar to the CI sound. A list of adjectives (Appendix: Table A3) assisted the participants in describing the CI sound. The simulation was modified according to the participants' response via the software sound tool GUI (Figure 3.3). This optimization procedure was repeated until no further improvement in similarity was subjectively achieved. Finally, the similarity score of the optimized simulation was recorded. In addition, the participant was asked for suggestions on how the simulation could be improved to evaluate the limitations of the perception of a signal transmitted through a CI.

Application Experiment

In the third task, the application experiment tested the effect of the sentences used. The parameter set of the optimized simulation was applied to two further sentences ('vier nasse Autos', ['four wet cars'] and 'neun weiße Tassen' ['nine white cups'], Wagener et al. 2005). As in the previous tasks, the simulated and reference sentences were presented, and the similarity score was rated by the participants. The participants in the 'Longitudinal Study during the First 6 Months of CI Experience' (Section 3.2.1), who participated at repeated measurements, additionally evaluated the optimized simulations from their first visit during their second visit.

3.2.4 Signal Processing

GUIs (Figures 3.2 and 3.3) were programmed for the experiments described in Section 3.2.3. Therefore, and for signal processing, the programming language Python[15] in the integrated development environment Spyder[16] was used. The Python package TkInter[17] was used to create the GUI. The Python library SciPy[18] (function: io.wavfile.read) was used to read audio WAVE files for the following processing steps. The input signal was digitized with a sampling rate of 44.1 kHz. After signal processing, the data were converted into a PCM format and saved as a WAVE file (Section 2.1.1, SciPy, Virtanen et al. 2020, function: io.wavfile.write). The library Winsound[19] (function: PlaySound) was used to play WAVE files.

Normalization

To generate a comfortable and consistent loudness in processed signals, a level normalization was inserted. A RMS normalization was performed according to Section 2.4.2 (Cychosz et al. 2024). Therefore, the RMS of the complete audio signal was calculated (Equation 2.6). The scaling factor was set to the maximum factor by which the audio signal can be scaled without inducing clipping. The normalization function was applied after each signal processing step except for the clipping function.

Low-, high-, band-pass filter

A Butterworth low-pass, high-pass and band-pass filter (Section 2.1.1, Figure 2.1) was implemented by using the Python library SciPy[18] (functions: scipy.signal.butter and scipy.signal.lfilter). The GUI offers the option to choose the order (first to 10th) and the cutoff frequency (between 0 and 8 kHz). This corresponds to the frequency range of CI signal coding strategies (Section 2.3.1, Appendix: Table A1).

The low-pass filter has a damped sound. The sound of a high-pass filtered signal is less voluminous and far away. The sound of the band-pass filtered signal was a combination of low- and high-pass filters.

Comb filter

A peaking comb filter (Section 2.1.1, Figure 2.1) was implemented by using the Python library SciPy[18] (functions: scipy.signal.iircomb and scipy.signal.lfilter). Since the fundamental frequency f_0 must be a divisor of the sampling frequency and meet the Nyquist theorem 2.3 ($f_0 < f_s/2 = 22.05\,\text{kHz}$ with $f_s = 44.1\,\text{kHz}$), the GUI gives the option to set f_0 between 1 Hz and 14.7 kHz. To generate a variety of sounds, the quality factor Q can be changed between 5 and 300.

[15]Python, van Rossum (1991), version 3.9.7
[16]Spyder, Raybaut (2009), version 5.1.5
[17]TkInter, Lundh 1999 version 8.6
[18]SciPy, Virtanen et al. (2020), version 1.7.1
[19]Winsound,Python Software Foundation (2016)

Depending on the parameters f_0 and Q, the sound of a comb filter ranges from echo-like, reverberant, metallic to sharp. It mimics the processing of a CI in that a comb filter transmits individual frequency bands such as a CI.

Pitch shift

The pitch of the audio signal was shifted by using the Python wrapper PyRubberband[20] (function: pitch_shift). The GUI gives the option to shift the pitch between 0 and 15 semitones in both directions (step-size = 1 semitone, toward larger or lower frequencies). Changing the pitch to larger frequencies can create, e.g., sound impressions such as a voice of a cartoon character, and mimic the frequency-to-place mismatch in cochlear implantation (Eisner et al. 2010).

Frequency shift

A frequency shift of the spectrum up or down by a fixed frequency was implemented by first calculating the DFT (Equations 2.4, Section 2.1.1) with the library NumPy[21] (functions: numpy.fft.rfft and numpy.fft.irfft). The DFT is shifted by the chosen frequency selected on the GUI. Afterwards, the inverse of the DFT (Equation 2.5) is calculated. The frequency to be shifted can be set between −30 and +300 Hz. By shifting the spectrum toward larger or smaller frequencies the harmonic relations are destroyed, and a disharmonic high- or low-frequency sound occurs.

Clipping

The audio signal is multiplied by a factor that is set by the GUI. The factor is between 1.0 (no clipping) and 20 (very strong clipping). By choosing the data type as an integer with a bit size of 16, the signal was clipped. This leads to an overmodulated sound impression with a sizzling noise.

Fast Fourier Transform-Vocoder

An FFT-vocoder, as described in Section 2.4.2 (Figure 2.7), was implemented. The signal was downsampled to a sampling rate of 16.0 kHz with the Python package Librosa[22] (functions: resample). A pre-emphasis was implemented by applying a 1st-order high-pass filter with a cutoff frequency of 4 kHz (Chung et al. 2011). The FFT-filter-bank was implemented by calculating the STFT (Section 2.1.1) of the signal by using the Python library SciPy[23] (function: scipy.signal.stft). Further signal processing corresponded to that described in Section 2.4.2. The upper and lower cutoff frequencies of the frequency bands were selected according to the default setting of the ACE[24] strategy (Section 2.3.1, Appendix: Table A1, Peters et al. 2018). The n ($n \in [1, 22]$) bands for the n-of-m algorithm were set via the GUI. The overlap-and-add procedure for temporal envelope reconstruction was performed by

[20] PyRubberband, McFee et al. (2015), version 0.3.0
[21] NumPy, Harris et al. (2020), version 1.20.3
[22] Librosa, McFee et al. (2022), version 0.9.1
[23] SciPy, Virtanen et al. (2020), version 1.7.1
[24] Custom Sound Pro Software, Cochlear Ltd. (2022b), Sydney, Australia, version 7.0

using the Python library TensorFlow[25] (function: tensorflow.signal.overlap_ and_ add).

The GUI provided the option to choose between a noise- or sine-carrier. Band-pass filtered Gaussian noise was generated as a noise-carrier, and the GUI offered the option of variable spread of excitation. A steep, moderate and flat slope of the filter (e.g., 4th, 2nd and 1st-order) corresponds to a weak, moderate and broad simulated spread of excitation (Cucis et al. 2021; Fu et al. 2005; Mehta et al. 2017). The modulated signal was upsampled to 44.1 kHz with the Python package Librosa[26] (function: resample).

Band-pass-Vocoder

A BP-vocoder (Figure 2.5) as described in Section 2.4.2 was implemented. Resampling and pre-emphasis was implemented as in the FFT-vocoder. To calculate the frequency-bands a band-pass-filter-bank was used. 4th-order Butterworth filters (SciPy[27], functions: scipy.signal.butter and scipy.signal.lfilter) were used. The signal was divided into m frequency bands, whereby m was set via the GUI ($m \in [1, 22]$). The filter-bank consisted of logarithmically spaced cutoff frequencies (Mehta et al. 2017). The amplitude envelopes were computed by low-pass filtering of the half-wave rectified signals of the m frequency bands (Fu et al. 2005). Therefore, a 4th-order Butterworth filter with a cutoff frequency of 160 Hz was used (Fu et al. 2005). The carrier type (sine or noise) and the simulated spread of excitation (weak, moderate or broad) could be selected via the GUI as for the FFT-vocoder.

Echo

An echo was created by adding the reference and a time-shifted audio signal. The GUI gives the option to choose no (0 ms), little (10 ms), medium (30 ms) or strong (90 ms) delay between the superposed signals.

Concatenation

The GUI offers the option to concatenate several signal processing steps. If the option was selected, all processing steps that were activated were applied to the audio signal successively. The concatenation function was implemented by applying one processing function on the output of another processing function until all processing functions that were activated were applied. The order of application of the processing steps is listed in Table A4 in the Appendix.

3.2.5 Data Analysis

Data analysis was performed using the software SPSS[28]. The data were analyzed descriptively by calculating the means, medians and SDs. The level of significance

[25] TensorFlow, Abadi et al. (2015), version 2.8.0
[26] Librosa, McFee et al. (2022), version 0.9.1
[27] SciPy, Virtanen et al. (2020), version 1.7.1
[28] SPSS, IBM (2021), version 28.0.0.0

was set to 0.05 for all the statistical tests. Bonferroni correction was used for post hoc comparisons. A visual inspection was used for testing data for normal distribution. Wilcoxon signed-rank tests were performed to examine the effect of time between the first visit and second visit in the ranking experiment on similarity scores. The symmetry of distribution was confirmed via visual inspection.

The effects of the sentence and simulation parameter sets on the similarity score in the ranking experiment for participants with at least 2 years of CI experience were calculated via repeated measures analysis of variance (ANOVA). The Greenhouse–Geisser adjustment was used to correct for violations of sphericity. The homogeneity of variance of the data was confirmed visually.

Wilcoxon signed-rank test was performed to determine the effect of simulation optimization compared with the ranking experiment on similarity scores. The simulation parameter set that produced the best median similarity score for sentence 1 (the sentence used in the optimization experiment), and the median of the best similarity scores for sentence 1 in the ranking experiment for each participant individually, was investigated. The symmetry of distribution was confirmed via visual inspection.

The Friedman test followed by sign tests were used to calculate the effect of sentences on similarity scores during the application experiment. The software Prism[29] and Inkscape[30] were used for visualization.

3.3 Results

3.3.1 Longitudinal Study during the First 6 Months of CI Experience

This case series included five participants (three male, two female). All the participants completed all the measurements. The first study visit took place 4 days after implant activation for all participants. The time between the first visit and second visit ranged from 172 days ($\approx$ 5.7 months) to 202 days ($\approx$ 6.6 months, median: 187 days $\approx$ 6.2 months). In the following, the first visit is referred to as the '4d-visit', and the second visit after approximately 6 months is referred to as the '6m-visit'. During the 4d-visit, the participants were aged between 35 and 65 years (median: 48 years). All 22 electrode contacts were activated for all participants at the 4d-visit. At the 6m-visit, three apical electrode contacts were deactivated in participant #102. All participants used the ACE strategy with $n = 8$. The participants' characteristics are summarized in Table 3.2.

Figure 3.4 shows the similarity scores for each participant for the 100 simulations in the ranking experiment. The variation in the similarity scores varied with the participant as well as with the parameter set and the sentence used. The similarity scores in the ranking experiment for each participant were not normally distributed, as assessed by visual inspection. The median of each participant for both visits is given in Figure 3.4. The median similarity score changed for all participants except

[29]Prism, GraphPad Software (2020), version 8.4.3
[30]Inkscape, Inkscape Community (2003), version 1.2

Table 3.2: Characteristics of the participants at the first (4 days after implant activation) and second (6 months after implant activation) study visit.

ID	Sex/ CI ear	Age/DoD [years]	Implant/ Processor	WRS [%] 4d/6m	4PTA [dB] 4d/6m	Etiology	Occupation	Socializing* 4d/6m
#101	m/l	50/0.9	CI632/ N7	35/45	11.3/13.8	ISSNHL	fotographer	5/5
#102	m/l	65/1.9	CI632/ N7	0/60	23.8/25.0	ISSNHL	pensioner (admin)	3/3
#103	f/r	35/1.9	CI612/ Kanso 2	40/40	11.3/11.3	SOL	medical assistant	2/3
#104	m/l	48/28.0	CI632/ N7	60/25	18.8/16.3	trauma	supervisor	7/> 7
#105	f/r	41/1.5	CI632/ Kanso 2	45/65	6.3/6.3	ISSNHL	scheduler	4/7

f: female, m: male, l: left, r: right, CI: cochlear implant, 4d: 4 days after activation, 6m: 6 months after activation, WRS: word recognition score measured with the German Freiburg monosyllables test (Hahlbrock 1953) at 65 dB SPL in quiet, 4PTA: four frequency pure tone average at 0.5, 1, 2 and 4 kHz in dB HL (hearing level, HL), DoD: duration of deafness, ID: identification number, ISSNHL: idiopathic sudden sensorineural hearing loss, SOL: subtotal ossifying labyrinthitis, admin: administrator.
* Social activity level was queried by asking 'How many times in the last 7 days have you met friends or talked to friends on the phone for more than 5 minutes?'.

for participant #104 significantly between both study visits (#101: $z = -7.41$, $p < 0.001$, $r = 0.74$, #102: $z = 7.23$, $p < 0.001$, $r = 0.72$, #103: $z = 7.15$, $p < 0.001$, $r = 0.72$, #104: $z = 1.28$, $p = 0.202$, $r = 0.13$, #105: $z = 7.51$, $p < 0.001$, $r = 0.75$). Figure 3.4 shows that all participants except #101 at the second visit evaluated simulation parameter sets 1 to 3, which correspond to simple filter functions (band-pass, high-pass and low-pass filters, Table 3.1), with larger similarity scores (yellow/orange horizontal areas in the heatmaps).

The modifications used to create the optimized simulations are shown graphically in Figure 3.5 and are named in detail in the Appendix in Table A5. Between one and three modifications were required to optimize the simulation for the 4d-visit, whereas between zero and five were needed during the 6m-visit. A frequency shift and a high-pass filter was most often required for optimization. The similarity scores of the optimized simulations (sentence 1) were between 8.0 and 10.0 during the 4d-visit and between 7.5 and 10.0 during the 6m-visit (Figure 3.6, mean ± SD of all optimized simulations of both visits: 8.9±0.8). The sound files of the optimized simulations, as well as the unprocessed reference signal (Wagener, Kollmeier, 2005) are included in the Supplemental digital content (1 to 13, Appendix: Table A7). In the application experiment, the similarity scores of simulations generated from optimized parameter sets and two further sentences, were between 1.0 and 9.5 during the first visit and between 7.0 and 9.0 during the second visit, respectively (Figure 3.6).

The starting point for participant #101 for the optimization experiment from the screening experiment was the FFT-vocoder (sine) simulation during the 4d-visit and

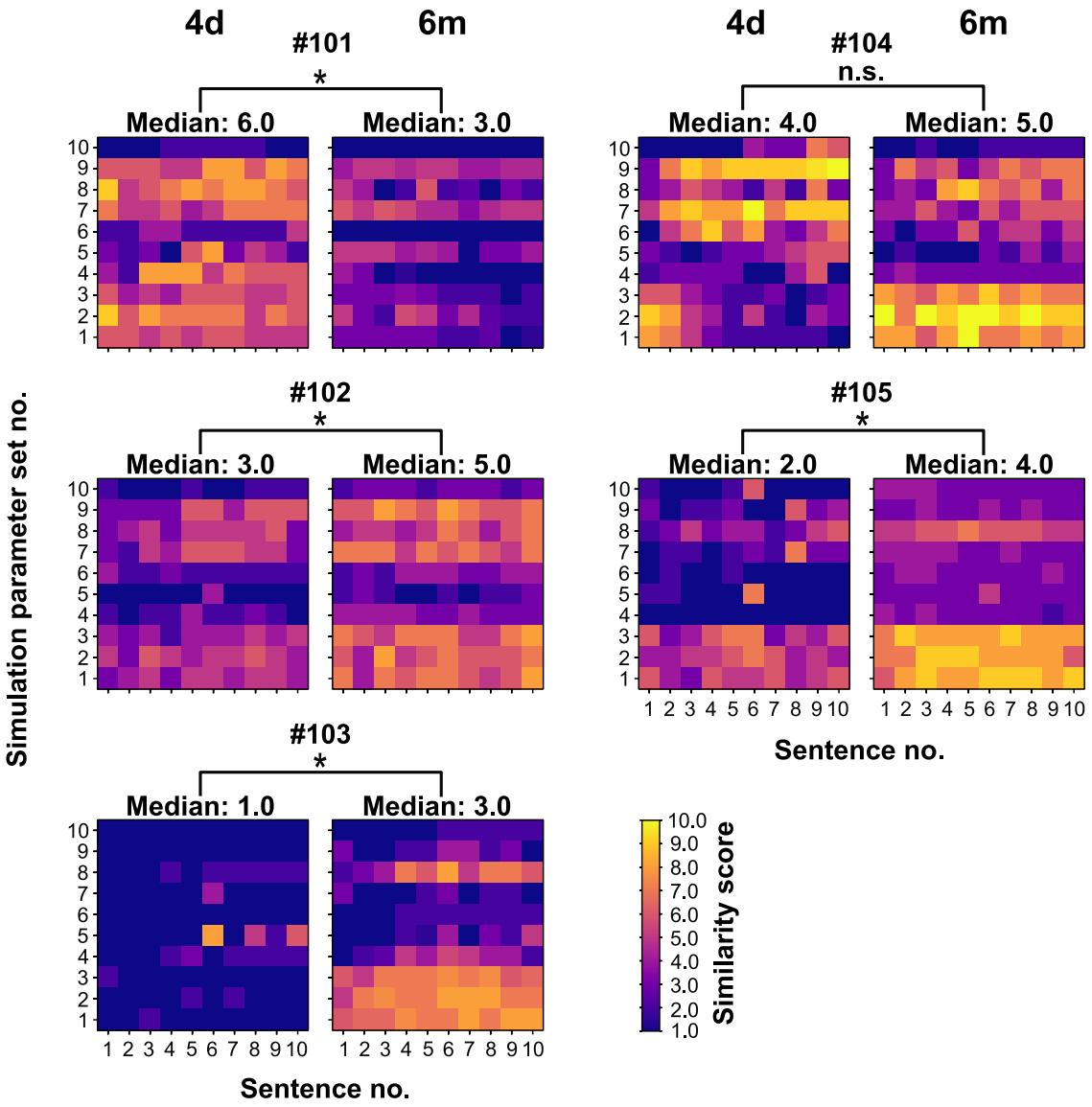

Figure 3.4: Similarity scores (1: no similarity, 10: signals are identical) of each participant (#101 to #105) for each cochlear implant (CI) simulation in the ranking experiment shown as heatmaps. 100 simulations were generated by applying ten simulation parameter sets to ten sentences. The sentences and parameter sets used are shown in Tables A2 and 3.1. Data from the 4 day (4d) and 6 month (6m) visits are shown. The median of all similarity scores for each visit and participant is shown. The significance test was performed with Wilcoxon signed-rank tests (* $p < 0.05$)

the BP-vocoder (noise) simulation during the 6m-visit (Figure 3.4). In the 6m-visit, the participant reported a shift in his evaluation criteria, stating that they had become stricter than those in the 4d-visit. He explained that the sound did not change during the first 6 months of CI experience, but the subjective perception of the sound had evolved (Table A5, sound sample, Supplemental digital content 3 and 4, Appendix: Table A7). This statement aligns with the finding that the recorded similarity scores were larger during the 4d-visit than during the 6m-visit across all the study tasks. For participant #101, changing sentences for simulation had no effect on the similarity score (Figure 3.6). The optimized simulation from

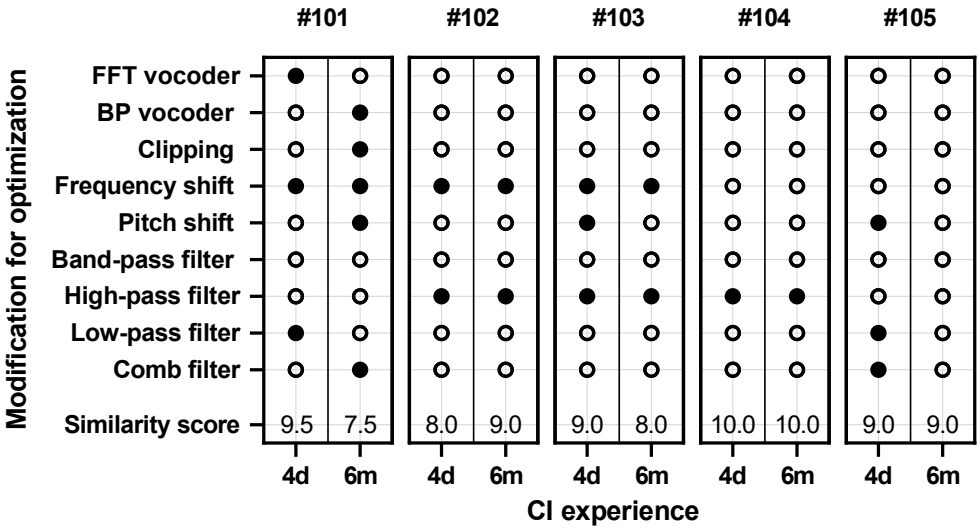

Figure 3.5: Parameters used (filled circles) or not used (open circles) for optimization of cochlear implant (CI) simulations for all participants (#101 to #105) for the 4 day (4d) and 6 month (6m) visits.The achieved similarity scores (1: no similarity, 10: signals are identical) of each optimized simulation are shown. For more details on the parameter settings, see Table A6.
BP: band-pass; FFT: fast Fourier transform

the 4d-visit was rated with smaller similarity scores (sentence 1: 6.5, sentence 2: 4.0, sentence 3: 7.0, Figure 3.6).

Participant #102 had an audiological outcome that was below expectations 1 month after CI activation. Upon re-evaluating the intracochlear position of the electrode array, initially considered appropriate on the basis of radiological reports, a tip fold-over in the three most apical electrode contacts was found so that the electrode contacts E18, E21, and E22 were deactivated. This led to an improvement in open word recognition from the 4d-visit (0 %) to the 6m-visit (60 %, Table 3.2). Participant #102 reported that the CI sound had remained the same during the first 6 months of CI experience, but acclimatization had occurred. The optimized simulation had a thin sound impression, as if caused by a low-pass filter (sound sample, Supplemental digital content 5 and 6, Appendix: Table A7). Figure 3.5 indicates that the modifications were consistent across both visits, whereas the similarity was assessed differently (Figure 3.5). The usage of other sentences for simulation led to similarity scores between 7.0 and 9.0 (Figure 3.6).

Participant #103 experienced subtotal ossifying labyrinthitis, which led to a special surgical and implantation technique (subtotal cochlectomy and reconstruction of the surgical defect). In the ranking experiment during the 4d-visit, the participant rated 80 out of 100 simulations with no similarity (similarity score = 1, Figure 3.4). The participant mentioned difficulty scoring the similarity and expressed a preference for a scale from 1.0 (no similarity) to 3.0 (identical signals). During the optimization, the participant struggled to describe her CI sound perception, resulting in a trial-and-error approach for optimization. The optimization resulted in a low-pitched sound impression as if caused by a frequency and pitch shift (sound sample, Sup-

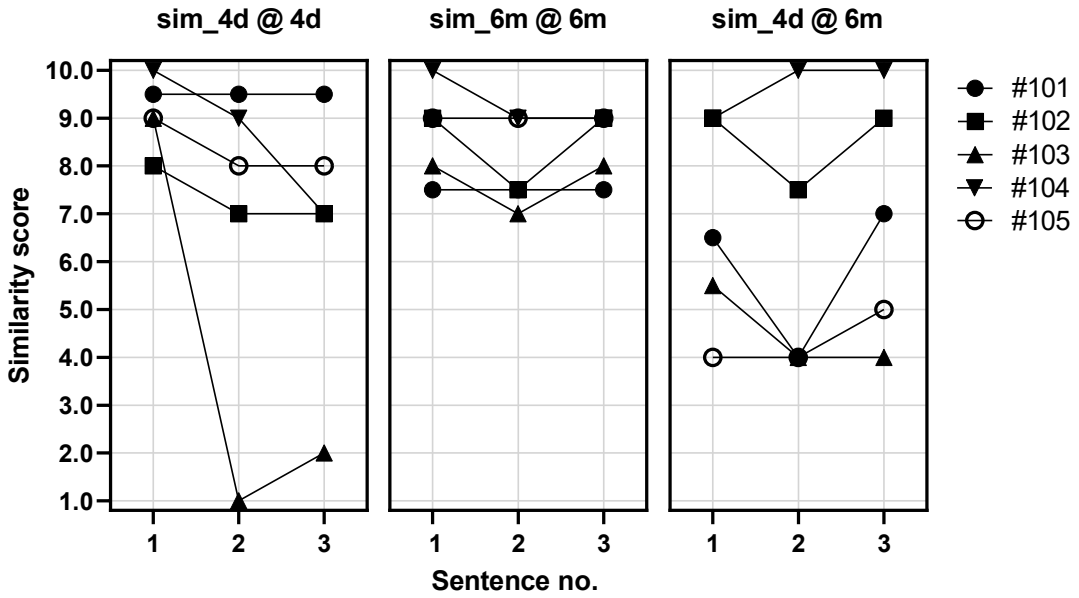

Figure 3.6: Similarity scores (1.0: no similarity, 10.0: signals are identical) of all the study participants for three sentences (1: 'drei rote Schuhe' ['three red shoes'], 2: 'vier nasse Autos' ['four wet cars'], 3: 'neun weiße Tassen' ['nine white cups'], Wagener et al. 2005). The similarities of the optimized simulations at the 4 day (4d) visit were scored twice: at the same visit (sim_4d @ 4d) and 6 months (6m) later (sim_4d @ 6m). The similarities of the optimized simulations of the 6m visit were scored once (sim_6m @ 6m).

plemental digital content 7, Appendix: Table A7). The usage of other sentences for simulation led to lower similarity scores (similarity score for sentence 1: 9.0, sentence 2: 1.0, sentence 3: 2.0; Figure 3.6). In the ranking and application experiments, participant #103 rated the simulations with larger similarity scores during the 6m-visit than during the 4d-visit. During the 6m-visit, the participant stated that the CI sound had changed in the last 6 months. For optimization, one fewer modification was required than for the 4d-visit (Figure 3.5, sound sample, Supplemental digital content 8, Appendix: Table A7). The usage of other sentences for simulation led to comparable similarity scores (similarity score for sentence 1: 8.0, sentence 2: 7.0, sentence 3: 8.0; Figure 3.6).

Participant #104 reported different sound perceptions during the ranking experiment of the 4d-visit depending on the sentence used. For sentences 3 to 10 (Table A2), he perceived a noisy envelope (as generated with a vocoder with a noise-carrier), and sentences 1 and 2 were perceived more clearly (as with a high-pass filter). Since the optimization experiment used sentence 1 as the reference signal, a high-pass filter led to the largest similarity score (10.0 = simulation and reference are identical, Figure 3.5, sound sample, Supplemental digital content 9, Appendix: Table A7). Supplemental digital content 10 provides an example of the noisy sound impression perceived by the participant in some sentences (FFT-vocoder with noise carrier, similarity score = 10.0). During the application experiment, the similarity scores were 9.0 and 7.0 for sentences 2 and 3, respectively (Figure 3.6). During the 6m-visit, the

participant explained that the CI sound had changed since the noisy envelope was no longer present in everyday hearing. Participant #104 scored the FFT-vocoder (noise) simulation in the ranking experiment in median with a smaller similarity score than the high-pass filter (Figure 3.4, simulation 7). The optimization resulted in a simulation based on a high-pass filter that was rated with the maximum similarity score (10.0, sound sample, Supplemental digital content 11, Appendix: Table A7). The usage of other sentences in combination with the optimized parameter set also led to simulations with large similarity (sentences 1 and 2: 9.0). The optimized simulation from the 4d-visit was also rated with large similarity scores (sentence 1: 9.0, sentence 2: 10.0, sentence 3: 10.0, Figure 3.6).

Participant #105 perceived her CI as 'high-pitched', 'squeaky', and 'metallic'. Three modifications were used to optimize the simulation (Figure 3.5, Appendix: Table A5 and sound sample, Supplemental digital content 12, Appendix: Table A7). When applied to sentences 1 and 2, the simulations were rated with a similarity score of 9.0. During the 6m-visit, the participant reported that the squeaky, high-pitched impressions were less present and more in the background than they were during the 4d-visit. The squeaky background sound could not be fully replicated with the software sound tool. However, the unmodified simulation scored a similarity of 9.0 (sound sample, Supplemental digital content 13, Appendix: Table A7). In the application experiment, unmodified sentences 2 und 3 were also scored with a similarity of 9.0. The optimized simulation of the 4d-visit, was rated with lower similarity scores (4.0 and 5.0, Figure 3.6) during the 6m-visit.

3.3.2 Cross-Sectional Study after at Least 2 Years of CI Experience

This study included 15 participants (seven male, eight female). All participants completed all the measurements. The participants were aged between 19 and 80 years (mean ± SD: 62 ± 18 years). An appropriate electrode array position was ensured by the postoperative radiological reports. In the processor-setting of the everyday use of participant #210, two medial electrode contacts were deactivated (short circuits), whereas all 22 electrode contacts were activated in the everyday settings of the other participants. All participants used the ACE strategy with $n = 8$. The participants' characteristics are summarized in Table 3.3.

Figure 3.7 shows similarity scores for all participants for all 100 simulations in the ranking experiment and similarity scores averaged across all participants as heatmaps. Most participants (#201, #202, #204, #205, #206, #208, #209, #210, #211, #212, #214, #215) scored parameter sets 1 to 3 (band-, high- and low-pass filter) and 8 (FFT-vocoder with sine-carrier, Table 3.1) with larger similarity than sets 4 to 6 and 10 (comb filter, frequency shift, BP-vocoder, Table 3.1). For participants #203 and #213, the heatmaps show an increased intensity depending on the sentence, especially for parameter sets 7 and 9 (vocoder). The heatmap of participant #207 shows no intensity maxima.

A repeated measures ANOVA with a Greenhouse-Geisser correction revealed that the mean similarity scores were significantly different between simulation parameter sets ($F(2.27, 31.77) = 21.12$, $p < 0.001$), but there was no significant main effect for

Table 3.3: Characteristics of the participants.

ID	Sex/ CI ear	Age/DoD [years]	Implant/ Processor	WRS [%]	4PTA [dB]	CI experience [years]	Etiology	CI usage [hours]*	Occupation/ Socializing**
#201	f/r	80/2.0	CI422/ N7	75	38.8	8.1	ISSNHL	14.1	pensioner (nurse)/7
#202	f/l	45/2.0	CI512/ N6	65	15.0	5.5	ISSNHL	5.5	carer/1
#203	m/l	38/1.0	CI632/ N7	60	7.5	2.3	ISSNHL	7.8	order picker/7
#204	f/l	73/60.0	CI512/ N6	55	31.3	5.9	cholesteatoma	7.1	pensioner (teacher)/7
#205	m/l	19/0.2	CI24RE (CA)/N7	85	7.5	9.9†	trauma	0.1†	illuminator/4
#206	f/r	78/5.0	CI632/ N7	55	33.8	2.1	ISSNHL	13.0	pensioner (pharmacist)/7
#207	f/r	63/12.0	CI512/ N7	55	21.2	6.0	ISSNHL	7.8	service worker/7
#208	f/r	50/0.2	CI522/ Kanso 2	80	16.0	5.6	ISSNHL	10.0	manager/0
#209	f/l	57/3.0	CI632/ N7	75	8.8	2.2	Meniere's disease	1.1††	pensioner (salesperson)/2
#210	m/l	72/40.0	CI532/ N7	75	30.0	4.2	otosclerosis	10.8	pensioner (painter)/3
#211	m/r	63/0.9	CI632/ N7	65	18.8	2.9	ISSNHL	4.6	pensioner (metalworker)/1
#212	m/l	80/46.0	CI512/ N6	65	48.8	6.3	cholesteatoma	12.3	pensioner (bank director)/3
#213	m/l	73/52.0	CI632/ N7	50	28.8	3.0	Meniere's disease	15.2	pensioner (supplier)/0
#214	m/l	58/28.0	CI512/ Kanso 1	50	6.3	6.8	ISSNHL	5.9	goldsmith/6
#215	f/r	77/3.0	CI632/ N7	75	31.3	3.9	Meniere's disease	8.0	pensioner (engineer)/2
mean		62/17		65	23	5.0		8.2	3.8
SD		18/21		13	13	2.6		4.5	2.8

f: female, m: male, l: left, r: right, CI: cochlear implant, WRS: word recognition score measured with the German Freiburg monosyllables test (Hahlbrock 1953) at $65\,\mathrm{dB\,SPL}$ in quiet, 4PTA: four frequency pure tone average at 0.5, 1, 2 and $4\,\mathrm{kHz}$ in dB HL (hearing level, HL), DoD: duration of deafness, ID: identification number, SD: standard deviation, ISSNHL: idiopathic sudden sensorineural hearing loss.

* CI usage is an average usage time (hours per day) recorded from the data logging of the processor.

** Social activity level was queried by asking 'How many times in the last 7 days have you met friends or talked to friends on the phone for more than 5 minutes?'

† Reimplantation $9.9\,\mathrm{years}$ before participating in this study. The first implantation was $11.4\,\mathrm{years}$ before participating in this study. Short duration of usage, as participant subjectively does not rely on CI.

†† Short duration of usage due to comorbidity.

sentences ($F(1.99, 27.85) = 1.85$, $p = 0.17$). Bonferroni-adjusted post-hoc analysis revealed significantly ($p < .001$) larger similarity scores for simulation parameter sets 1 to 3 and 8 than for parameter sets 4 to 6 and 10 ($M_{Diff,1,4} = 4.78$, $CI_{1,4}[1.08, 8.52]$, $M_{Diff,1,5} = 4.88$, $CI_{1,5}[0.99, 8.78]$, $M_{Diff,1,6} = 4.30$, $CI_{1,6}[0.30, 8.30]$, $M_{Diff,1,10} = 5.16$, $CI_{1,10}[1.36, 9.06]$, $M_{Diff,2,4} = 3.65$, $CI_{2,4}[1.57, 5.74]$, $M_{Diff,2,5} = 3.74$, $CI_{2,5}[1.89, 5.59]$, $M_{Diff,2,6} = 3.15$, $CI_{2,6}[0.84, 5.47]$, $M_{Diff,2,10} = 4.01$, $CI_{2,10}[1.76, 6.26]$, $M_{Diff,3,4} = 3.44$, $CI_{3,4}[1.38, 5.50]$, $M_{Diff,3,5} = 3.53$, $CI_{3,5}[1.20, 5.86]$, $M_{Diff,3,6} = 2.94$, $CI_{3,6}[0.79, 5.09]$, $M_{Diff,3,10} = 3.80$, $CI_{3,10}[1.52, 6.08]$, $M_{Diff,8,4} = 3.43$, $CI_{8,4}[1.55, 5.32]$, $M_{Diff,8,5} = 3.52$, $CI_{8,5}[1.67, 5.37]$, $M_{Diff,8,6} = 2.93$, $CI_{8,6}[1.18, 4.68]$, $M_{Diff,8,10} = 3.79$, $CI_{8,10}[1.94, 5.64]$).

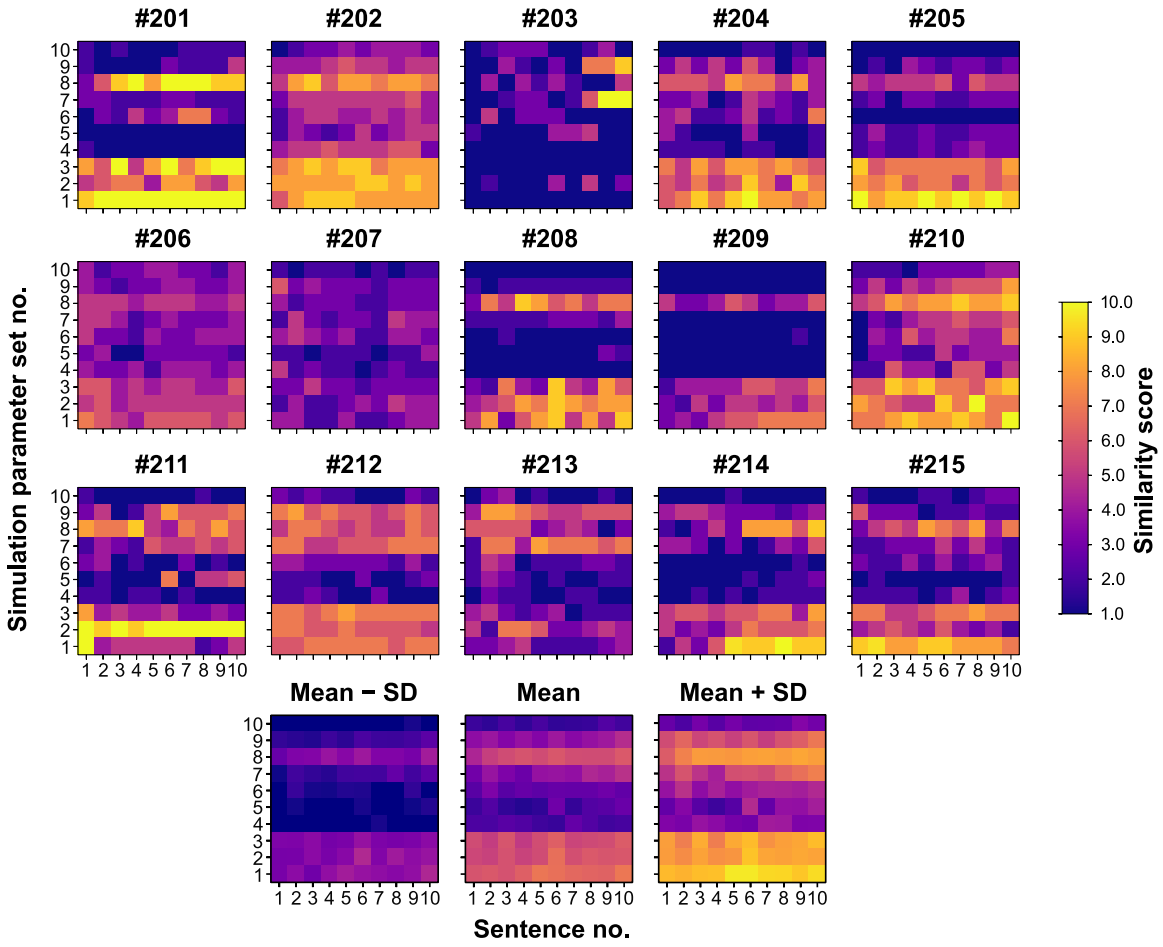

Figure 3.7: Similarity scores (1: no similarity, 10: signals are identical) of each participant (#201 to #215) for each simulation in the ranking experiment shown as heatmaps. 100 simulations were generated by applying ten simulation parameter sets to ten sentences. The sentences and parameter sets used are shown in Tables A2 and 3.1. The last row shows the average similarity scores across all participant and plus or minus the standard deviations (SD).

The subjective descriptions of sound perception before the optimization experiment ranged from 'normal' to 'high pitched' to 'robotic' (Appendix: Table A6). The sound files of the optimized simulations and of the reference signal (Wagener, Kollmeier, 2005) are listed in the Supplemental digital content (1 and 14 to 28, Appendix: Table A7). In the optimization experiment, between none and three modifications were required to replicate the CI sound in the best possible way.

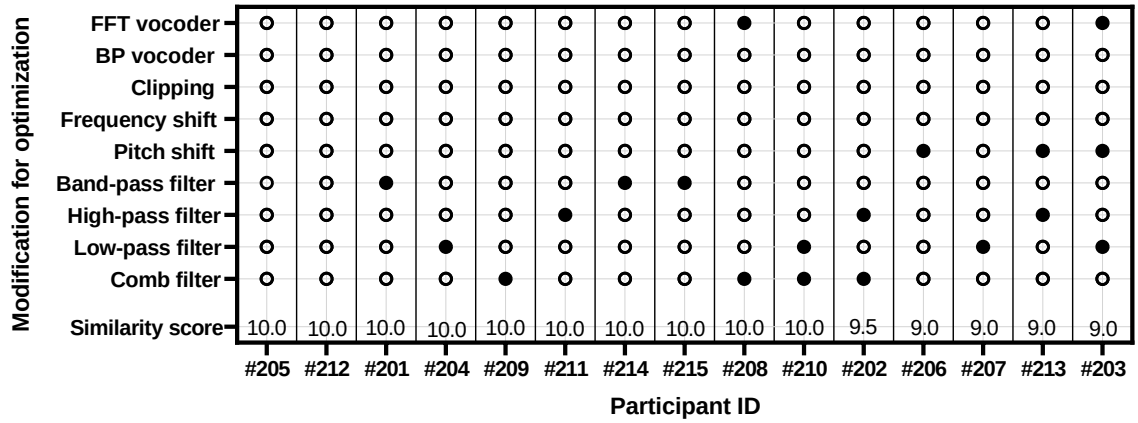

Figure 3.8: Parameters used (filled circles) or not used (open circles) for optimization of simulations for all participants (#201 to #215). The achieved similarity scores (1: no similarity, 10: signals are identical) of each optimized simulation are shown. For more details on the parameter settings, see Table A6. The participants' identification numbers (IDs) are sorted by the similarity score in the first step and by the number of needed modifications in the second step.
BP: band-pass; FFT: fast Fourier transform

Figure 3.8 and Table A6 in the Appendix show the modifications needed for optimization of the simulations. Two of the optimized simulations required no modifications (#205 and #212). Eight simulations were modified by one parameter, four simulations required two parameters, and one simulation required three modifications. A low-pass filter or a comb filter was used most often for this purpose (Figure 3.8). Sound descriptors such as 'normal' also occurred with strong modifications of the optimized simulation, such as a vocoder (participant #203). On average, the optimized simulations were rated with a similarity score of 9.7 ± 0.5 (median: 10.0). For 67 % (10 of 15) of the participants, a simulation with a perfect match (similarity score = 10.0) could be created. Four participants (27 %) rated the similarity of their optimized simulation as 9.0 and one participant (7 %) rated it as 9.5. Among the participants who scored a similarity score of less than 10.0, some could not describe which sound impressions were missing in the simulation. Otherwise, the CI was described as more feminine or less clear. Two of the participants (#207 and #215) stated that the feeling of hearing with the CI was different from hearing with the contralateral ear. After optimization, the participants were asked again for a subjective description of which sound aspect was not yet replicated by the simulation. After 10 of 15 optimizations, participants stated that no further optimizations were necessary.

The Wilcoxon signed-rank test revealed that the median similarity score in the optimization experiment was significantly larger than the median similarity score of the simulation parameter set 1 for sentence 1 (median: 6.0, $Z = 3.184$, $p < 0.001$) and than the median of the best similarity scores for sentence 1 in the ranking experiment for each participant (median: 7.0, $Z = 3.195$, $p < 0.001$).

Similarity scores from the application experiment are shown in Figure 3.9. Sentence

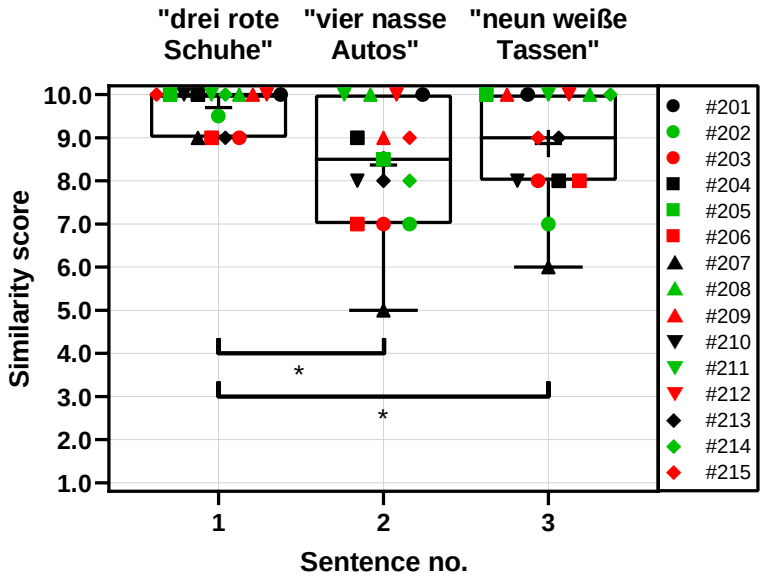

Figure 3.9: Similarity scores (1.0: no similarity, 10.0: signals are identical) of all the study participants for three sentences (1: 'drei rote Schuhe' ['three red shoes'], 2: 'vier nasse Autos' ['four wet cars'], 3: 'neun weiße Tassen' ['nine white cups'], Wagener et al. 2005). The optimization procedure was performed with sentence 1 and the modifications were applied to sentences 2 and 3. The boxes show the lower and upper quartiles (25th and 75th percentiles). The horizontal lines mark the median, and the crosses mark the means of the similarity scores across all the study participants. Whiskers indicate the minimum similarity score. * indicates statistically significant differences between similarity scores of different sentences ($p < 0.05$, Bonferroni-corrected, Friedman test followed by sign tests).

2 had a mean similarity score of 8.4 ± 1.5, while sentence 3 has a mean score of 8.9 ± 1.3. Some participants scored all sentences the same (e.g., #208), whereas others scored the sentences differently (e.g., #207). No participant scored sentences 2 and 3 with larger similarity than sentence 1. The Friedmann test showed a significant difference between similarity scores of the three sentences ($\mathcal{X}^2(2) = 16.60$, $p < 0.001$). Differences in similarity scores of sentences 1 and 2 ($Z = 3.02$, $p = 0.003$), as well as sentences 1 and 3 ($Z = 2.27$, $p = 0.048$) were statistically significant according to the sign test. The difference between the similarity scores for sentences 2 and 3 was not statistically significant ($Z = 7.00$, $p = 0.21$).

3.4 Discussion

The aim of this study was to create German-language CI simulations for devices with 22 electrode contacts. In addition, the CI sound in the three phases of rehabilitation (basic therapy, follow-up therapy and aftercare = rehabilitated) was recorded via CI simulations. A further aim was to investigate whether the application of the simulation parameters to two other sentences still approximates the CI sound.

The study design presented in this chapter was suitable for comparing the similarity of acoustic simulations with the perception of a signal transmitted through a CI. This was demonstrated in two study cohorts, one with little CI experience (4 days and 6 months) and one with extensive CI experience (2 years, rehabilitated). This study design has a very subjective character, as there is no objective method for measuring the sound perception of a CI, as described in Section 2.4. The optimization and rating of similarity during the optimization experiment depend not only on the individual participant's description and evaluation criteria (which may have changed between the visits in the study cohort with little CI experience, e.g., #101), but also on the proceeding and competence of the experimenter. Due to the subjective character of the study, it is not possible to validate the results, but good communication between the experimenter and the participant was essential for the success of the study.

For this reason, the ranking experiment was conducted before the optimization experiment, in contrast to the study design of Dorman et al. (2020), which mainly consisted of the optimization experiment. Through the ranking experiment, the participants were presented with a series of simulations and sound impressions, thus prompting them to focus on their CI sound perception. This enabled them to communicate this perception to the experimenter. Simultaneously, the ranking experiment can evoke a bias in the rating of similarity, as the participants have already heard the sentence to be simulated several times on both ears, which may have led to an adaptation. However, the ranking experiment used ten sentences, thereby minimizing the impact of familiarization.

In the rehabilitated study cohort ($n = 15$), the similarity scores of the ranking experiment showed a significant effect of the simulation parameter sets on the rating of the similarity. In the study cohort with little CI experience, statistics were omitted because of the small case number ($n = 5$). The ranking experiment revealed in both study cohorts that simple filters (low-, high-, and band-pass filters) achieved better similarity scores (Figures 3.4 and 3.7) than the other simulation parameter sets did (Table 3.1). In addition, the FFT-vocoder with a sine carrier (simulation parameter set no. 8, Table 3.1 and Figure 3.7) was rated with large similarity by most of the participants. This may be due to the similar processing mechanisms of the implemented FFT-vocoder to the ACE[31] coding strategy used by all participants (Sections 2.3.1 and 2.4.2, Nogueira et al. 2005). The FFT-vocoder tended to perform better with sine carriers than with noise carriers. This finding is in agreement with the results of Dorman et al. (2017), who reported median similarity scores of 2.9 and 1.9 (scale: 0 to 10, Dorman et al. 2017) for sine and noise carriers, respectively. In contrast, Peters et al. (2018) found larger similarity for noise carriers than for sine carriers.

CI simulations with large similarity were generated for both study cohorts (mean similarity score, study cohort with little CI experience: 8.9 ± 0.8, rehabilitated study cohort: 9.7 ± 0.5). The similarity of the optimized simulations increased significantly compared to those without optimization in the ranking experiment. The similarity scores achieved are comparable to the results of Dorman et al. (2020), who achieved an average similarity score of 8.8 ± 0.9 (Dorman et al. 2020). In a review by Dorman

[31] Custom Sound Pro Software, Cochlear Ltd. (2022b), Sydney, Australia, version 7.0

et al. (2024), the authors reported a mean similarity score of 9.6±0.3, which resulted from the ten best similarity scores (greater than 9.5) from a total cohort of 30 study participants.

Like in the studies of Dorman et al. the CI sound was very individual in all three phases of rehabilitation (Supplemental digital content 1 to 28, Appendix: Table A7, e.g., 2019; 2020; 2022; 2024). The number of modifications for optimization (between zero and five, Figures 3.5 and 3.8), as well as the strengths of the modifications (Tables A5 and A6), were variable.

In the study cohort with little CI experience across both visits, a frequency shift or a high-pass filter ($n = 6$) was most often required to optimize the simulations. The result of these modifications is a high-frequency (frequency shift) or thin and tinny (high-pass) sound. The high-frequency sound impressions found for many of the participants with little CI experience may be caused by the frequency-to-place mismatch explained in Section 2.4. The frequency range of an electrode contact and the physiologically correct place for processing that frequency range can differ, especially in cases of short electrode arrays (Baumann et al. 2006; Canfarotta et al. 2020; Dorman et al. 2019b). Another possible cause of the frequent use of a high-pass filter includes the frequency response of the insert earphone used. Due to their design, insert earphones have a high-pass filter effect (Lehnhardt et al. 2009), so that the CI sound is compared with a high-pass filtered sound from the contralateral ear. Since not all participants required a high-pass filter (see also participants with CI experience > 2 years), it is unlikely that the frequency response of the insert earphones had a major effect.

In comparison, a low-pass or comb filter ($n = 4$) was most frequently used to optimize the simulations in the rehabilitated participants. In the rehabilitated participants, a frequency shift was never used to optimize the simulations. A pitch shift was used three times in both study cohorts. This finding is in agreement with the results of Reiss et al. (2007) and McDermott et al. (2009), who reported that pitch perception changes with CI experience toward lower frequencies. This is explained by neuronal plasticity (Section 2.4), as the brain is reorganizable in response to new stimuli, using memories and experiences (Bernhardi et al. 2017; Gazerani 2025). During rehabilitation, all participants had a normal hearing contralateral ear. This input facilitated the learning process. The rehabilitated participants had at least 2 years of experience hearing with CI, which may have led to a reduction in the perceived frequency-to-place mismatch. Notably, rehabilitated participants often even needed a low-pass filter to optimize the simulations, which leads to a damped sound in the simulations. A possible explanation for this finding includes a overregulation of neuronal plasticity and the use of an age-dependent hearing threshold as a criterion for normal hearing in the contralateral ear was used. Thus, some participants had hearing loss (4PTA) greater than 30 dBHL (hearing level, HL, Table 3.3), and compared the CI sound with an already low-pass filtered contralateral ear (due to hearing loss). However, among the four participants (#203, #204, #207, #210) for whom a low-pass filter was applied, only two had high-frequency hearing loss (#207, #210). Participant #204 also had a hearing loss of 31.3 dBHL (4PTA), but this hearing loss did not range from high frequencies.

In addition to low-pass filters, comb filters were also often used to optimize sim-

ulations. In the signal processing of CIs, the input sound signal is divided into logarithmic frequency bands by a filter-bank (Section 2.3.1). In comparison, a comb filter also divides the sound signal into several frequency bands, but these are not spaced logarithmically (Section 2.1.1, Figure 2.1d). Comb filters produce a metallic, tinny sound (flanging, Section 2.1.1), so this step in the signal processing of CIs may cause the often used description of CI sound: tinny. To improve the naturalness of sound perception in CIs, a promising direction for future research is enhancing the filter bank used in the ACE strategy.

Notably, in the ranking experiment, the post hoc test after the repeated measures ANOVA resulted in a significantly lower average similarity score for simulation parameter set 4 (comb filter) than for set 3 (low-pass filter). This is due to the different cutoff frequencies and quality factors used in the ranking experiment compared with the optimization experiment. For the parameter sets of the ranking experiment, the parameters were based on the literature and partly used a 'first guess' to reproduce the typical sound descriptions (e.g., 'tinny'). This shows the relevance of the optimization of simulations to individual perceptions to improve the similarity score.

In the subjective description of the CI sound, the descriptor 'normal' was used four times for the rehabilitated participants, whereas the participants with little CI experience did not use this description once. Participant #205 used the description 'normal' and did not need to change the simulation to achieve perfect similarity. However, some participants used the description 'normal' with other descriptions that suggest a deviation of the sound impression from a normal hearing ear (e.g., #203: 'female, softer'). For participant #203, a vocoder was used to create the optimized simulation. A vocoder leads to a strong spectral change. However, participant #203 described this sound as 'normal'. Dorman et al. (2022) made similar observations and suspected that the description 'normal' is probably used as a synonym for 'familiar'.

The result that 10 of the 15 rehabilitated participants stated that no further optimizations had to be made fits with the results that they rated the similarity with a 10.0. This also shows that the software sound tool already covers many aspects of CI sound. For participants with little CI experience, several aspects of sound could not be fully replicated via the software sound tool. This finding is in agreement with the reduced mean similarity in the study cohort with little CI experience (8.9 ± 0.8) than in the cohort with rehabilitated participants (9.7 ± 0.5). Sound aspects that could not be simulated by the software sound tool developed for this study were, for example, synthetic sound characteristics such as robotic and emphasis (Tables A5 and A6). For subsequent projects, the change in emphasis could be realized by increasing the sound pressure level of certain speech components. The reduced similarity of the optimized simulations compared with the CI sound may be due to the limited CI experience. On the one hand, the participants are still in the learning phase, and neuronal plasticity has not yet been exhausted, thus the CI sound is still very unfamiliar. An artificial sound is more difficult to simulate than a sound that comes very close to that of a normal hearing ear. On the other hand, the participants had a shorter period to address unfamiliar CI sound and may had difficulties describing it, consequently complicating the optimization process on the basis of these descriptions.

Despite the small study population ($n = 15$ and $n = 5$), certain sound characteristics occurred several times. For example, to optimize the simulations for participants #201, #214 and #215, a band-pass filter was used in all the cases, and only the cutoff frequencies had to be chosen differently. For participants #201 and #214, the simulation parameter sets were identical. For participants #202 and #209, a comb filter was used for both simulations, which resulted in similar sounds of simulations. Participants #205 and #212 did not require any modifications to the reference signal. This is remarkable as it shows that the sound of a CI can be very similar to that of a normal hearing ear (similarity score = 10.0) and that CI sound can be similar or even identical between individuals.

However, CI sound is very individual. This may be due to differences in programming of the processors, inhomogeneities of etiology, duration of use, duration of deafness, depth of insertion, surgical technique, complications (tip foldover, $n = 1$) or implant type (Section 2.4). Even if the study cohorts are characterized in terms of their CI experience, CI experience may still influence the CI sound even after 2 years of CI experience.

Dorman et al. (2022) investigated the influence of CI experience on the parameters necessary to create CI simulations via a case series of five participants. The authors created CI simulations at two time points. Therefore, a frequency shift was most often needed to approximate the CI sound. This is in accordance with our observation in the study cohort with little CI experience. Dorman et al. (2022) reported little to no change in (especially high-frequency) CI sound during the examined time period. The authors concluded that the CI sound cannot be compensated by neuronal plasticity within the first 3 years of CI experience if short electrode arrays (active length: 15.0 mm, total length: 18.5 mm, Advanced Bionics AG 2022) are used. The authors assumed that this is due to a large frequency-to-place mismatch caused by short electrode arrays (Dorman et al. 2022). This is consistent with the explanation of some of our participants with little CI experience, that the sound had not changed but that the perception of the characteristics of the sound had changed (#101, #104, #105). In addition, participant #103 stated that the CI sound had changed between the two visits. For all participants except participant #102, different simulation parameters were used between the visits. The differences in the results of this study and those of Dorman et al. (2022) may be due to the different inclusion criteria used in the two studies. The CI experience of participants at both visits varied across the studies. Our participants had 4 days (4d-visit) and 6 months (6m-visit) of CI experience. In comparison, the CI experience between the two visits in the study by Dorman et al. (2022) was more inhomogeneous (first visit between 3 and 20 months, second visit between 17 and 47 months). The participants had CIs from different manufacturers that come with differences in their technical designs (e.g., lengths of the electrode arrays) and signal processing. Furthermore, there are interindividual differences in participants, such as the etiology and duration of deafness, and different software sound tools have been used for simulation optimization. These factors may affect the CI sound (Section 2.4), but further research is necessary to support these considerations. More fundamental studies of tonal sound perception based on electrical to acoustic pitch matching experiments (McDermott et al. 2009; Reiss et al. 2007; Tan et al. 2017) found a change in pitch perception with increasing CI experience, which is in accordance with our results.

If the simulations of the rehabilitated study cohort are examined as a function of CI experience, all participants with more than 6 years of CI experience (#201, #205, #212, #214) either needed no or only a weak modification (broad band-pass filter) to optimize the simulation and obtain a perfect match (similarity score = 10). This may indicate that neuronal plasticity is not exhausted even after the completion of follow-up therapy. Moreover, neuronal plasticity can compensate for frequency-to-place mismatches in CI users with relatively short electrode arrays (e.g., #212: CI512: active length: 14.25 mm, total length: 19.2 mm, Cochlear Ltd. 2022a).

When the parameters of the optimized simulations were applied to two other sentences, the application experiment (rehabilitated study cohort) showed that although the sign test showed significant differences in the similarity scores of sentences 2 and 3 compared with the optimized simulation with sentence 1, the similarity was still rated with large similarity on average (sentence 2: 8.4±1.5, sentence 3: 8.9±1.3, Figure 3.9). In addition, the sentences in the ranking experiment had no significant main effect ($F(1.99, 27.85) = 1.85$, $p = 0.17$). Furthermore, the mean similarity scores of the optimized simulations applied to sentences 2 and 3 are comparable to the mean similarity score of (8.8 ± 0.9) obtained in the study by Dorman et al. (2020).

One limitation of this study is the small number of study participants ($n = 15$, $n = 5$). In addition, only the audio signal from one male speaker was used for simulation. In future projects, CI simulations based on speech signals with female speakers, speakers of other languages or music should be created to capture CI sound to a greater extent. Furthermore, all study participants had CIs from one manufacturer, so no statement can be made about sound perception with other implants on the basis of these study results. However, since studies with a similar study design have already been conducted with CIs from other manufacturers (e.g., Dorman et al. 2019a; 2020; 2022), the focus of this study was on creating simulations with large similarity for CIs from a single manufacturer. Nevertheless, this was an explorative study design and is suitable for generating hypotheses. In particular, a number of noteworthy observations could be made on the basis of individual study participants. These observations will now be discussed.

For participant #102, three electrode contacts were deactivated between the 4d-visit and the 6m-visit. Deactivation of electrode contacts led to a change in the frequency distribution of the individual electrode contacts (frequency bands). After deactivating electrode contacts the participant developed word recognition (4d-visit: 0 %, 6m-visit: 60 %, Table 3.2). This finding is in accordance with the results of Zwolan et al. (1997), who deactivated non-discriminable electrode contacts in a study cohort of eleven CI participants, which led to an improvement in speech recognition. Since participant #102 stated that the CI sound did not change between visits, it can be concluded that deactivating electrode contacts does not necessarily lead to an impairment of the CI sound. This should be taken into account when programming CI sound processors.

For participant #104, a reduction in speech recognition occurred from 60 % to 20 % between the 4d- and the 6m-visit (Table 3.2). According to the participant, this was due to stress. Nevertheless, he stated that the CI sound had changed between both visits. For sentences 3 to 10 (Table A2), the participant reported the per-

ception of a noisy envelope, whereas the sound impressions for sentences 1 and 2 (Table A2) were clear during the 4d-visit. The participant previously reported a noisy sound impression during the first processor-activation, during single-channel stimulation at the basal electrode contacts (E1 to E14, frequency range: 1188 Hz to 7938 Hz, Appendix: Table A1), whereas the other electrode contacts were described as clear-sounding pulsed tones. For this reason, the different sound perceptions of the individual sentences can be attributed to the different frequency components in the sentences. During the 6m-visit, he stated that the noisy impression was no longer present in everyday hearing. For a perfect match in the optimization experiment, a lower cutoff frequency of the high-pass filter (1000 Hz) was used in the 6m-visit than in the 4d-visit (2000 Hz, Table A5). This means that the CI sound in the 6m-visit was closer to the hearing of the normal hearing ear than it was in the 4d-visit. The results of both participants (#102 and #104) show that the CI sound does not necessarily have to be linked to speech recognition. This fits with the results of Gfeller et al. (2003), who reported only a weak correlation between speech recognition and sound quality.

Participant #205 did not use the system in everyday life (average daily CI usage time: 0.1 hours), but still has a word recognition of 85 % (corresponding to the best word recognition score of the entire study cohort, Table 3.2). Furthermore, he reported no difference between the CI sound and his normal hearing, contralateral ear (Table A6). These good results of auditory processing (word recognition and CI sound), together with the short daily usage time, may be caused by a short duration of deafness (two months), as the participant was implanted shortly after a trauma. Although the participant was reimplanted due to an implant defect 9.9 years before participating in the study, he still has a large CI experience of 11.4 years (first implantation). In addition, he was implanted in childhood and had intensive all-day usage at that time. As children have larger neuronal plasticity (Johnston 2009), these factors may be possible causes for the CI sound being close to that of a normal hearing ear.

Speech recognition and CI sound are not necessarily related in the investigated CI participants. Some participants in the rehabilitated study cohort did require no or weak modifications in their CI simulations, rated them with a maximum similarity, and yet still did not achieve 100 % speech recognition (Table 3.3, Figure 3.8). Since the CI simulations, as defined in Section 2.4.1, are intended to replicate the CI sound and not simulate the functionality or processing mechanisms of a CI, this discrepancy between CI simulation and speech recognition is understandable. Sound perception and speech recognition are distinct phenomena, after all.

This observation was noteworthy during the study, prompting us to ask participants about it. Some participants were asked whether they could explain why their CI sound was so close to that of a normal hearing ear, yet they did not recognize all the words in the speech test. All the participants confidently confirmed that they understood the study tasks correctly. However, they could not provide a definitive explanation, but noted that the sensation of hearing with a CI was different, requiring more concentration to recognize speech.

Possible explanations include learning effects due to the experimental design, as participants had already heard the sentences multiple times in both ears (adaptation).

As discussed above, this effect is likely small; for example, participant #205 stated at the beginning of study participation, that his CI sound was equal to that of his normal hearing contralateral ear. Another factor could be the cognitive load associated with processing the CI transmitted signals. If the brain is already heavily engaged in processing CI sound, this could limit the resources available for speech recognition. This hypothesis is supported by neurocognitive studies showing that processing speech in acoustically challenging environments requires additional cognitive effort (Eckert et al. 2016) and by the participants' statements that understanding with a CI requires more concentration.

Due to the large similarities of the CI simulations presented in this study compared with the CI sound (12 out of 25 optimized CI simulations were rated with a maximum similarity), they are suitable for scientific and educational purposes. They enable a realistic assessment of the sound perception of CI users. The application experiment showed that the application to other sentences also resulted in a large similarity to the CI sound, suggesting these simulations can be used in future studies investigating sound perception with CI. This allows such studies to be conducted on participants with normal hearing, facilitating the recruitment of large study populations. Additionally, study designs that are challenging or impossible with actual CIs, such as those involving electroencephalography (EEG) or functional magnetic resonance imaging (fMRI), can benefit from these simulations. However, it is important to remember that these CI simulations do not replicate the processing mechanisms of a CI, but rather the CI sound.

Furthermore, they can be used to educate patients and all interprofessionals involved in the care process. Of course, the CI simulation only simulates the possibilities of CI sound, which, as already discussed, is very individual and the one CI sound does not exist. Both, the technical characteristics of the CIs (signal processing, hardware, etc.) and patient-related data (CI experience, duration of deafness, etc.) may influence CI sound. Additionally, the simulations provided in this thesis primarily reflect the CI sounds experienced by SSD CI users. For example, bilateral CI users may experience CI sounds that differ from those of SSD CI users due to differences in adaptation mechanisms influenced by contralateral hearing. To increase CI simulations' utility, future projects should develop German-language simulations for other CI manufacturers. Moreover, further research into the causes of individual differences in CI sound is essential, as this could enable predictions of CI sound quality for CI candidates and support decision-making processes. The CI simulations do not represent additional effects related to cochlear implantation, such as changes in quality of life or social interactions (Andries et al. 2021; Cychosz et al. 2024). To ensure extensive consultation, the CI simulations should therefore be used as supportive tools and not be presented without further explanation.

3.5 Conclusions

The method presented in this chapter was successfully used to generate German-language CI simulations for devices with 22 electrode contacts. CI simulations were generated in the form of sound samples that reproduce CI sound with large similarity in the three phases of rehabilitation (basic therapy, follow-up therapy and aftercare).

Even if certain sound characteristics (e.g., a muffled sound perception as if through a low-pass filter) occurred more frequently, the simulations show that the CI sound is very different among the participants in basic therapy, follow-up therapy and aftercare. In addition, the simulations revealed that the CI sound can also change to a more normal perception within the first 6 months of CI experience. The results of individual participants showed that deactivation of electrode contacts does not necessarily result in a change in CI sound ($n = 1$) and that speech recognition and CI sound are not necessarily related ($n = 2$). Applying the parameters of the optimized simulations to two other sentences led to significantly lower similarity scores, which nevertheless corresponded to a large degree of similarity.

Further research is needed to explain the large interindividual differences in CI sound between the participants. One possibility is to investigate influencing factors such as etiology, duration of deafness, insertion depths, surgical techniques, implant types or CI experience.

The CI simulations can be used for scientific and educational purposes because of their large similarity to CI sound. However, CI simulations are primarily used to simulate the CI sound and cannot reflect other factors, such as communication skills or quality of life that may change as a result of cochlear implantation.

4 New Quantification Methods for Cochlear Implant Sound Quality

4.1 Background Information

In Chapter 3, various modifications were required to create CI simulations with large similarity to the CI sound of individual participants. This variety of parameters illustrates the individuality of CI sound. To investigate possible factors influencing the individuality of CI sound, a quantification is necessary. A suitable measure for quantification is sound quality. A variety of outcome measurements are used to prove the success of cochlear implantation. These tests include speech recognition tests in quiet and in noise, sound localization tests, and quality of life or sound quality measurements (Arndt et al. 2017).

As discussed in Section 2.5.1, there are currently only limited ways to determine the sound quality of a CI. Most evaluations are based on psychoacoustic/subjective assessments by CI users themselves (self-reported CI sound quality), as there are no objective measurement methods of human perception (Amann et al. 2014). For example, a questionnaire to record the Hearing Implant Sound Quality Index (HISQUI_{19}, Amann et al. 2014) is available. Many factors are included in questionnaires, such as the sound quality itself, as well as personal, emotional and psychological factors, e.g., previous hearing experience, cognitive abilities or expectations (Amann et al. 2014). In addition, in questionnaires, each CI sound of an individual can only be evaluated by that individual person. On the one hand, this leads to reduced statistical power and, on the other hand, makes it more difficult to identify other factors influencing sound perception.

Sound quality is a multidimensional variable and there is no consistent definition. In the treatment of hearing loss, sound quality in terms of perceived richness with the hearing device (e.g., hearing aid, CI) is relevant (Caldwell et al. 2017). Since a small deviation from CI sound compared with normal hearing is desirable (Blauert et al. 1997), this chapter will focus in particular on quantifying the deviation in sound perception between CI ear and a normal hearing ear.

The CI simulations described in Chapter 3 therefore provide a completely new way of investigating the CI sound quality. The sound quality of acoustic signals is often measured by subjective rating methods (e.g., random access, semantic differential, category scaling and magnitude estimation, Fastl 2005; Roy et al. 2012b, Section 2.5). Each of these methods provides specific information on questions such as 'which signal is better?' or 'how much better is a signal?' (Fastl 2005).

In this chapter, two methods for quantifying sound quality are presented: a subjective method using a combination of psychoacoustic assessment methods on normal

hearing subjects (Chung et al. 2006) and an objective method using spectral analysis of CI simulations. The CI simulations of the rehabilitated study cohort are considered here, since the participants with little CI experience showed more problems in describing the CI sound and the CI simulations of the rehabilitated study cohort had larger similarity to the CI sound.

The aim of this chapter is therefore to quantify the sound quality of CIs on the basis of CI simulations of rehabilitated participants from Chapter 3. Two methods of quantification are presented and evaluated to develop a new method for measuring the sound quality of CI simulations.

4.2 Materials and Methods

A prospective, non-interventional, experimental study was conducted. All study measurements were performed at the Department of Otorhinolaryngology, Head and Neck Surgery at the University Hospital Halle (Saale), Germany, in July 2023. The ethical review board of University Medicine Halle approved the study protocol and the informed consent forms according to the Declaration of Helsinki with approval number: 2023-144. Informed consent forms for study participation were obtained from all study participants.

4.2.1 Participants

All the study participants were normal hearing adults and native German speakers (inclusion criteria). Pure-tone audiograms for both ears were measured for all participants via a clinical AT1000[32] and HDA300 headphones[33] in a soundproof booth. The inclusion criterion was a pure-tone hearing threshold for air-conduction, averaged over 0.5, 1, 2, and 4 kHz (4PTA), corresponding at least to the age- and sex-related 95th percentile according to DIN EN ISO 7029 (2017). The sample size calculation was based on the results of earlier studies (e.g., Morise et al. 2018; Roy et al. 2012b; Roy et al. 2015) and an assumption of a SD of the primary endpoint of 15 (CI sound quality, MUSHRA). Including a drop out of three participants, this results in a sample size of 15 participants under the requirement of determining the mean value with a 95 % confidence interval and a confidence interval length of 20 (Dhand et al. 2014).

4.2.2 Psychoacoustic Procedures

The experiment was performed in a quiet room with HD201 headphones[33]. The participants rated all CI simulations with different simulation parameter sets from Chapter 3 (Supplemental digital content 1, 14 to 28, Appendix: Table A7) in terms of their sound quality in a combination of pairwise comparison, MUSHRA and semantic differential tasks (Chung et al. 2006; Fastl 2005; ITU-R 2015). As a result, 13 of the 15 CI simulations were rated.

[32] AURITEC, Hamburg, Germany
[33] Sennheiser, Wedemark, Germany

A GUI, developed for this purpose, guided the participants through the three study tasks. It was used for simplified and quick application by the study participants. The GUI was developed in Python[34] in the integrated development environment Spyder[35] with the package TkInter[36]. The library Winsound[37] (function: PlaySound) was used to play WAVE files. The GUI exported the acquired data automatically to Microsoft Excel[38] for data storage. Each participant was introduced to the study with the same wording at the beginning of the participation. A written experimental instruction was presented before each study task. An adviser stayed in the experimenter room to answer questions arising while handling the GUI.

The participants' data (name, sex, age, native language, occupation), musical education ('How many years did you take lessons in a musical instrument or singing?') and social activity level ('How many times in the last 7 days have you met friends or talked to friends on the phone for more than 5 minutes?') were queried for later characterization of the study cohort (Li et al. 2016).

Training Task

Before starting the study tasks, the participants completed a training task. The training task consisted of a short version of the three study tasks. The aim of the training task was that the participants heard the simulations and reference signal at least once and learned how to handle the GUI. During the training task, the participants were instructed to set the sound volume to a subjectively comfortable level. During the training task all components of the GUI were explained via short instructions.

Pairwise Comparison

In the first study task, a pairwise comparison was performed (Figure 4.1). Each simulation was compared with each other, so that 78 ($n * (n-1)/2$ with $n = 13$) pairs were generated. The pairs were randomly presented to the participants. The participants were able to listen to each simulation several times. The participants had to choose their preference between both simulations concerning the sound quality. Figure 4.1 shows a screenshot of the GUI of the pairwise comparison during the training task.

MUSHRA

For the random access-task, an adaptation of the MUSHRA was chosen, since the original MUSHRA is recommended for a maximum of nine sound samples (ITU-R). The 'MUSHRA-drag&drop' method according to Völker et al. (2015) was performed since it enables a visualization of the ranking and thus allows an increased number of sound samples to be examined (Völker et al. 2015, Section 2.5). The GUI presented

[34]Python, van Rossum (1991), version 3.9.7
[35]Spyder, Raybaut (2009), version 5.1.5
[36]TkInter, Lundh (1999) version 8.6
[37]Winsound,Python Software Foundation (2016)
[38]Excel, Microsoft Corporation, Mircosoft Office Professional Plus 16

Figure 4.1: Screenshot of the graphical user interface (GUI) for pairwise comparison during training task with short instructions. On the left, all the components of the GUI are explained. On the right, two cochlear implant (CI) simulations to be compared can be listened to via two buttons. The simulation with the better sound quality is selected via one of the two other buttons below.

a continuous horizontal MUSHRA scale from the left (bad sound quality = 0) to the right (excellent sound quality = 100, Figure 4.2). The scale consisted of five categories (0 to 20: 'Sehr schlecht'/['Bad'], 20 to 40: 'Schlecht'/['Poor'], 40 to 60: 'Mittelmäßig'/['Fair'], 60 to 80: 'Gut'/['Good'], 80 to 100: 'Exzellent'/['Excellent']).

13 boxes presented the simulations on the GUI. Those were movable on the scale via drag and drop. The actual scale-value of the moved box was written on top of the scale. By clicking at the box, the simulation was played back. A 14th box served as reference signal (unmodified audio signal) and was fixed at the scale at 100. Simulation #205 (= simulation #212) served as 'hidden reference', since participants #205 and #212 did not need any changes in the audio signal to reflect his CI sound. Since the 'anchor signal' is typically a low-pass filtered version of the reference signal and to avoid further increasing the number of sound samples, the low-pass filtered simulations #207 and #204 were used as 'anchor signals'. The participants were able to listen to each audio signal in any order several times (ITU-R 2015). The pairwise comparison task was used to identify a rough order in which the simulations on the GUI on the MUSHRA-scale were arranged in equal distances as a function of how often it was preferred in the pairwise comparison task. The participants were instructed to rate the sound quality concerning the deviation in comparison to the reference signal. Several simulations were allowed to be related to the same sound quality. The participants were instructed that at least one simulation had to be assigned a sound quality of 100 and that the simulation with the lowest sound quality did not have to be assigned a scale value from the bad category (ITU-R 2015).

Semantic Differential

The last study task was a semantic differential task. The GUI displayed sliders with an adjective at one end (artificial, high-frequency) and the opposite adjective (natural, low-frequency) at the other end (Figure 4.3). The participant decided how appropriate these adjectives were for each of the simulations by placing the sliders

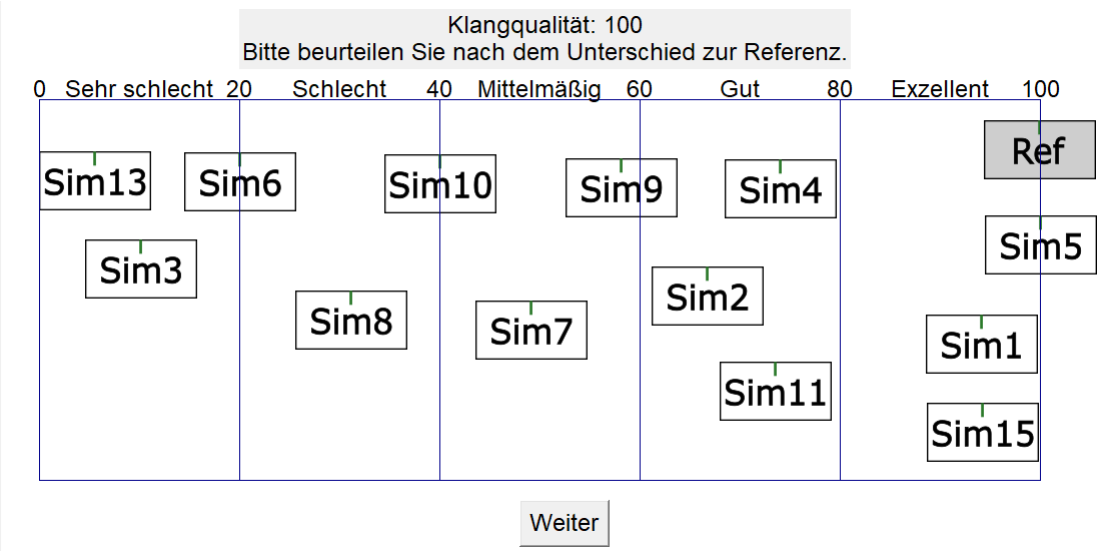

Figure 4.2: Screenshot of the graphical user interface (GUI) for the Multi-Stimulus Test with Hidden Reference and Anchor (MUSHRA)-'drag&drop' task (Völker et al. 2015). The horizontal MUSHRA scale is shown on the top (from 'Sehr schlecht'/['Bad'], over 'Schlecht'/['Poor'], over 'Mittelmäßig'/['Fair'], over 'Gut'/['Good'], to 'Exzellent'/['Excellent']). Boxes present the cochlear implant (CI) simulations. Boxes are moveable via drag and drop. Simulations can be listened to by clicking on the boxes.

between the adjectives. The participants were able to listen to the reference signal at any time. The outcome of the semantic differential task is referred to as 'pitch deviation' and 'naturalness' in the following.

4.2.3 Data Analysis

To calculate an objective measure for the deviation of the simulation spectra in comparison to the reference spectra, a spectral analysis was performed. The frequency spectra over time (STFTs, Section 2.1.1) were calculated and plotted as spectrograms by using the Python[39] libraries SciPy[40] (function: signal.spectrogram) and Matplotlib[41] (function: pyplot.pcolormesh). The FFT length was set to 2048. The linear spaced frequency bands of the STFT-spectrogram, were mapped to 128 logarithmically spaced frequency bands via the package Librosa[42] (function: melspectrogram). The absolute values of the differences between the spectra of the simulations and the reference signal (spectral deviation) were calculated and summed for each simulation. The spectra were plotted as spectrograms with the package Matplotlib[41] (function: pyplot.pcolormesh). Data analysis was performed using the software SPSS[43]. The data were analyzed descriptively by calculating the means, medians and SDs of the sound quality ('MUSHRA drag&drop'), number of preferences (pairwise comparison), pitch deviation, naturalness (semantic differential)

[39]Python, van Rossum (1991), version 3.9.7
[40]SciPy, Virtanen et al. (2020), version 1.7.1
[41]Matplotlib, Hunter (2007), version 3.4.3
[42]Librosa, McFee et al. (2022), version 0.9.1
[43]SPSS, IBM (2021), version 28.0.0.0

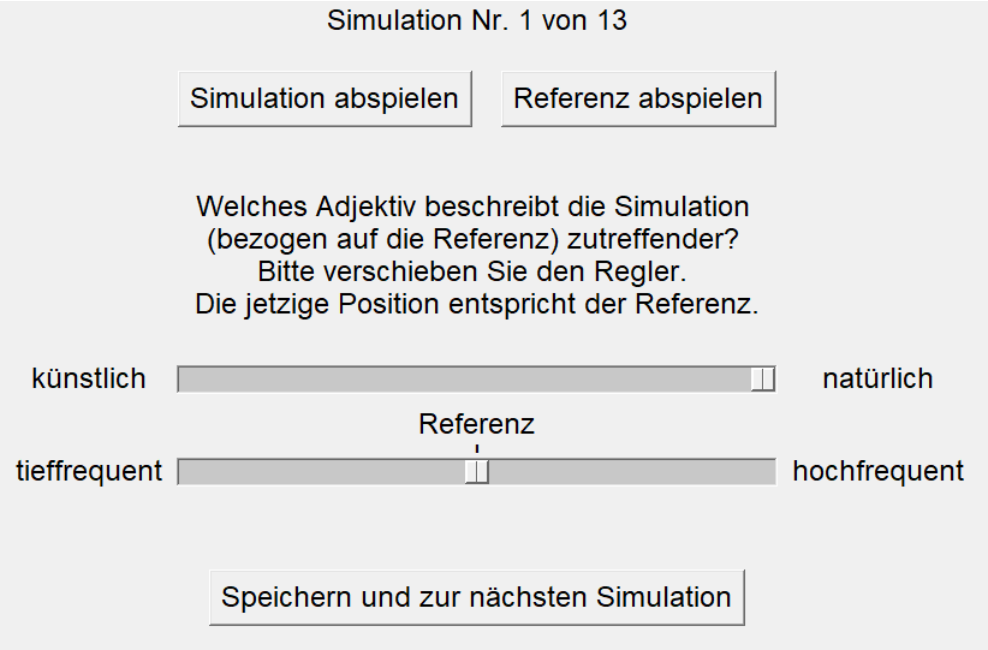

Figure 4.3: Screenshot of the graphical user interface (GUI) for the semantic differential task. On the top, one cochlear implant (CI) simulation and the reference signal can be listened to via two buttons. Sliders were movable between the adjective pairs ('künstlich' ['artificial'), 'natürlich' ['natural'] and 'tief-freqeunt' ['low-frequency'] and 'hochfrequent' ['high-frequency']).

and spectral deviation. Correlations between sound quality, number of preferences, naturalness and spectral deviation were analyzed via linear regression. Spearman's correlation coefficient was calculated to test for significance. The software Prism[44] and Inkscape[45] were used for visualization.

[44]Prism, GraphPad Software (2020), version 8.4.3
[45]Inkscape, Inkscape Community (2003), version 1.2

4.3 Results

This study included 15 participants (four male, eleven female). The participants were aged between 18 and 29 years (mean ± SD: (24 ± 3) years). The mean 4PTA for both ears was (6 ± 2) dBHL. All participants completed all the study tasks. Participants' characteristics are summarized in Table 4.1.

Table 4.1: Characteristics of the participants for the sound quality study.

ID	Sex	Age [years]	4PTA left/right [dB]	Occupation	Socializing*	Musical edu.** [years]
#301	f	25	5.0/5.0	student (medical physics)	5	0
#302	f	23	6.3/5.0	student (German studies)	4	0
#303	f	25	8.8/7.5	student (music)	10	17
#304	f	18	5.0/7.5	trainee (logopedics)	6	3
#305	m	25	5.0/7.5	food chemist	3	0
#306	f	26	5.0/2.5	trainee (logopedics)	5	0
#307	f	20	2.5/2.5	trainee (logopedics)	2	10
#308	f	25	5.0/7.5	student (anglistic)	3	10
#309	f	24	7.5/8.8	student (art)	5	0
#310	m	25	5.0/6.3	student (mathematics)	5	19
#311	m	23	6.3/7.5	student (biology)	4	0
#312	f	24	8.8/10.0	student (psychology)	10	0
#313	f	29	6.3/8.8	student (pedagogy)	4	8
#314	f	22	6.3/5.0	student (physics)	6	15
#315	m	25	2.5/3.8	medical physicist	2	3
mean		24	5.7/6.3		5	5.7
SD		3	1.8/2.4		2	7.0

f: female, m: male, 4PTA: four frequency pure tone average at 0.5, 1, 2 and 4 kHz in dB HL (hearing level, HL), ID: identification number, SD: standard deviation.
* Social activity level was queried by asking 'How many times in the last 7 days have you met friends or talked to friends on the phone for more than 5 minutes?'
** Musical education level was queried by asking 'How many years did you take lessons in a musical instrument or singing?'.

Spectral Analysis

Figure 4.4 shows spectrograms for each CI simulation from Chapter 3 and its spectral deviation (absolute values of difference spectrograms) compared with the reference signal (top of the figure). The spectral deviation varied with frequency for each CI simulation and was largest for simulation #213 and smallest for simulations #205 and #212, which equate with the reference signal.

Figure 4.5 shows the sum of the spectral deviation for each simulation. The simulations were ranked according to the sum. The sums were between 0 dB and $5.0 * 10^5$ dB. Averaged over all the simulations, the mean sum of the spectral deviation was $(1.8 \pm 1.5) * 10^5$ dB.

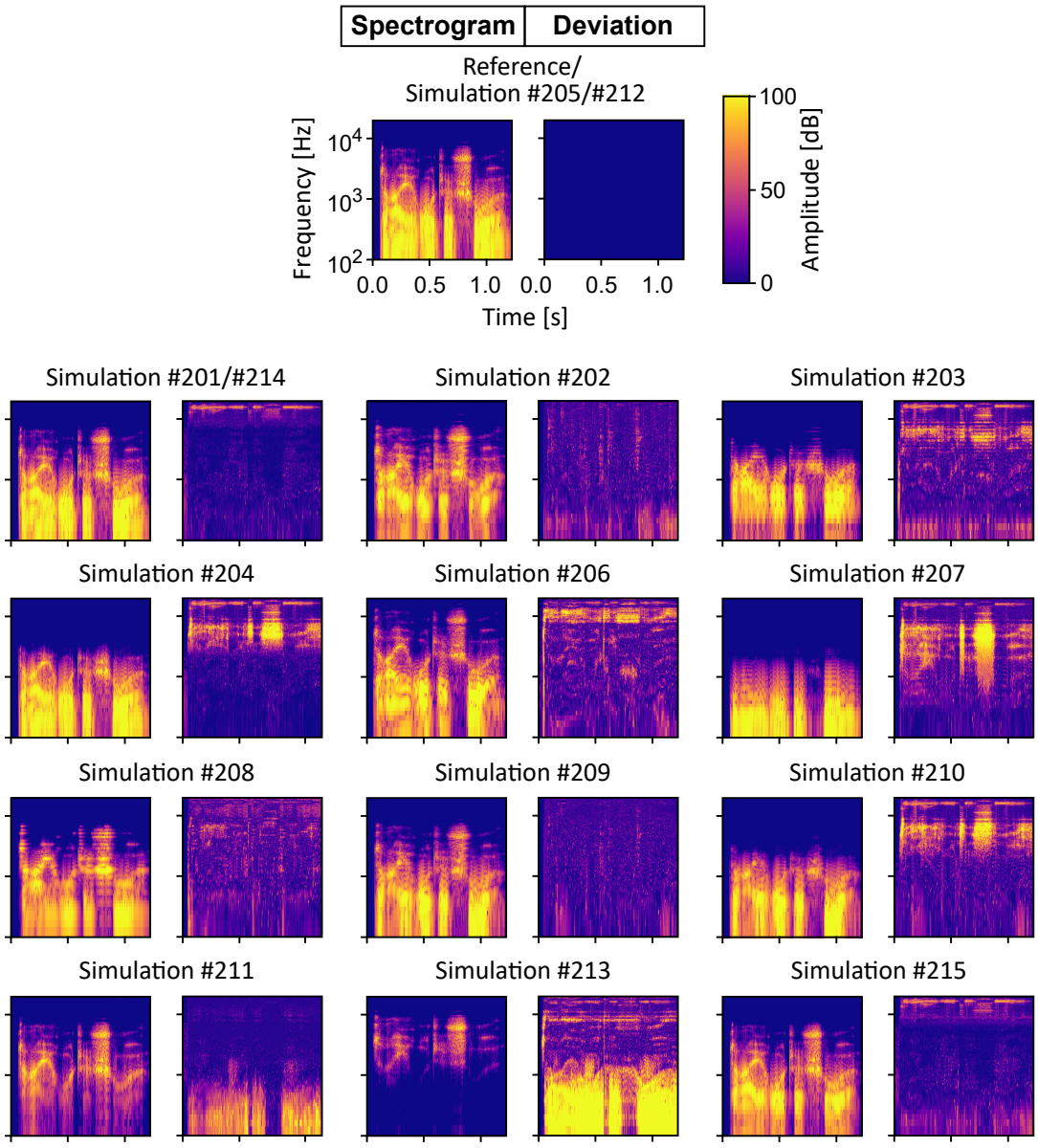

Figure 4.4: Spectrograms of cochlear implant (CI) simulations for participants with CI experience larger than two years. Each spectrogram is named by the participants'/simulations' identification number (ID) from the CI simulation study in Chapter 3. At the top of the figure the spectrogram of the reference (unmodified) signal ('drei rote Schuhe', ['three red shoes'], Wagener et al. 2005) is shown. For each simulation the spectral deviation (absolute values of difference spectrogram, reference − simulation) is shown in addition to the spectrogram. Redundant CI simulations, i.e., that based on the same parameter sets (simulation #201 = simulation #214, simulation #205 = simulation #212 = reference), were shown once. The frequency and amplitude axes are shown logarithmically.

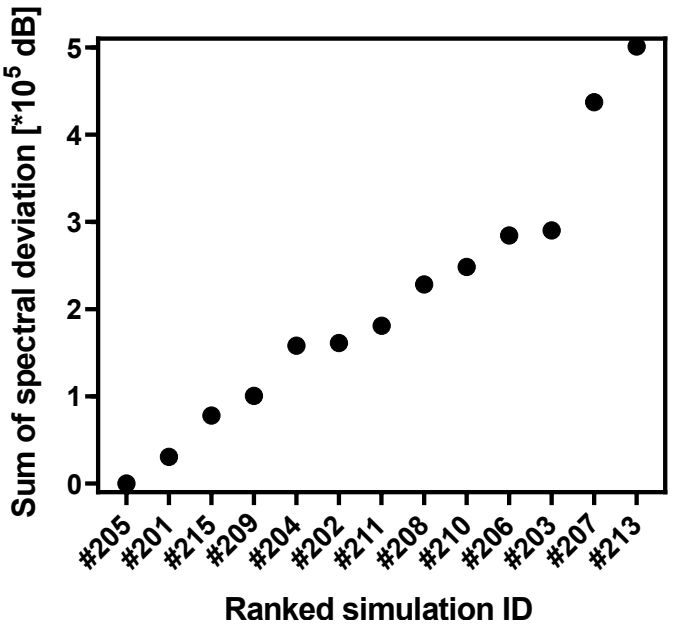

Figure 4.5: Sum of the spectral deviation for each cochlear implant (CI) simulation. The simulation identification numbers (IDs) were ranked according to the sum of the spectral deviations.

Psychoacoustic Analysis

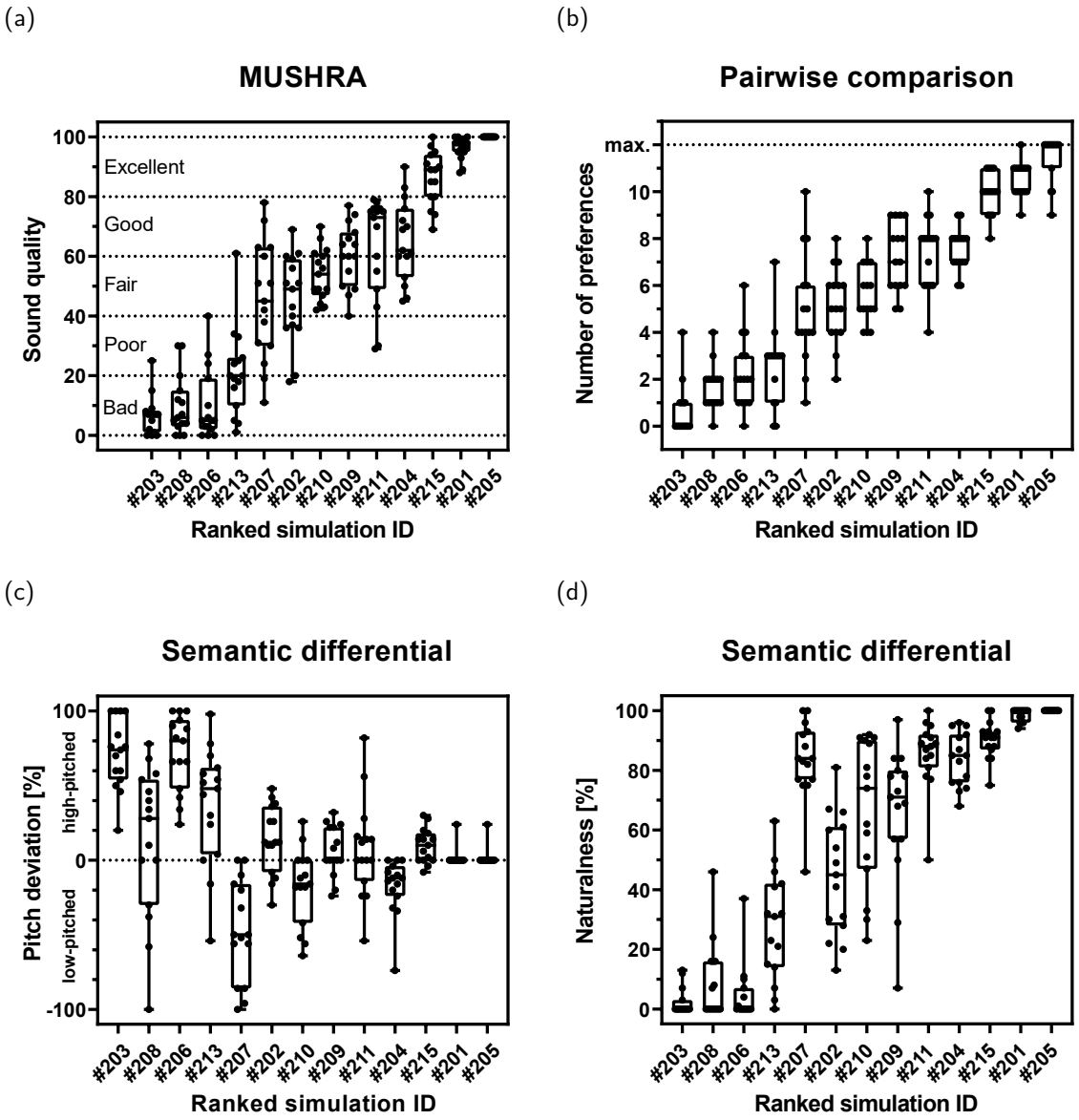

Figure 4.6: Boxplots presenting (a) sound quality (Multi-Stimulus Test with Hidden Reference and Anchor, 'MUSHRA drag&drop', Völker et al. (2015)), (b) number of preferences (pairwise comparison), (c) pitch deviation (semantic differential) and (d) naturalness (semantic differential) for each simulation. The simulation identification numbers (IDs) were ranked according to the sound quality in the MUSHRA task. Each point is one score of one normal hearing participant. The boxes show the lower and upper quartiles (25th and 75th percentiles). The horizontal lines mark the median.

To assess the variance of the results, Figure 4.6 shows the rating of each CI simulation for each normal hearing participant in the MUSHRA, pairwise comparison and semantic differential task. The simulations were ranked according to the rated mean sound quality in the MUSHRA task (Figure 4.6a). The sound quality was scored best on average for simulation #205 and worst for simulation #203. Averaged over all simulations, a mean sound quality in the MUSHRA of (51 ± 33) was scored. The

statistical dispersion was smaller at the edges of the scale (near 0 or 100) than for fair sound quality in the MUSHRA, paired comparison and semantic differential task for naturalness (Figures 4.6a, 4.6b and 4.6d). For simulation #207 the statistical dispersion was the largest during MUSHRA task. Averaged over all simulations, a mean naturalness of $(58 \pm 38)\,\%$ was scored. In the pairwise comparison, simulation #205 was most often preferred, whereas simulation #203 was the least preferred on average (Figure 4.6b). The pitch deviation had the smallest statistical dispersion for simulations #205 and #201 and the largest for simulation #208 (Figure 4.6c). Averaged over all simulations, a mean pitch deviation of $(11 \pm 41)\,\%$ was scored.

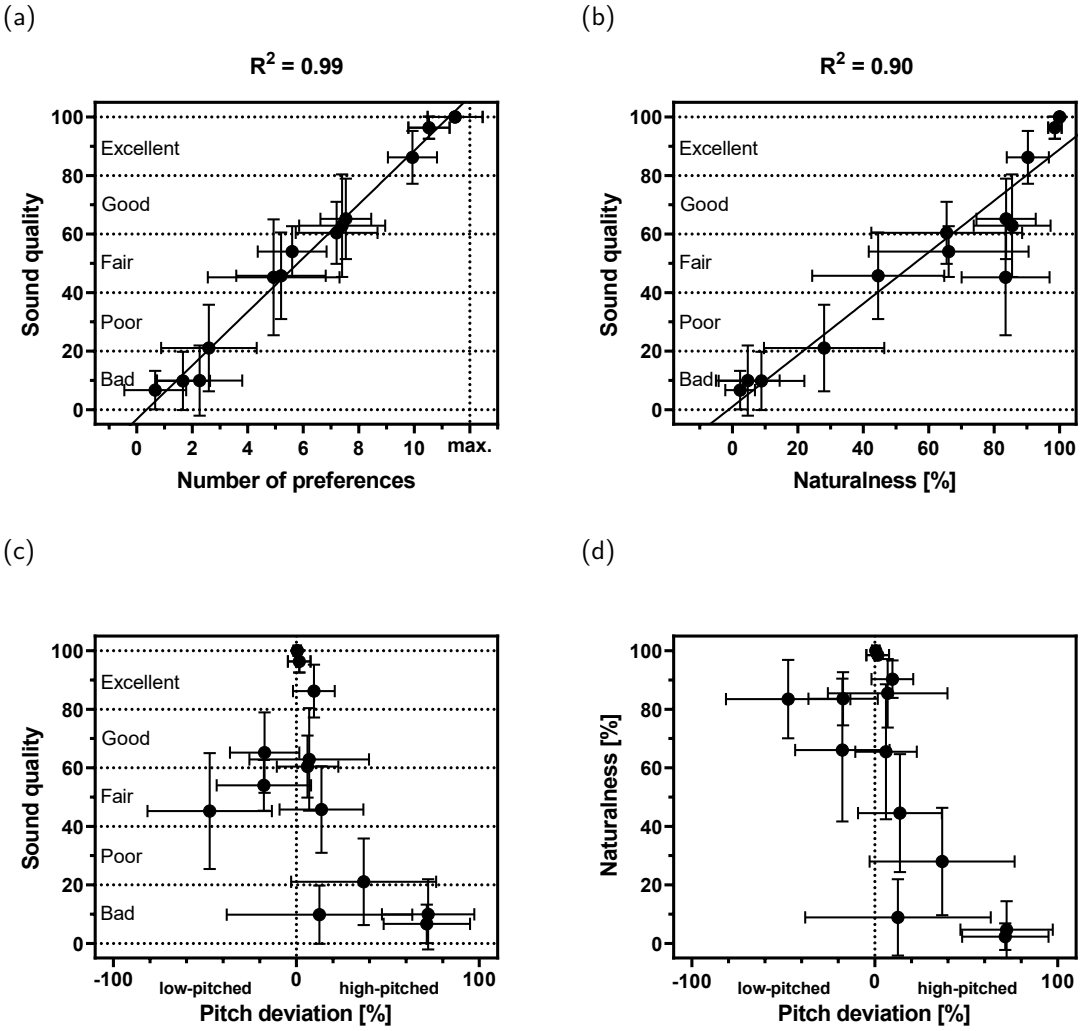

Figure 4.7: Relations between the means and standard deviations of (a) sound quality (Multi-Stimulus Test with Hidden Reference and Anchor, 'MUSHRA drag&drop', Völker et al. (2015)) and number of preferences, (b) sound quality and naturalness, (c) sound quality and pitch deviation and (d) naturalness and pitch deviation. Each point represents one cochlear implant (CI) simulation. The solid lines show linear regression curves, and the coefficient of determination R^2 is given on the graphs.

Figure 4.7 shows the means and SDs of the sound quality, number of preferences, naturalness and pitch deviation plotted against each other. The sound quality and

number of preferences, as well as naturalness and sound quality, showed significant linear correlations in Spearman correlation tests ($r_s(15) = 1.00$, $p < 0.05$ and $r_s(15) = 0.97$, $p < 0.05$, respectively, Figures 4.7a and 4.7b). For an excellent sound quality (> 80), a small pitch deviation ($< 20\,\%$) was necessary, but bad sound quality (< 20) occurred also with small pitch deviation. Large pitch deviations ($> 40\,\%$) led to fair to bad sound quality (Figure 4.7c). For a large naturalness ($> 90\,\%$) small pitch deviations were necessary, but pitch deviations to lower pitches produced also larger naturalness. Large pitch deviations ($> 60\,\%$) to higher pitch tended to lead to a reduction in naturalness (Figure 4.7d).

Comparison of Spectral and Psychoacoustic Analysis

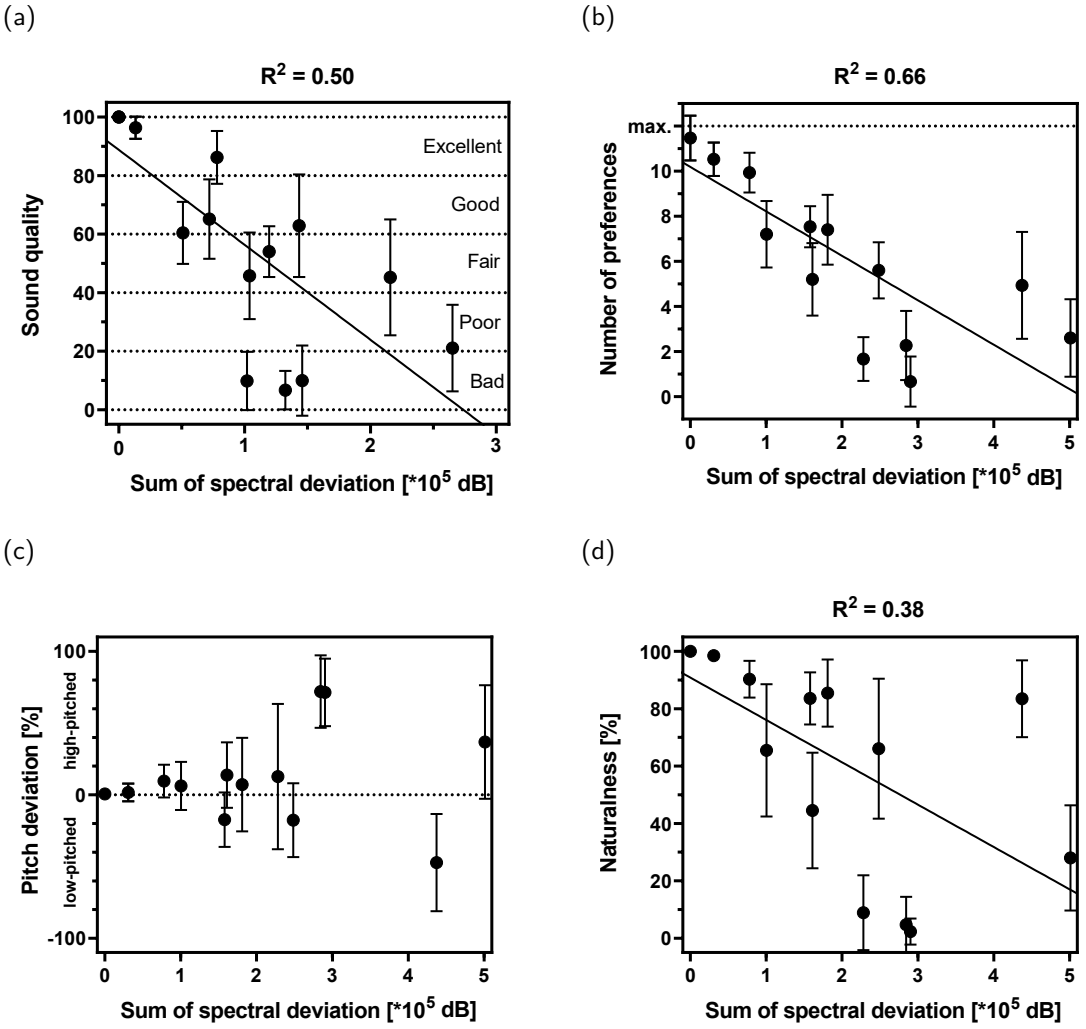

Figure 4.8: Relations between the means and standard deviations of (a) sound quality (Multi-Stimulus Test with Hidden Reference and Anchor, 'MUSHRA drag&drop', Völker et al. (2015)) and the sum of the spectral deviation, (b) number of preferences and the sum of the spectral deviation, (c) pitch deviation and the sum of the spectral deviation and (d) naturalness and the sum of the spectral deviation. Each point represents one cochlear implant (CI) simulation. Solid lines show linear regression curves, and the coefficient of determination R^2 is given on the graphs.

Figure 4.8 shows the means and SDs of the sound quality, number of preferences, naturalness and pitch deviation as a function of the sum of the spectral deviations for each simulation. Spearman correlation analysis identified significant correlations between the sound quality, number of preferences, naturalness and spectral deviation ($r_s(15) = -0.90$, $p < 0.05$, $r_s(15) = -0.90$, $p < 0.05$ and $r_s(15) = -0.82$, $p < 0.05$). In particular, the sound quality, number of preferences and naturalness increased with decreasing spectral deviation (Figures 4.8a, 4.8b and 4.8d). Figure 4.8c showed a reduced pitch deviation with smaller spectral deviation ($< 1.0 * 10^5$ dB).

4.4 Discussion

The aim of this chapter was to develop a new method for measuring the sound quality of CI sound via psychoacoustic and objective methods. The quantification of CI sound quality on the basis of CI simulations by normal hearing people assessment and by spectral analyses was suitable for comparing the sound quality aspects of different CI users.

The spectral (Figure 4.4, Figure 4.5), as well as the psychoacoustic evaluation of the CI simulations (Figure 4.6) confirm the individuality of sound perception. This is in good accordance with the results of Chapter 3 in which various modifications were required to create CI simulations for individual participants. Thus, the variability in CI simulations is reflected in the CI sound quality measures of this chapter. Further investigations are necessary to identify factors influencing this variability in CI sound quality.

The results of the single study tasks are consistent, since a more natural sound leads to a better sound quality (Figure 4.7b) and, e.g., a high-pitched sound leads to worse sound quality (Figure 4.7c). The assessment of sound quality in MUSHRA and in the pairwise comparison was based on different questions (comparison of the sound deviation from the reference signal or comparison of the sound quality among the simulations). Thus, the subjective pleasantness could influence the evaluation during the pairwise comparison, whereas these evaluation criteria may have a smaller effect during the MUSHRA. However, sound quality and the number of preferences were strongly linear correlated ($R^2 = 0.99$). This may be because the pairwise comparison task was used to identify a rough order in which the simulations on the GUI on the MUSHRA-scale were arranged or because the sound quality between each pair in the pairwise comparison was also assessed by the deviation from the reference signal, which was heard in the training task once by each participant.

The accuracy of the study design is shown since no (#205) or weak modifications (broad band-pass filter, #201) in the CI simulations lead to excellent sound quality, a large number of preferences, no or little pitch deviation and large naturalness (Figure 4.6). During the MUSHRA, all participants identified the hidden reference (#205). Furthermore, no participant scored the anchor signals (#204, #207) with a score larger than 90, which is important for sufficient reliability of the participant's evaluation (ITU-R 2015). The study cohort was very homogenous concerning the age. Sound quality is a measure that is dependent on human perception so that an age dependency of evaluation is possible. Since the focus of the MUSHRA and the semantic differential tasks was set on the sound quality in terms of deviation from the reference signal (= normal hearing), the age-dependent effect is considered rather small.

However, sound quality (MUSHRA), the number of preferences (pairwise comparison) and naturalness (semantic differential) show large statistical dispersion, especially for simulations with fair sound quality. At the edges of the scales (near 0 or 100, no unit or %, respectively), the statistical dispersion was smaller. The statistical dispersion of pitch deviation was small for simulations #201, #205 and #215, which are simulations with no or very weak sound modifications (Table A6, band-pass filters with broad passbands), but was larger for all other simulations. The large

statistical dispersion shows that sound quality is a very subjective, multidimensional quantity (Zwicker et al. 2007), that is rated very individually (Section 2.5).

As discussed in Section 2.5.1 and Section 4.1, most CI sound quality evaluations are based on subjective assessments by CI users themselves, e.g., questionnaires (self-reported CI sound quality, Amann et al. 2014). In such questionnaires, the CI sound of an individual can only be evaluated by that individual person. Particularly, with the results of this chapter on how individual sound quality is rated (large statistical dispersion), the statistical power of such questionnaires must be considered. By using the method introduced in this chapter, increasing statistical power by calculating averages over sound quality ratings of larger participant cohorts ($n > 1$) is possible. Nevertheless, this method does not substitute CI users' questionnaires or self-reported CI sound quality. First, this method is not applicable to all CI users because of the strict inclusion criteria (SSD) for generating CI simulations in Chapter 3. Generating CI simulations for bilateral or bimodal (hearing aid and CI) supplied persons using the method described above is currently not possible. Secondly, this method does not capture all aspects that a questionnaire does. As discussed in Section 3.4, CI simulations only offer an assessment of CI sound, they do not simulate other effects associated with cochlear implantation. Nonetheless, this newly developed method for recording sound quality can contribute to investigate factors influencing CI sound quality. A comparison of the self-reported CI sound quality assessed by the CI users participating in the study of Chapter 3 and the CI sound quality determined in this chapter would be interesting.

However, the aim of determining CI sound quality from CI simulations resulted from the individuality of CI simulations. For this reason, sound quality was not previously assessed via questionnaires in the study in Chapter 3. Since a change in sound quality with increasing CI experience is likely, a questionnaire was not made after the study in Chapter 3 had been completed.

In the validation study of the HISQUI_{19}, the authors analyzed data from 75 CI participants and reported a mean self-reported CI sound quality index of 75 (Amann et al. 2014). The original scale ranged from 19 to 133. When converted to a 0 to 100 scale such as the MUSHRA scale, this corresponds to a sound quality of 49 (Amann et al. 2014). Mertens et al. (2015) investigated data from the HISQUI_{19} (Dutch version) for 65 adult CI users and found a mean self-reported CI sound quality index of 65 ± 21 (converted to a 0 to 100 scale: 40 ± 2). Considering these results under conversion to the MUSHRA scale, both studies found, on average, fair sound quality. This study found on average a fair sound quality (51 ± 33) from CI simulations. Although direct comparisons between the sound quality outcomes of different study designs are difficult, as discussed in Section 2.5, due to lack of a consistent definition of sound quality, the results of this study are in good accordance with earlier studies (Amann et al. 2014; Mertens et al. 2020; Saki et al. 2023).

The subjective characteristics of sound quality, depending on the human perception, is one reason why there is no standard measuring tool to record sound quality objectively. The calculation of spectral deviation by subtracting the simulations' and references' spectrograms was an attempt to capture CI sound quality in terms of deviation from normal hearing since in treatment of hearing loss a small deviation from CI sound compared to normal hearing is desirable (Caldwell et al. 2017). Even

when considering the more objective method of calculating the spectral deviation, a certain degree of subjectivity is also involved here, since the CI simulations were determined and evaluated on the basis of subjective descriptions. The spectral deviation was significantly, moderately correlated with the sound quality, number of preferences and naturalness (Figure 4.8) and thus only roughly approximated these quantities. The simulation with the largest pitch deviation toward low pitches (simulation #207) was scored with fair sound quality, whereas simulations with similarly large pitch deviations toward high pitches were scored with bad sound quality (#203 and #206, Figure 4.7c). Thus, pitch deviations to high pitches showed a greater effect on the perceived sound quality than shifts to low pitches. This finding may be caused by the cognitive processing and the human perception. The calculated spectral deviation did not consider such differences in human perception. Thus, one possible approach to improve the objective measure of sound quality in a future project is to determine and use scaling factors that weight certain spectral cues according to human perception or a neural network model including several objective and subjective measures in a sound quality prediction model (e.g., Zhang et al. 2019).

4.5 Conclusions

The two new methods presented in this chapter were successfully used to quantify the sound quality of CIs on the basis of CI simulations. On average, a fair CI sound quality was found in the psychoacoustic experiment, which combined a pairwise comparison, MUSHRA and a semantic differential task. The objective method used to assess sound quality by calculation of the spectral deviation between CI simulations and reference signal showed a significant correlation with psychoacoustic results based on human perception. Although the psychoacoustic results for sound quality showed large statistical dispersion, both the psychoacoustic and the spectral results showed large variability in median sound quality.

Improvements in modeling or calculating sound quality via spectral analyses are possible in future projects by developing a neural network model. Further research is needed to explain the large interindividual differences in CI sound quality between CI simulations. One possibility is to investigate influencing factors such as etiology, duration of deafness, insertion depths, surgical techniques, implant types or CI experience.

5 Influencing Factors of Cochlear Implant Sound Quality

5.1 Background Information

Many studies have investigated factors influencing speech recognition (Blamey et al. 2013; Canfarotta et al. 2022; Hoppe et al. 2021; Kim et al. 2018; Lazard et al. 2012). Technical characteristics of CIs as well as patient-related data were investigated to predict or identify correlations to the postoperative speech recognition with CIs. To mention only a few investigated factors: electrode array design (perimodiolar or lateral wall), CI processor programming (e.g., percentage of active electrode contacts, Lazard et al. 2012), onset of deafness (pre- or postlingual), duration of deafness, preoperative performance (with or without hearing aid), hearing performance of the contralateral ear, etiology, and CI electrode array insertion depths (Blamey et al. 2013; Canfarotta et al. 2022; Hoppe et al. 2021; Kim et al. 2018; Lazard et al. 2012).

Moreover, Chapter 3 showed that even CI users with strong modifications in CI simulations were able to achieve a good speech recognition (#208, word recognition score at 65 dB SPL: 80 %, Table 3.3). Furthermore, Chapter 4 showed large inter-individual variability in CI sound quality determined from CI simulations. Gfeller et al. (2003) reported only a weak correlation between speech recognition during speech tests and sound quality in music perception. However, limited research has examined the factors that influence CI sound quality, which highlights the importance of investigating these influencing factors (Bessen et al. 2021; Gfeller et al. 2008; Mertens et al. 2015; Saki et al. 2023). These studies captured sound quality with questionnaires (e.g., HISQUI_{19}, Amann et al. 2014) or appraisal tests and investigated the correlation between self-reported CI sound quality and possible influencing factors. In particular, age at implantation, age at onset of hearing loss and CI experience moderately affect the self-reported sound quality (Bessen et al. 2021; Gfeller et al. 2008; Mertens et al. 2015; Saki et al. 2023). The methods used for measuring sound quality include many aspects, such as the ability to discriminate (e.g., HISQUI_{19}: 'Can you effortlessly hear the ringing of the phone?', Amann et al. 2014). Furthermore, these are self-reported sound qualities, so that there is only one rater for each sound quality and emotional factors in evaluation might be large. These studies receive statistical power by including a large number of participants ($n \geq 65$). Compared with these studies, in Chapter 4, the CI sound quality was investigated in terms of deviation in sound perception between a CI ear and a normal hearing ear. To date, no studies have investigated factors influencing CI sound quality defined in that way.

As discussed in Chapter 3, CI simulations are suitable for educational purposes, as they allow a realistic assessment of the sound perception of CI users through large

similarities with CI sound. As the CI sound is very individual, the CI simulation only simulates possibilities of CI sound. To provide extensive consulting further analysis of influencing factors is necessary. The aim of this chapter is therefore to investigate correlations between patient-related factors and CI sound quality parameters (CI sound quality, pitch and spectral deviation) determined from CI simulations.

5.2 Materials and Methods

A retrospective non-interventional, experimental data analysis of the CI participants' characteristics from Chapter 3 and the study results of Chapter 4 was conducted. The ethical review board of University Medicine Halle approved the study protocol and the informed consent forms with approval number: 2023-144.

The participants' data were previously collected within the study described in Chapter 3 and from the corresponding patient records (approval number: 2022-048).

5.2.1 Data Analysis

Data analysis and visualization were performed using the software Prism[46], SPSS[47] and Inkscape[48]. The CI sound quality parameters and CI participants' data were graphically visualized as scatter plots to identify possible influencing factors. Additionally, correlations between sound quality and spectral deviation and participants' data were analyzed by linear and non-linear regression. Coefficients of determination were calculated.

The following participants' data were used for investigation: electrode array design (implant type), percentage of active electrode contacts, duration of deafness/onset of deafness, maximum preoperative word recognition score (unaided), preoperative word recognition score in the Freiburg monosyllable test (Hahlbrock 1953) in open sound field with frontal presentation at 65 dB SPL with hearing aid, 4PTA of the contralateral ear, postoperative word recognition score at 65 dB SPL with CI, etiology, age at implantation, CI experience, social activity level, age at study participation, average CI usage time recorded from the data logging of the processor, sex, surgical technique (cochleostomy, subtotal cochlectomy, round window approach), anatomical data (cochlear size, malformations), CI electrode array insertion angle and intracochlear spread of the electric field (transimpedances).

To evaluate the spread of the electric field, the SCINSEV method of Cochlear Ltd.[49] called transimpedance measurement was used (Section 2.3). Investigated transimpedances were measured postoperatively with stimulation currents of 100 or 110 current level in 'MP2 Stim Rec' measurement mode. The pulse width and measurement time point were 37 μs. Incomplete transimpedance recordings caused by open or short circuits were excluded from the investigation. As a characteristic parameter for transimpedances, the percentage decrease in neighboring electrode

[46]Prism, GraphPad Software (2020), version 8.4.3
[47]SPSS, IBM (2021), version 28.0.0.0
[48]Inkscape, Inkscape Community (2003), version 1.2
[49]Custom Sound EP Software, Cochlear Ltd. (2020), Sydney, Australia, version 6.0

contacts was calculated for a basal (E4), medial (E12) and apical (E19) electrode contact. According to Wagner et al. (2025), the off-diagonal transimpedance values were used as reference values. The percentage decrease to the second neighbor electrode contact was calculated toward the apical and basal directions (Wagner et al. 2025). Both decreases (toward the apical and basal) were averaged. The random error of transimpedance measurement was set to 0.2 % (Kopsch 2021). Gauss' law of error propagation was used to determine the error of the percentage decrease in transimpedances.

Anatomical data were measured from preoperative CT or CBCT, with primary slice thicknesses smaller than 0.6 mm. CT or CBCT data were evaluated in the software Otoplan[50]. The diameter A, width B, height H and CDL were measured according to Section 2.6.1 with automatic detection. The automatically set markers for determining the specified lengths were subsequently visually inspected and optimized if deviations between automatic detection and visual detection occurred. The measurement error was estimated for diameter A, width B and height H for each participant's CT or CBCT, individually. Gauss's law of error propagation was used to determine the error of CDL.

The electrode array insertion angles were measured from postoperative CT, CBCT or planar X-ray images. Planar X-ray images had to be recorded in Stenver, cochlear or Altschul view (Section 2.6.2, Figure2.10). Planar X-ray images were excluded from investigation if the anatomical structures (superior semicircular canal, vestibule) or the most apical electrode contact were not identifiable (Figure 2.13). If multiple postoperative images were available, a tomographic image was preferred over planar imaging. Insertion angle measurements were performed according to the description in Section 2.6.2 (Figure 2.11b, Marsh et al. 1993; Cohen et al. 1996; Xu et al. 2000) using the image processing software ImageJ[51].

5.2.2 Estimation of Insertion Angle Precision

As described in Section 2.6.2, to measure the insertion angle adequately from planar X-ray images, X-ray imaging should be performed in the cochlear view (Xu et al. 2000). To estimate the systematic error that occurred in the insertion angle measurement due to deviations from the cochlear view, a three-dimensional (3D) model was created.

The 3D model was based on the CBCT data of participant #204 with a primary slice thickness of 0.125 mm (Figures 5.1a and 5.1c). The requirements for the data set for the 3D model were availability of pre- and postoperative CBCT data from the same patient, absence of malformation or incorrect electrode array placement, and that the cochlea did not have a particularly large ($>$ 40 mm) or small CDL ($<$ 28 mm, Távora-Vieira et al. 2023). The CDL of participant #204 was 35.3 mm, and the CI electrode array type was CI512 (Cochlear Ltd. 2022a).

For further processing the pre- and postoperative CBCT data were anonymized. The inner ear was reconstructed in the software Otoplan[50] and exported in an STL file

[50] Otoplan, Cascination AG, Bern, Switzerland in cooperation with MED-EL, Innsbruck, Austria, version 3.0.0

[51] ImageJ, Rasband (1997), version 1.54p

format (Figure 5.1b). The electrode array was reconstructed from the postoperative CBCT with the software 3D Slicer[52] and was also exported in an STL file format. The 3D model of the electrode array was revised with the software FreeCad[53] by removing of the extracochlear electrode array cable. The 3D models of the electrode array and inner ear were fused in Python[54] in the integrated development environment Spyder[55] with the library Open3D[56] (Figure 5.1d). Fusion was conducted by visual adjustment according to the postoperative CBCT data.

Electrode contacts were modeled by 35 spheres aligned along the electrode array model. The modeled electrode contacts served as fixed measurement points to measure the insertion angles. Six further electrode contacts were inserted at the electrode array model tip, following the spiral trend of the electrode array model (Figure 5.1e). The 3D model was rotated to the cochlear view by comparison with the cochlear view of the pre- and postoperative CBCT (Figures 5.1a and 5.1c).

The center points of the superior semicircular canal, vestibule and electrode array (approximation for the modiolus) were identified by extracting the superior semicircular canal, vestibule and upper part of the electrode array from the 3D model.

The semicircular canal and the vestibule were extracted with the software FreeCad[53] from the 3D model (Figure 5.1f). The STL files of the 3D models included the surface of the models as triangulated mesh. The center point of the vestibule was calculated by averaging the coordinates of each triangle for the three directions in space individually. The apex point of the semicircular canal was calculated by using the projection in the cochlear view to calculate the center point coordinates in the x and y directions (the coordinate system was defined according to that presented in Figure 5.1g) by averaging the relevant coordinates. The z-coordinate for the center point was calculated by averaging all the z-coordinates of all the triangles of the extracted semicircular canal model. The center point of the electrode array model was calculated by averaging the coordinates of the 22 most apical electrode contact spheres. The center points were marked with green spheres (Figure 5.1g).

To simulate variations in the X-ray projection technique, the 3D model was rotated around two axes. The angle between the midsagittal plane and the X-ray detector, as well as the angle between the IOML and the central beam (Figure 2.10) was simulated by rotating the 3D model around the y (angle α) and x-axes (angle β, Figures 5.1g and 5.2). α and β angle model therefore variations in angles between the midsagittal plane and the X-ray detector and between the IOML and the central beam, respectively (Section 2.6.2, Figure 2.10).

The cochlear view was used as the reference view with $\alpha = \beta = 0\,^{\circ}$. Figure 5.2 shows the extrinsic rotation of the 3D model. Extrinsic means, that rotation was performed around the primary, fixed coordinate axes x, y, z not around the new, rotated coordinate axes x, y and z. The first rotation was around the y-axis (angle α), and the second rotation was around the x-axis (angle β, Figure 5.2). Equation 5.1 gives the calculation formula for the rotation matrix. Rotation was performed by

[52] 3D Slicer, The Slicer Community (2025), version 5.6.1
[53] Freecad, Riegel et al. (2001), version 0.21.2
[54] Python, van Rossum (1991), version 3.9.7
[55] Spyder, Raybaut (2009), version 5.1.5
[56] Open3D, Zhou et al. (2018), version 0.19.0

(a)

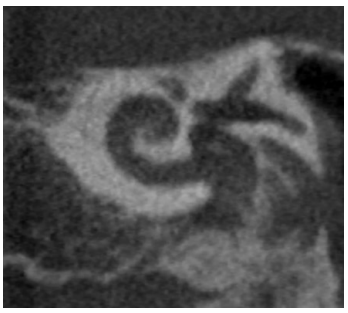

(b)

(c)

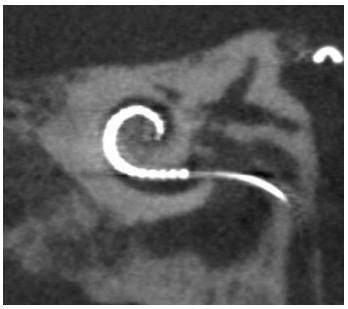

(d)

(e)

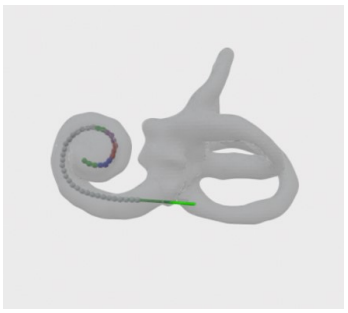

(f)

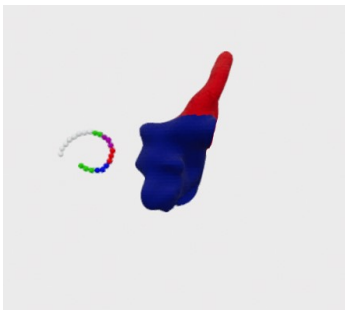

(g)

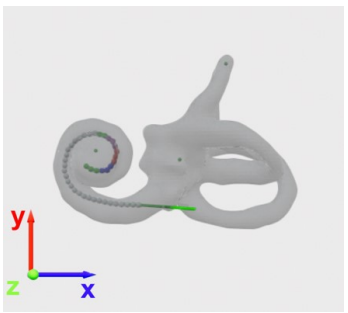

(h)

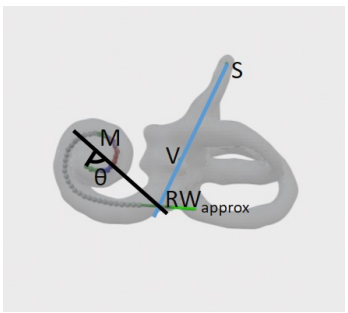

Figure 5.1: Design of the 3D model for estimation of systematic error in insertion angle measurement due to deviations from the cochlear view. (a) Preoperative cone-beam computed tomography (CBCT) data of participant #204 in the cochlear view (coronal). (b) Inner ear reconstruction from the data in (a) shown as a 3D model. (c) Postoperative CBCT data of participant #204 in the cochlear view (coronal). (d) Fused electrode array and inner ear 3D model. Electrode array model was inserted into the 3D model in (b) according to the view in (c). (e) Electrode contacts modeled as spheres aligned along the electrode array model in the inner ear model. Apical, colored electrode contact spheres mark electrode contacts used for insertion angle measurements. (f) Structures used to define markers for insertion angle measurements. Apical electrode contact spheres (modiolus approximation) and the vestibule model used for center point definition. Superior semicircular canal volume for apical point definition. (g) Complete 3D model and definition of the coordinate systems. The green spheres mark the markers used for the insertion angle measurements. (h) 3D model shown in the projection angle $\alpha = \beta = 0\,^\circ$ with markers and reference lines for insertion angle measurement according to Xu et al. 2000. M: modiolus, S: superior semicircular canal, V: vestibule, RW: round window, Θ: insertion angle
Radiological data were made available with the kind permission of Prof. Kösling (Department of Radiology, Martin Luther University Halle-Wittenberg, University Medicine Halle, Halle, Germany).

multiplying the rotation matrix 5.3 and all coordinates of the 3D model.

$$R = R_z(\gamma = 0) \cdot R_x(\beta) \cdot R_y(\alpha) \tag{5.1}$$

$$= \begin{pmatrix} 1 & 0 & 0 \\ 0 & 1 & 0 \\ 0 & 0 & 1 \end{pmatrix} \cdot \begin{pmatrix} 1 & 0 & 0 \\ 0 & \cos(\beta) & -\sin(\beta) \\ 0 & \sin(\beta) & \cos(\beta) \end{pmatrix} \cdot \begin{pmatrix} \cos(\alpha) & 0 & \sin(\alpha) \\ 0 & 1 & 0 \\ -\sin(\alpha) & 0 & \cos(\alpha) \end{pmatrix} \tag{5.2}$$

$$= \begin{pmatrix} \cos(\alpha) & 0 & \sin(\alpha) \\ \sin(\alpha)\sin(\beta) & \cos(\beta) & -\sin(\beta)\cos(\alpha) \\ -\sin(\alpha)\cos(\beta) & \sin(\beta) & \cos(\alpha)\cos(\beta) \end{pmatrix} \tag{5.3}$$

The 3D model was validated by comparing the insertion angles of the 3D model (last electrode contact sphere covered completely by the electrode contact model, Figure 5.1e) measured in the cochlear view ($\alpha = \beta = 0\,^\circ$) and CBCT data (Figure 5.1c).

Insertion angle measurements were performed for the 14 most apical, colored electrode contact spheres (Figure 5.1h). Measurements were performed for variable α and β projection-angles. α was varied between $0\,^\circ$ and $-55\,^\circ$ in steps of $5\,^\circ$ and β was varied between $-20\,^\circ$ and $45\,^\circ$ in steps of $5\,^\circ$. The image processing software ImageJ[57] was used for the insertion angle measurements. The insertion angles were measured according to the method described in Section 2.6.2. Figure 5.1h shows one exemplary measurement on the basis of the 3D model for one projection angle ($\alpha = \beta = 0\,^\circ$). The round window is approximated by the intersection of the line

[57] ImageJ, Rasband (1997), version 1.54p

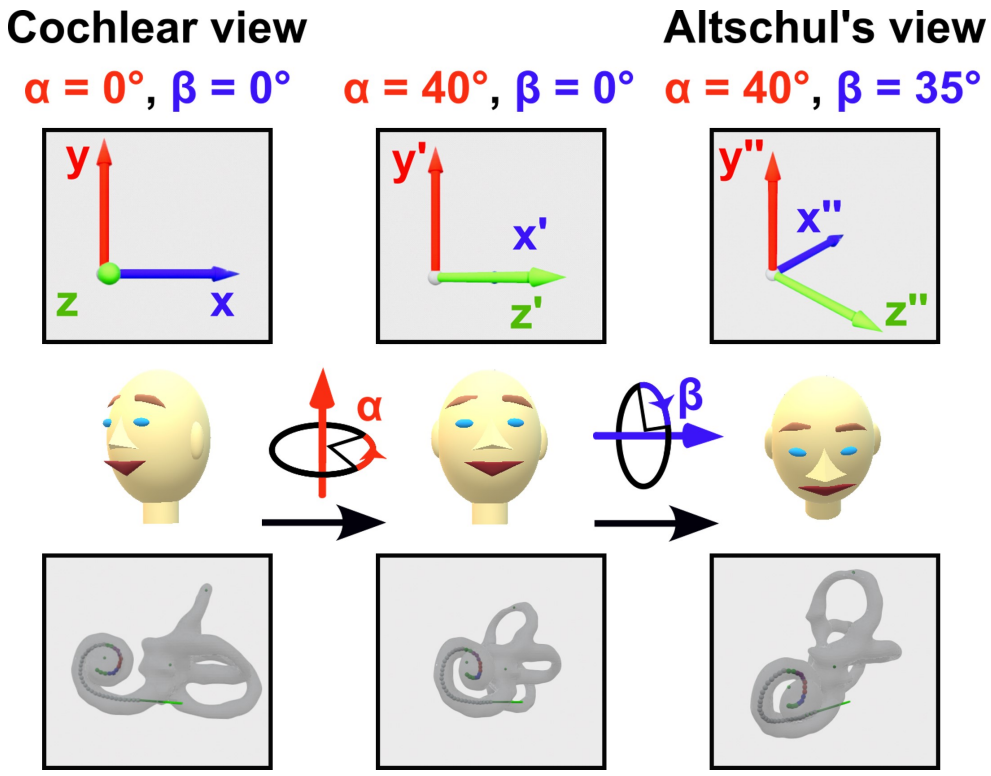

Figure 5.2: Schematic visualization of the extrinsic rotation of the 3D inner ear model, associated head positions and coordinate systems for variable projections (from the cochlear view to the Altschul view). Definition of the coordinate systems and rotation axes.

connecting the apex of the superior semicircular canal and the centrum of the vestibule (green spheres) with the electrode array. The reference line was drawn from the modiolus approximation to the round window approximation. The insertion angle was measured from each of the colored electrode contact spheres relative to the reference line (Marsh et al. 1993; Cohen et al. 1996; Xu et al. 2000).

The relative error related to the insertion angle in the cochlear view of each electrode contact sphere was calculated. The relative errors were analyzed as a function of the two projection angles α and β.

5.3 Results

5.3.1 Precision of Insertion Angle Measurement

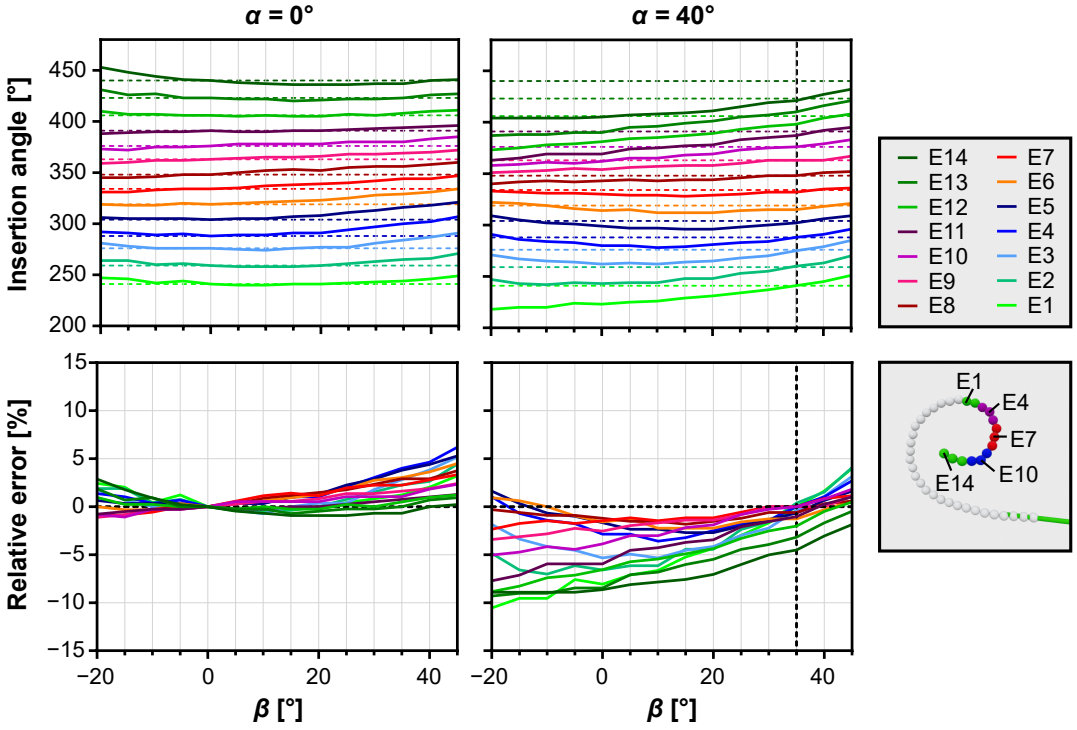

Figure 5.3: Insertion angles and its relative errors measured for all electrode contact spheres (E1 to E14) from the 3D inner ear model for variable β projection angles and two fixed α projection angles ($\alpha = 0\,^\circ$ and $40\,^\circ$). The errors were calculated relative to the insertion angles measured in the cochlear view ($\alpha = \beta = 0\,^\circ$). The colored dashed lines represent insertion angles measured in cochlear view for each electrode contact sphere. The black vertical line represents the projection angle for Altschul view.

The 3D model of the inner ear is shown in Figure 5.1g. The insertion angle of the last electrode contact sphere covered completely by the electrode contact model had an insertion angle of $347\,^\circ$ and the CBCT led to an insertion angle of $344\,^\circ$ for the most apical electrode contact. This corresponds to a relative error of $0.9\,\%$ in the insertion angle between the 3D model and the CBCT data.

Figure 5.3 shows the insertion angles and relative errors for variable β projection angles and two fixed α projection angles ($\alpha = 0\,^\circ$ and $40\,^\circ$). For $\alpha = 0\,^\circ$, the relative error increased with increasing deviation from the cochlear view ($\beta = 0\,^\circ$). The relative error depends on the absolute insertion angle/position of the electrode contact sphere within the cochlea. For $\alpha = 40\,^\circ$, the relative error decreased for larger β-values. For $\alpha = 40\,^\circ$ and $\beta = 35\,^\circ$, which corresponds to Altschul view (Figure 2.10), the relative error was smaller than $5\,\%$ (absolute value) for all electrode contact spheres but increased if β decreased. For deep inserted electrode contact spheres and $\beta = -20\,^\circ$ the relative error is around $10\,\%$ (absolute value). Figure 5.4 shows the relative errors of the insertion angles for the 14 electrode contact spheres as a function of the α and β projection angles. The relative error is color coded and

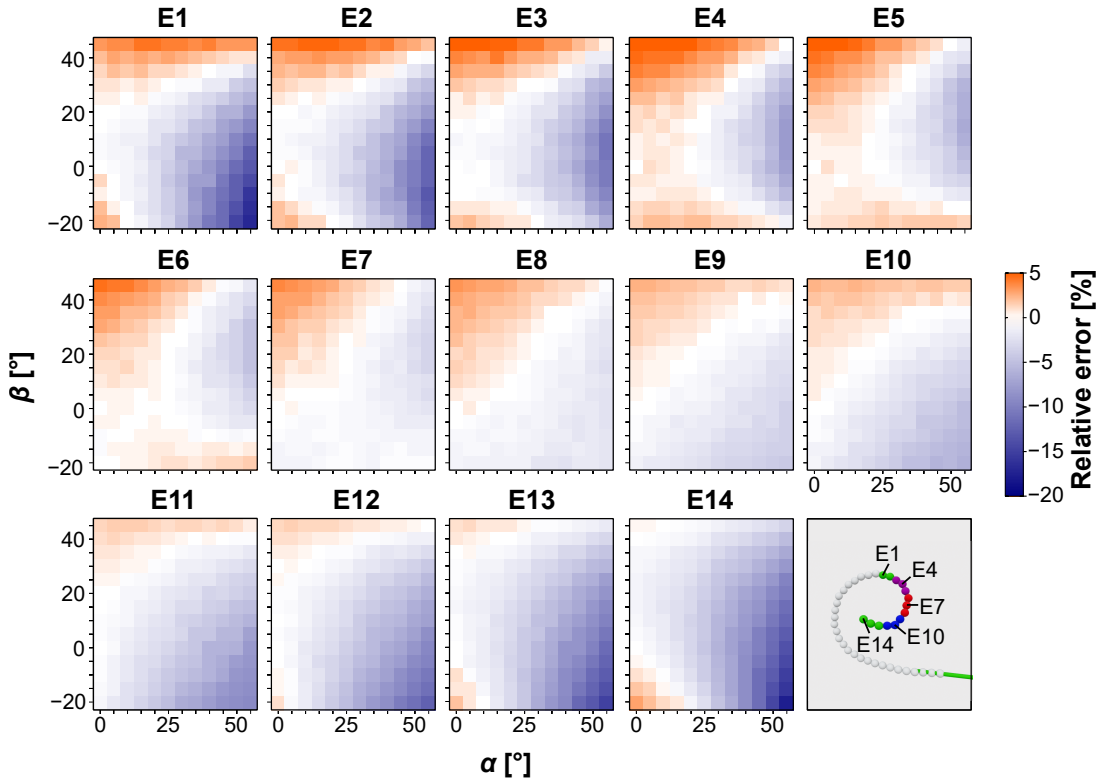

Figure 5.4: Heatmaps of the relative errors of the insertion angles measured for all electrode contact spheres (E1 to E14) from the 3D inner ear model for variable α and β projection angles. The errors were calculated relative to the insertion angles measured in the cochlear view ($\alpha = \beta = 0\,°$).

varied as a function of the projection angles as well as a function of electrode contacts. Both negative and positive relative errors occurred. Relative error averaged over all electrode contacts spheres and over the considered range of projection angles was $(2.6 \pm 2.8)\,\%$. For further consideration, it is assumed, that the relative error of the insertion angle from planar X-ray images was smaller than $10\,\%$ (Figure 5.3).

5.3.2 Influencing Factors of Cochlear Implant Sound Quality

This retrospective data analysis included CI sound quality parameters and patient-related data from 15 CI participants who participated in the study described in Chapter 3, (Cross-Sectional Study after at Least 2 Years of CI Experience). As inclusion criteria (Section 3.2), all CI participants had a CI indication acquired postlingually. Table 3.3 shows all the participants' data queried during the study visit. Further data (maximum preoperative word recognition score (unaided), preoperative word recognition score in the Freiburg monosyllable test in open sound field with frontal presentation at 65 dB SPL with hearing aid, surgical technique, cochlear diameter, cochlear width, cochlear height, CDL, CI electrode array insertion angle and transimpedances) were registered from the corresponding patient records.

An investigation of the influence of the number of deactivated electrode contacts on CI sound quality was not performed since only one participant had two deactivated electrode contacts ($n = 1$, #210). No participant had an inner ear malformation.

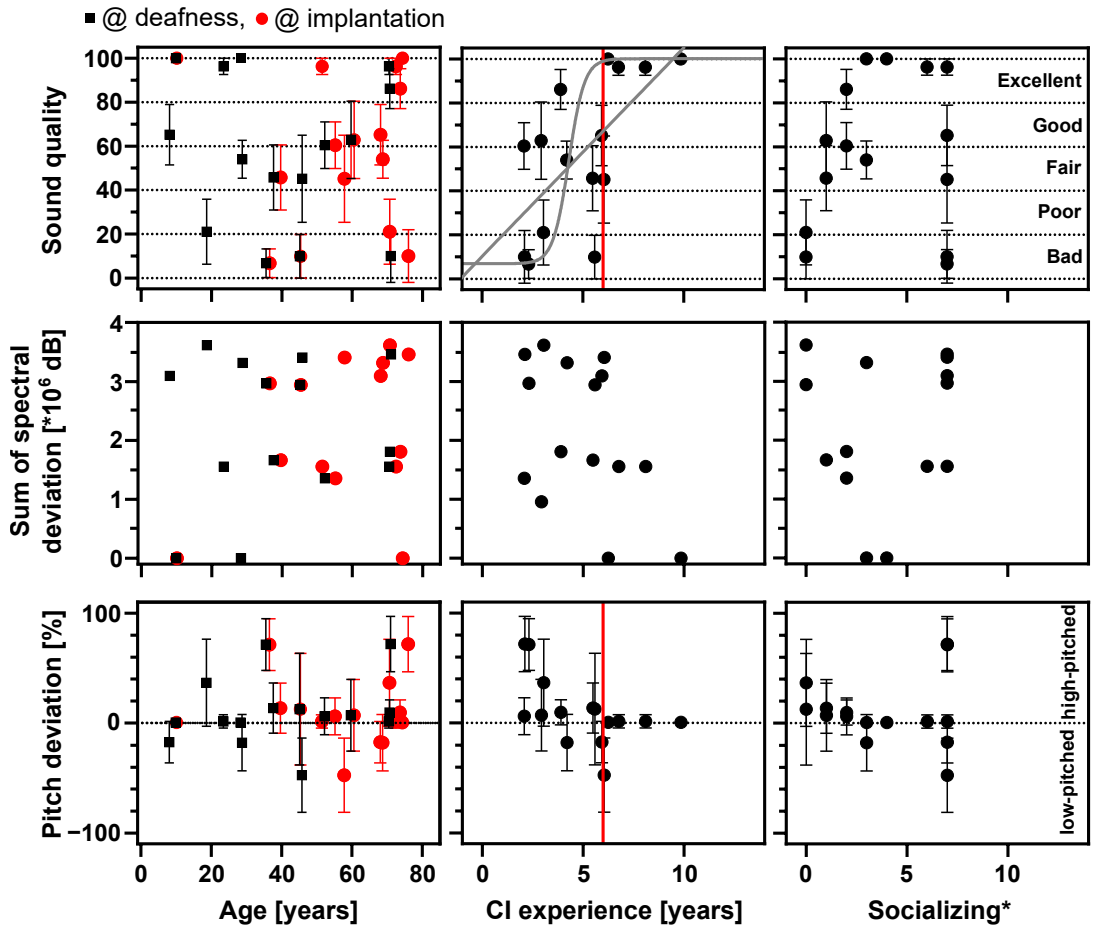

Figure 5.5: Relations between cochlear implant (CI) sound quality parameters (CI sound quality, pitch and spectral deviation) and age at onset of deafness, age at implantation, CI experience and social activity level, respectively. The gray curves are linear regression and logistic regression lines ($R^2_{linear} = R^2_{logistic} = 0.41$). The red line marks 6 years of CI experience, where the sound quality saturates with CI experience. All further factors showed no correlation ($R^2 \leq 0.2$).
* Social activity level was queried by asking 'How many times in the last 7 days have you met friends or talked to friends on the phone for more than 5 minutes?'.

For 12 CI participants the preoperative word recognition score in the Freiburg monosyllable test in open sound field with frontal presentation at 65 dB SPL with a hearing aid was not documented in the patient records. For this reason, an investigation of this factor was not performed.

Figure 5.5 shows scatter plots of CI sound quality parameters and age at onset of deafness, age at implantation, CI experience and social activity level, respectively. For all of these factors, complete data sets were available. Age at onset of deafness and age at implantation were not correlated with sound quality, spectral deviation ($R^2 \leq 0.2$) and pitch deviation. CI experience showed moderate linear and logistic correlation with sound quality ($R^2_{linear} = R^2_{logistic} = 0.41$). The sound quality and pitch deviation varied strongly for CI experiences smaller than 6 years, but saturated

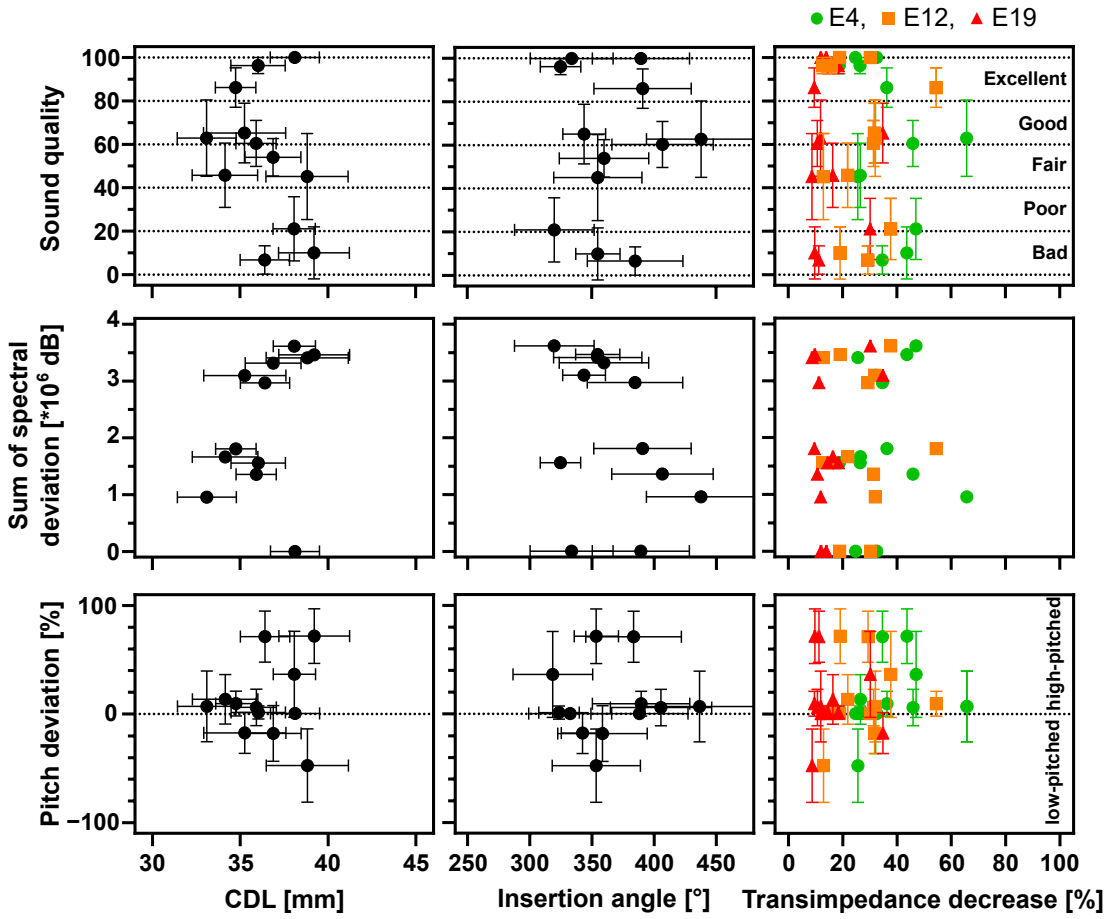

Figure 5.6: Relations between cochlear implant (CI) sound quality parameters (CI sound quality, pitch and spectral deviation) and the cochlear duct length (CDL), insertion angle and transimpedance decrease at electrode contacts E4, E12 and E19, respectively. Error bars of the insertion angles measured from cone beam computed tomography (CBCT) represent $5\,\%$ of the measured values. Error bars of the insertion angles measured from planar images represent $10\,\%$ of the measured values. The measurement errors of the CDL and transimpedance decrease were calculated with Gauss's law of error propagation. The transimpedance decrease errors were smaller than $0.3\,\%$ for all the data points, so that error bars were neglected. No factor was correlated with CI sound quality or spectral deviation ($R^2 \leq 0.2$).

to excellent sound quality and no pitch deviation for large CI experiences (> 6 years). CI experience and spectral deviation, as well as social activity level and CI sound quality parameters were not correlated ($R^2 \leq 0.2$). Sound quality increased for increasing social activity levels up to three social contacts per week, saturated up to six social contacts and varied strongly for seven contacts per week. The pitch deviation decreased for increasing social activity levels up to three social contacts per week and varied strongly for seven contacts per week.

Figure 5.6 shows scatter plots of CI sound quality parameters and CDL, insertion angle and transimpedance decrease at electrode contacts E4, E12 and E19, respectively. For participants #205, #208 and #214 no preoperative CT or CBCT data with primary slice thicknesses smaller than 0.6 mm were available. Thus, for 12 CI

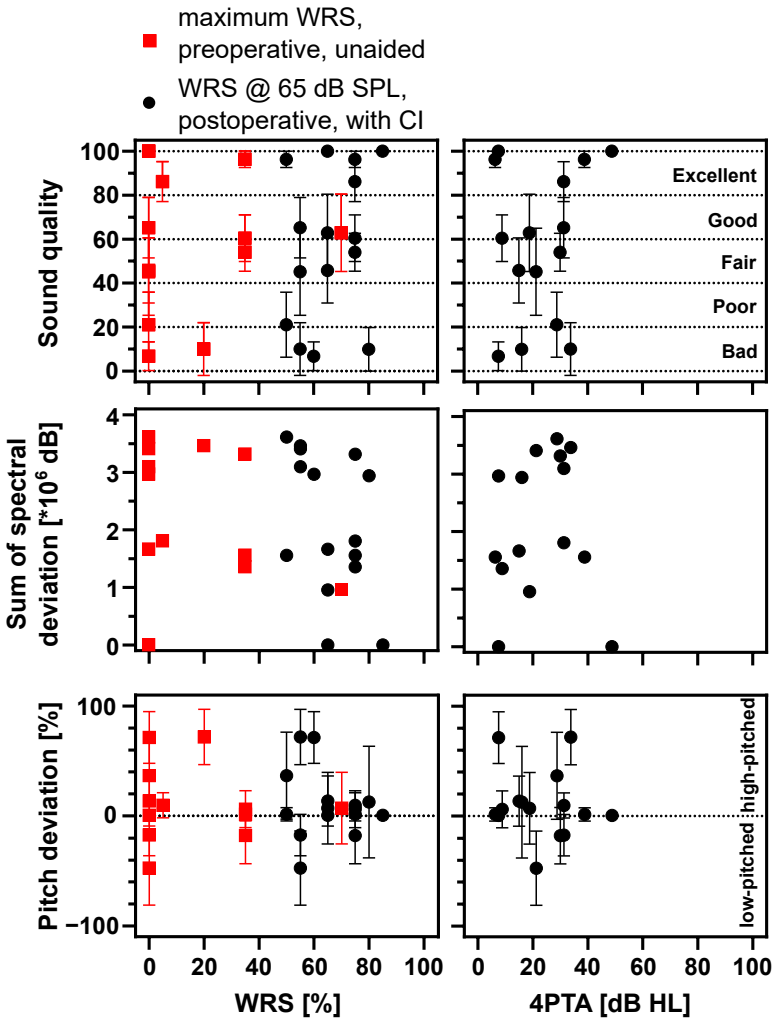

Figure 5.7: Relations between cochlear implant (CI) sound quality parameters (CI sound quality, pitch and spectral deviation) and the maximum preoperative word recognition score (WRS, unaided), postoperative WRS at 65 dB SPL with CI and four frequency pure tone average (4PTA), respectively. No factor was correlated with CI sound quality or spectral deviation ($R^2 \leq 0.2$).

participants, the CDLs were measured. The mean (± SD) CDL was (36.4±2.0) mm. For participants #202, #208 and #214 the insertion angle could not be measured from postoperative radiological images, caused by a lack of availability or unfavorable projection (last electrode contact was projected on the residual electrode array). Insertion angle data were available for 12 participants. The mean (± SD) insertion angle was (368 ± 38) °. A postoperative measured CBCT was available for three participants. Nine participants had postoperative planar X-ray images in Altschul view. Transimpedances were available for 13 participants. The scatter plots in Figure 5.6 show no correlation between the described factors ($R^2 \leq 0.2$).

Figure 5.7 shows scatter plots of CI sound quality parameters and maximum preoperative word recognition score (unaided), postoperative word recognition score at 65 dB SPL with CI and 4PTA, respectively. The preoperative maximum word recognition score was not available for participants #208 and #214. Thus, for 13 participants, an evaluation was possible. The 4PTA and the word recognition score

with CI were available for all participants. However, the data considered in Figure 5.7 show no correlation between the described factors ($R^2 \leq 0.2$).

Further scatter plots with possible influencing factors, such as duration of deafness, age at study participation, usage time, cochlear size (height H, width B, diameter A), electrode array type, etiology, sex and surgey technique, are shown in Figures A1 and A2 in the Appendix. The surgical technique was not available for participants #208 and #214. For 12 CI participants height H, width B and diameter A were available (see above). For all other factors, data sets were available from all 15 CI participants. All factors shown in Figures A1 and A2 in the Appendix, had no correlation with the sound quality, the spectral deviation or pitch deviation (Figure A1: $R^2 \leq 0.2$).

5.4 Discussion

5.4.1 Influencing Factors of Cochlear Implant Sound Quality

The aim of this chapter was to investigate the correlations between patient-related factors and CI sound quality parameters (CI sound quality, pitch and spectral deviation) determined from CI simulations. Mainly, a correlation between CI sound quality and CI experience was found (> 6 years, $R^2_{linear} = R^2_{logistic} = 0.41$). Especially, a saturation of sound quality and pitch deviation of excellent quality, and no deviation was observed if the CI experience was large. The sound perception of the CI participants with more than 6 years CI experience closely approximates the sound perception of a normal hearing ear. In this study, however, only CI simulations of fully rehabilitated CI users were considered (Chapter 4). Thus, even after two years of CI experience and completion of the 'follow-up therapy' (Section 3.1), the CI sound quality may change.

The correlation between CI sound quality and CI experience is in accordance with e.g., Reiss et al. (2007) and McDermott et al. (2009). They found in acoustic to electric pitch-matching experiments that pitch perception and perceived frequency-to-place mismatch changed with CI experience (McDermott et al. 2009; Reiss et al. 2007). Additionally, Bessen et al. (2021) found that self-reported CI sound quality and CI enjoyment were significantly positively correlated with CI experience. These findings highlight the importance of learning, adaptation and neuronal plasticity in the rehabilitation of CI users and CI sound quality. The results of this chapter showed that CI sound quality, in terms of deviation in sound perception with CI compared to a normal hearing ear, can change with CI experience.

Dorman et al. (2022) reported little to no change in CI sound (especially in pitch) within the first 3 years of CI experience and concluded that the CI sound cannot be compensated by neuronal plasticity during this time period if CI users have short electrode arrays. However, our data analysis of cochlear size (CDL, height H, width B, diameter A), and the insertion angle showed no correlation with CI sound quality parameters (Figure 5.6 and A1). In this study , the mean ($\pm$ SD) CDL and insertion angle was (36.4 ± 2.0) mm and $(368 \pm 38)\,^\circ$, respectively. These findings were comparable with those of previous studies, e.g., Paouris et al. (2023) reported a mean CDL of (35.5 ± 1.9) mm for automatically detected CDLs with the software

Otoplan[58] in 109 ears and Landsberger et al. (2015) found a mean insertion angle of $(381 \pm 51)^\circ$ for 44 implanted CIx12[59] electrode arrays.

Hearing loss or deafness leads to functional reorganization of the central auditory system (Kral et al. 2016; McKay 2018). Thus, the ability of an individual's nervous structures in the brain to reorganize and adapt itself to new stimuli (Bernhardi et al. 2017), postoperatively, is highly relevant. It is reasonable that CI sound quality also depends on the strength of preoperative reorganization of the central auditory system or the incidence of exposure to new stimuli postoperativly. Since this study was a retrospective data analysis, factors that measure preoperative reorganization directly, such as electroencephalography (EEG), were not included in the data analysis. Instead, this research investigated the duration of deafness, the age at onset of deafness, the age at implantation and the age at study participation, which may be related indirectly to the preoperative reorganization of the nervous system. CI usage time and social activity level were examined as factors for the incidence of exposure to new stimuli that affect postoperative reorganization.

However, none of these factors were correlated with the CI sound quality parameters in this study. Bessen et al. (2021) reported significant, moderate correlations between self-reported CI sound quality and age, age at implantation and age at onset of hearing loss (r between -0.3 and -0.4, Bessen et al. 2021). Saki et al. (2023) found no correlation between age at implantation and self-reported CI sound quality, but found a significant correlation between duration of deafness and CI sound quality. Mertens et al. (2015) found a moderate correlation between age at study participation and self-reported CI sound quality ($r = 0.35$, Mertens et al. 2015). Thus, previous studies have identified different influencing factors. The differences in the results from the literature in comparison to the results of this data analysis can be explained by the investigation of different sound qualities. Previous studies have considered only self-reported CI sound quality, whereas the approach presented in this thesis is based on the evaluation of the sound quality of CI simulations. As described in Section 2.5.1, most questionnaires used to measure self-reported sound quality include many factors, such as the ability of discrimination (e.g., HISQUI_{19}: 'Can you effortlessly hear the ringing of the phone?', Amann et al. 2014) but personal, emotional and psychological factors also have a large impact since each sound quality is only rated by one rater (self-reported). Since a small deviation from a CI sound compared with normal hearing is desirable (Blauert et al. 1997), this thesis focused on CI sound quality in terms of the deviation in sound perception between a CI ear and a normal hearing ear. On the one hand, it was evaluated by normal hearing people, and on the other hand, evaluated by a more objective method by calculating the spectral deviation of the CI simulations compared with the reference signal. Considering different sound qualities results in a limited comparability of the literature with these data analyses.

This data analysis also revealed no correlations between the sound quality parameters and implant type and sex, respectively (Figure A2), which is in accordance with previous studies (Gfeller et al. 2008; Mertens et al. 2015; Saki et al. 2023). Large spread of the electric field, leads to 'spectral smearing' that showed a moder-

[58] Otoplan, Cascination AG 2024, Bern, Switzerland in cooperation with MED-EL, Innsbruck, Austria, version 3.0.0

[59] Cochlear Ltd., Sydney, Australia

ate correlation with the spread of excitation in previous studies (Kopsch et al. 2022; Söderqvist et al. 2021), leading to a reduced spectral resolution (Bingabr et al. 2008; Tang et al. 2011; van den Honert et al. 1987; Zeng et al. 2014; Zwolan et al. 1997). For that reason, a moderate correlation of transimpedances and CI sound quality was expected (Section 2.4). However, this data analysis showed no effect of the spread of the electric field (transimpedance decrease) on CI sound quality parameters (Fgure 5.6). A possible explanation is that investigated transimpedances were measured at different time points, postoperatively, whereas Wagner et al. (2025) found a change of transimpedances in time course. To reduce this effect, transimpedance data measured at a specific time point would have had to be analyzed.

Many studies have investigated factors influencing speech recognition (Blamey et al. 2013; Canfarotta et al. 2022; Hoppe et al. 2021; Kim et al. 2018; Lazard et al. 2012) and have reported several factors and prediction models (Sections 5.1 and 2.4). It has been suggested that the factors that influence speech recognition also influence CI sound quality. The data analysis showed no correlation between CI sound quality parameters and pre- or postoperative word recognition scores (Figure 5.7). This fits with the results of Gfeller et al. (2003), who reported only a weak correlation between speech recognition and sound quality in music perception, whereas Mertens et al. (2015) reported a moderate effect of speech recognition on self-reported CI sound quality ($r = 0.36$, Mertens et al. 2015). As already discussed in Section 3.4, CI sound perception and CI sound quality do not have to be linked with speech recognition.

This remarkable discrepancy between CI sound quality and word recognition raises important questions regarding the underlying mechanisms involved. In particular, some participants had excellent sound quality but were unable to achieve full speech recognition (e.g., #205, word recognition score at 65 dB SPL: 85 %, sound quality: 100), whereas others with bad sound quality demonstrated a high level of speech recognition (e.g., #208, word recognition score at 65 dB SPL: 80 %, MUSHRA sound quality: (9 ± 10)), suggesting complex interactions between acoustic and cognitive processes. Possible explanations have already been discussed in Section 3.4 and include, e.g., the cognitive load associated with processing CI transmitted signals. If the brain is already heavily engaged in processing the CI sound and its sound quality, this could limit the resources available for speech recognition. This hypothesis is supported by neurocognitive studies showing that processing speech in acoustically challenging environments requires additional cognitive effort (Eckert et al. 2016).

The fact that the 4PTA did not affect the pitch deviation (Figure 5.7) supports the discussion in Section 3.4, where it was noted that the participants often used a low-pass filter to optimize the simulations. Thus, the hearing losses in some participants greater than 30 dB HL of the contralateral ear (4PTA, Table 3.3), did not lead to pitch deviation in CI simulations.

Nevertheless, correlations between the above-mentioned factors and CI sound quality would have been expected, but none were found. CI usage time and social activity were recorded at the study visit. However, the incidence of exposure to CI stimuli over the entire postoperative period, rather than at just one point in time, would have been more relevant. Furthermore, one limitation of this study is the small number of CI simulations ($n = 15$). An analysis of multifactorial relationships, for example, through multiple regression, was therefore not meaningful. In addition,

some factors that could influence sound quality, such as cognition (Lee et al. 2003), were not considered. In future projects, the generation of a larger number of CI simulations and investigation of further factors would be meaningful to enable better analysis of factors influencing CI sound quality or to enable a prediction of CI sound quality for CI users or candidates.

5.4.2 Precision of Insertion Angle Measurement

The preview of the insertion angle measurement from planar X-ray images as a function of the two projection angles α and β (Figure 5.2) led to an estimation of a systematic, relative error. The systematic error varied with the angles α and β. Both an overestimation (orange) and an underestimation (blue) of the insertion angle are possible in dependency of the projection angle. The effect of variable angles between the central beam and the midsagittal plane (corresponding to α) were also investigated by Svrakic et al. (2015) (Section 2.6.2). The authors reported that systematic errors of up to 8 % are caused by the projection angle, which is, however, on the order of magnitude of the interrater variability (Svrakic et al. 2015). This finding is in good accordance with the systematic errors found with the 3D model developed in this chapter ($< 10\,\%$), even though the second angle β was considered.

Furthermore, the 3D model revealed that the systematic error depends not only on the projection angles but also on the absolute, intracochlear position/insertion depth of the electrode contacts. One possible explanation is that the anatomical structures and the trajectory of the electrode array are not symmetrical. Varying the projection angles also varies the projected spatial relation of the individual electrode contacts to each other. This finding is in accordance with the results of Alahmadi et al. 2024, who compared the insertion angles measured from CT and planar X-ray images for all inserted electrode contacts. The investigated X-ray images were acquired in the cochlear view, and the difference in the insertion angles measured from CT images compared with those from planar X-ray images varied between 0.3 ° and 9.8 °. Although the X-ray images were acquired in the standardized cochlear view, a mean relative error of 9 % occurred at most basal electrode contacts, for example. The systematic error evoked by deviation of radiological projection angles is consequently in the order of magnitude of the measurement error, which occurred already by evaluation of planar X-ray images in the cochlear view compared with CT evaluations (Alahmadi et al. 2024).

For this reason, in the clinical context, the performance of planar imaging according to Altschul view instead of the cochlear view is also justified. It should be explicitly pointed out that the model presented in this chapter did not take all aspects of the insertion angle measurement into account. Further measurement errors in the insertion angle measurement arise, e.g., from the placement of the markers corresponding to the anatomical structures (modiolus, the apex of the superior semicircular canal and the centrum of the vestibule, Figure 2.11).

This consideration is not only relevant for investigating possible factors influencing sound quality but also has clinical relevance. The latest version of the software Otoplan[60] offers the option of calculating anatomy-based fitting on the basis of

[60]Otoplan, Cascination AG (2024), Bern, Switzerland in cooperation with MED-EL, Innsbruck,

planar X-ray images. In this context, the clinical audiologist should be aware of the measurement errors of the insertion angles from planar imaging to adjust the anatomy-based fitting accordingly. In general, the relevance of the measurement accuracy of the insertion angle should always be considered when addressing clinical questions, and tomographic imaging should be considered if high measurement accuracy is necessary and if an increased radiation dose is justifiable. To keep radiation dose as low as possible, special detectors, such as a low-dose photon-counting detector can be used in CT imaging (Spahn et al. 2025).

5.5 Conclusions

This chapter presented an explorative data analysis of factors influencing not self-reported CI sound quality. Despite the relatively small number of CI simulations, CI sound quality and CI experience showed a moderate correlation. Especially, a saturation in sound quality to excellent quality was found for CI experiences larger than 6 years. Further factors did not show any correlations with CI sound quality parameters. To improve the investigation of CI sound quality influencing factors and to enable a prediction of postoperative CI sound quality, an increase in the number of CI simulations to evaluate sound quality is necessary.

Furthermore, this chapter contributes to the radiological evaluation of cochlear implantations. The 3D model developed in this chapter showed that measuring the insertion angle of planar X-ray images with variable projection angles led to systematic errors. In addition, the systematic error of the insertion angle also depends on the absolute depth of insertion of electrode contacts into the cochlea. If X-rays are acquired in Altschul view instead of the cochlear view, relative errors of less than 10 % are assumable.

Austria, version 3.1.0

6 Thesis Conclusions and Outlook

This thesis investigated the sound perception and sound quality perceived by CI users. A software-based sound tool was designed that enabled the creation of CI sound simulations on the basis of the descriptions of CI users. The participants were able to compare the auditory impressions of the normal hearing, contralateral ear with the reference signal perceived through the CI. By adjusting various simulation parameters via a software sound tool, it was possible to generate German-language CI simulations with a large degree of similarity to the CI sound, for the first time. No comparable CI simulations existed for devices with 22 intracochlear electrode contacts. Furthermore, CI sounds could be replicated for CI participants at different stages of rehabilitation. The results revealed considerable interindividual variability in sound perception, even among rehabilitated users, highlighting the individuality of auditory experiences with CIs.

In contrast to earlier studies, which relied primarily on discrimination tasks or subjective self-assessments (e.g., questionnaires) to evaluate sound quality, this thesis enabled, for the first time, an assessment of CI sound quality on the basis of CI simulations. Through various psychoacoustic experiments, the sound quality of CI simulations was rated by normal hearing participants. This approach not only allowed a comparative assessment between CI sound and normal hearing but also facilitated a multi-rater evaluation that extended beyond the subjective view of the CI user alone.

On average, the simulations were rated as having fair sound quality, and individual CI simulations sound quality ranged from 'bad' to 'excellent'. The sound quality was scored with large statistical dispersion, highlighting the strong subjectivity of sound quality. To address this dispersion of sound quality, an objective measure was introduced: the spectral difference between the spectrograms of the CI simulations and the reference signal. This spectral deviation showed a moderate correlation with the CI sound quality ratings provided by the participants with normal hearing. To enable better prediction of sound quality from CI simulations via objective measures, future studies should consider developing sound quality models that incorporate the psychoacoustic properties of human auditory perception.

To explore the individuality of CI sound quality, several potential influencing factors were examined. CI experience emerged as the most relevant factor: in particular, a saturation effect was observed. Especially, a saturation in sound quality to excellent quality was found for CI experiences larger than 6 years. This finding suggests that, over time, the auditory perception of a CI can closely approximate the sound perception of a normal hearing ear in SSD CI users. This observation highlights the relevance of neuronal plasticity in the rehabilitation process after cochlear implantation. No further CI sound quality influencing factors were found, which may be due to multifactorial interactions. To enable more comprehensive analyses, such as

multiple regression, an increased number of CI simulations is meaningful for future projects.

Since in general, CI performance strongly depends on the actual CI electrode array position in the cochlea, a 3D model was developed to estimate the systematic error of the electrode array insertion angle as a function of the X-ray projection angle. The resulting systematic error was similar in magnitude to the error previously reported when planar X-ray imaging was compared with tomographic imaging (Alahmadi et al., 2024). Therefore, the relevance of the measurement accuracy of the insertion angle should always be considered when addressing clinical questions. If high precision is required and increased radiation exposure is justifiable, tomographic imaging should be considered.

Several noteworthy individual observations emerged throughout this thesis. For instance, CI participants with little CI experience demonstrated that auditory perception can change significantly within the first 6 months after cochlear implantation. Additionally, deactivating electrode contacts did not lead to noticeable changes in sound perception, and auditory perception and speech recognition did not correlate.

Due to the large similarity between CI simulations and CI sound, these simulations offer valuable potential for scientific and educational purposes, as they allow a realistic assessment of the sound perception of CI users. Given that the technical parameters of implants and processors may also influence CI sound, future research should develop CI simulations for CI users implanted with CIs from other manufacturers and CI simulations with further acoustic signals (e.g., female speaker and music) to enable extensive consulting. Notably, the CI simulations presented in this thesis are primarily used to simulate CI sound and cannot reflect other factors that may change as a result of cochlear implantation (e.g., communication skills and quality of life). Thus, CI simulations should therefore be used as a supportive tool and should not be presented without further explanation.

Appendix

Table A1: Upper and lower cutoff frequencies f_c of the frequency bands according to the default setting of the Advanced Combination Encoder (ACE) strategy (Cochlear Ltd. 2022b).

Electrode contact	22	21	20	19	18	17	16	15	14	13	12
Lower f_c [kHz]	188	313	438	563	688	813	938	1063	1188	1313	1563
Upper f_c [kHz]	313	438	563	688	813	938	1063	1188	1313	1563	1813
Electrode contact	11	10	9	8	7	6	5	4	3	2	1
Lower f_c [kHz]	1813	2063	2313	2688	3063	3563	4063	4688	5313	6063	6938
Upper f_c [kHz]	2063	2313	2688	3063	3563	4063	4688	5313	6063	6938	7938

Table A2: Sentences from the Oldenburg children's sentence test used for the ranking experiment (1st test list: the first 10 sentences, Wagener et al. 2005). An English translation is given in brackets.

No.	Sentence	
1.	'Drei rote Schuhe'	['Three red shoes']
2.	'Vier nasse Autos'	['Four wet cars']
3.	'Neun weiße Tassen'	['Nine white cups']
4.	'Sieben grüne Bilder'	['Seven green pictures']
5.	'Vier Grüne Schuhe'	['Four green shoes']
6.	'Acht kleine Autos'	['Eight small cars']
7.	'Sieben rote Blumen'	['Seven red flowers']
8.	'Fünf schöne Tassen'	['Five beautiful cups']
9.	'Fünf schöne Steine'	['Five beautiful stones']
10.	'Acht kleine Messer'	['Eight small knifes']

Table A3: Adjective list for describing CI sound and handling to participants during the optimization experiment.

Hochfrequent	Schrill	Nachhallend
Übersteuert	Klar	Verschmiert
Metallisch	Monoton	Verrauscht
Elektrisch	Blechern	Verzerrt
Fremd	Doppelt	Spitz
Dröhnend	Leise	Stumpf
Melodisch	Brummend	weit entfernt
Verschwommen	Gedämpft	Laut
Roboterartig	Hohl	Nah
'Darth-Vader'[1]-ähnlich	Schmutzig	Voll
'Chipmunks'[2]-ähnlich	Tieffrequent	Pfeifend
'Mickey-Maus'[3]-ähnlich	Nasal	Piepsig

[1] A trademark of the Lucasfilm Ltd. LLC, a subsidiary of the Walt Disney Company.
[2] A trademark of the Bagdasarian Productions, LLC and the Walt Disney Company.
[3] A trademark of the Walt Disney Company.

Table A4: Order of application of the processing steps

No.	Processing
1.	BP-vocoder
2.	FFT-vocoder
3.	Echo
4.	Comb Filter
5.	Low-pass Filter
6.	High-pass Filter
7.	Band-pass Filter
8.	Frequency shift
9.	Pitch shift
10.	Clipping
11.	Normalisation

BP: band-pass, FFT: fast Fourier transform.

Table A5: Longitudinal study during the first 6 months of CI experience: Parameters and similarity scores for simulation optimization during the 4 day (4d) and 6 month (6m) visits.

ID	Subjective description*	Vocoder	Clipping	Pitch/frequency shift	Filter	Similarity score for sentence 1	2	3	Further need for optimization**
#101 4d	robotic, emotionless	FFT: carrier = noise, SOE-order = 1, $n = 2$		frequency: 360 Hz	LP: 6th order, $f_c = 1800$ Hz	9.5	9.5	9.5	CI sounds harsher, more robotic and monotonous
#101 6m	scratchy, dry, overdriven	BP: carrier = noise, SOE-order = 4, $m = 15$	1.5	frequency: 360 Hz, pitch: 6.5 semitones	Comb $f_0 = 98$ Hz $Q = 5$	7.5	7.5	7.5	CI sounds more scratchy and like cartoon character
#102 4d	like a synthetic computer voice			frequency: 375 Hz	HP: 4th order, $f_c = 3600$ Hz	8.0	7.0	7.0	CI sounds more synthetic
#102 6m	like a synthetic computer voice			frequency: 375 Hz	HP: 4th order, $f_c = 3600$ Hz	9.0	7.5	9.0	difficult to describe
#103 4d	bright, clear, tinny			frequency: 395 Hz, pitch: −4.5 semitones	HP: 4th order, $f_c = 2100$ Hz	9.0	1.0	2.0	difficult to describe
#103 6m	slightly more natural than before			frequency: 220 Hz,	HP: 4th order, $f_c = 1800$ Hz	8.0	7.0	8.0	voice pitch somehow different, difficult to describe
#104 4d	noisy envelope, unclear				HP: 4th order, $f_c = 2000$ Hz	10.0	9.0	7.0	Sentence 3: noisy envelope
#104 6m	no noisy enevlope anymore				HP: 4th order, $f_c = 1000$ Hz	10.0	9.0	9.0	Nothing
#105 4d	like a voice changer, blurred, unnatural, far away			pitch: 8.5 semitones	Comb: 4th order, $f_0 = 98$ Hz, $Q = 5$, LP: 4th order, $f_c = 1000$ Hz,	9.0	8.0	8.0	Emphasis is different with the CI
#105 6m	squeaky, far away					9.0	9.0	9.0	CI sounds more squeaky

ID: identification number, CI: cochlear implant, BP: band-pass, LP: low-pass, HP: high-pass, FFT: fast Fourier transform, SOE: spread of excitation, f_c: cutoff filter frequency, f_0: fundamental frequency, Q: quality factor, m: number of frequency bands, n: number of selected frequency bands with the largest energy, 4d: 4 days after activation, 6m: 6 months after activation, sentence 1: 'drei rote Schuhe' ['three red shoes'], sentence 2: 'vier nasse Autos' ['four wet cars'], sentence 3: 'neun weiße Tassen' ['nine white cups'] (Wagener et al. 2005).
* The participants' subjective descriptions of their CI sound before starting the study tasks. ** The participants' suggestions on how the simulation could be improved to evaluate the limitations of the software sound tool were queried after the optimization procedure.

Table A6: Cross-Sectional Study after at Least 2 Years of CI Experience: Parameters and similarity scores for simulation optimization.

ID	Subjective description*	FFT-Vocoder	Pitch shift	Filter	Similarity score for sentence			Further need for optimization**
					1	2	3	
#201	little high pitched			BP: 4th order, $f_c = 200$ and $8000\,\mathrm{Hz}$	10.0	10.0	10.0	nothing
#202	mechanical			Comb: $f_0 = 100\,\mathrm{Hz}$, $Q = 5$ HP: 4th order, $f_c = 500$	9.5	7.0	7.0	difficult to describe
#203	normal, female, softer	carrier = sine, SOE-order = 4, $n = 22$	6 semitones	LP: 3rd order, $f_c = 1200\,\mathrm{Hz}$	9.0	7.0	8.0	CI is a little more feminine and pleasant
#204	little muffled			LP: 7th order, $f_c = 100\,\mathrm{Hz}$	10.0	9.0	8.0	nothing
#205	normal				10.0	8.5	10.0	nothing
#206	technical, high pitched		10 semitones		9.0	7.0	8.0	difficult to describe
#207	normal, feeling is different			LP: 2nd order, $f_c = 100\,\mathrm{Hz}$	9.0	5.0	6.0	distorted, feeling is different with CI
#208	robotic	carrier = sine, SOE-order = 2, $n = 8$		Comb: $f_0 = 98\,\mathrm{Hz}$, $Q = 5$	10.0	10.0	10.0	nothing
#209	tinny, high pitched			Comb: $f_0 = 98\,\mathrm{Hz}$, $Q = 5$	10.0	9.0	10.0	nothing
#210	normal			Comb: $f_0 = 98\,\mathrm{Hz}$, $Q = 5$ LP: 4th order, $f_c = 1500$	10.0	8.0	8.0	nothing
#211	thin			HP: 4th order, $f_c = 1000\,\mathrm{Hz}$	10.0	10.0	10.0	nothing
#212	normal, sometimes little tinny				10.0	10.0	10.0	nothing
#213	high pitched, thin		4 semitones	HP: 4th order, $f_c = 2400\,\mathrm{Hz}$	9.0	8.0	9.0	CI sounds less clear
#214	high pitched, more natural than in the beginning			BP: 4th order, $f_c = 200$ and $8000\,\mathrm{Hz}$	10.0	8.0	10.0	nothing
#215	feeling is a little different			BP: 4th order, $f_c = 400$ and $6300\,\mathrm{Hz}$	10.0	9.0	9.0	nothing

ID: identification number, CI: cochlear implant, BP: band-pass, LP: low-pass, HP: high-pass, FFT: fast Fourier transform, SOE: spread of excitation, f_c: cutoff filter frequency, f_0: fundamental frequency, Q: quality factor, m: number of frequency bands, n: number of selected frequency bands with the largest energy, sentence 1: 'drei rote Schuhe' ['three red shoes'], sentence 2: 'vier nasse Autos' ['four wet cars'], sentence 3: 'neun weiße Tassen' ['nine white cups'] (Wagener et al. 2005).
* The participants' subjective descriptions of their CI sound before starting the study tasks. ** The participants' suggestions on how the simulation could be improved to evaluate the limitations of the software sound tool were queried after the optimization procedure.

Table A7: Supplemental digital content. All digital content files have an audio WAVE file format.

No.	File name	Description
1	reference_sentence1	Reference audio signal for optimization experiment (sentence 1).
2	reference_sentence3	Reference audio signal of sentence 3.
	Longitudinal Study during the first 6 month of CI Experience	
3	#101_sentence1_4d	Optimized simulation for participant #101 during the 4d-visit.
4	#101_sentence1_6m	Optimized simulation for participant #101 during the 6m-visit.
5	#102_sentence1_4d	Optimized simulation for participant #102 during the 4d-visit.
6	#102_sentence1_6m	Optimized simulation for participant #102 during the 6m-visit.
7	#103_sentence1_4d	Optimized simulation for participant #103 during the 4d-visit.
8	#103_sentence1_6m	Optimized simulation for participant #103 during the 6m-visit.
9	#104_sentence1_4d	Optimized simulation for participant #104 during the 4d-visit.
10	#104_sentence3_4d	Sound sample that captures the noise-envelope perception, that participant #104 described in sentence 3 during the 4d-visit.
11	#104_sentence1_6m	Optimized simulation for participant #104 during the 6m-visit.
12	#105_sentence1_4d	Optimized simulation for participant #105 during the 4d-visit.
13	#105_sentence1_6m	Optimized simulation for participant #105 during the 6m-visit.
	Cross-Sectional Study after at Least 2 Years of CI Experience	
14	#201_sentence1	Optimized simulation for participant #201.
15	#202_sentence1	Optimized simulation for participant #202.
16	#203_sentence1	Optimized simulation for participant #203.
17	#204_sentence1	Optimized simulation for participant #204.
18	#205_sentence1	Optimized simulation for participant #205.
19	#206_sentence1	Optimized simulation for participant #206.
20	#207_sentence1	Optimized simulation for participant #207.
21	#208_sentence1	Optimized simulation for participant #208.
22	#209_sentence1	Optimized simulation for participant #209.
23	#210_sentence1	Optimized simulation for participant #210.
24	#211_sentence1	Optimized simulation for participant #211.
25	#212_sentence1	Optimized simulation for participant #212.
26	#213_sentence1	Optimized simulation for participant #213.
27	#214_sentence1	Optimized simulation for participant #214.
28	#215_sentence1	Optimized simulation for participant #215.

4d-visit: Study visit 4 days after cochlear implant activation, 6m-visit: Study visit 6 months after cochlear implant activation.

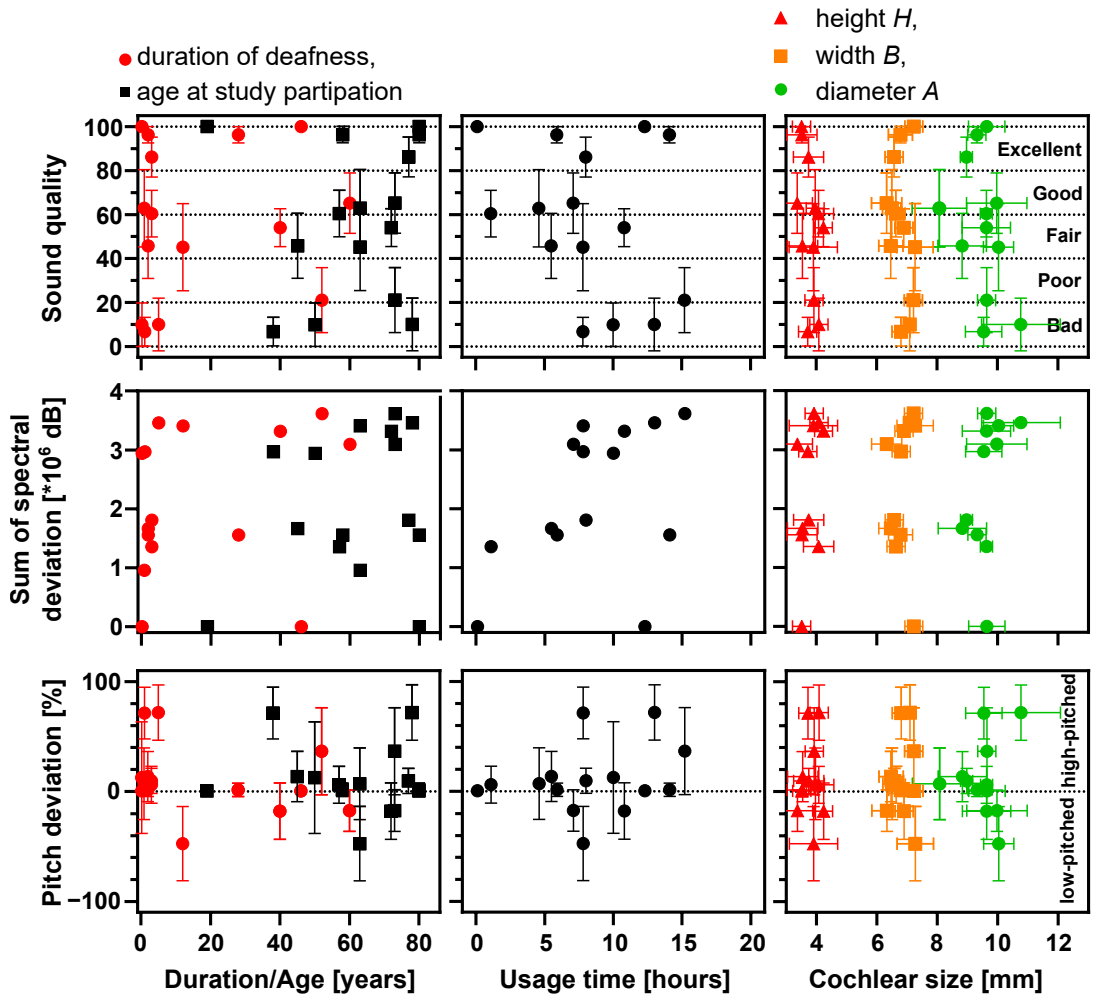

Figure A1: Relations between cochlear implant (CI) sound quality parameters (CI sound quality, pitch and spectral deviation) and duration of deafness, age at study participation, average CI usage time (data logging) and cochlear size (height H, width B, diameter A), respectively. No factor was correlated with CI sound quality or spectral deviation ($R^2 \leq 0.2$).

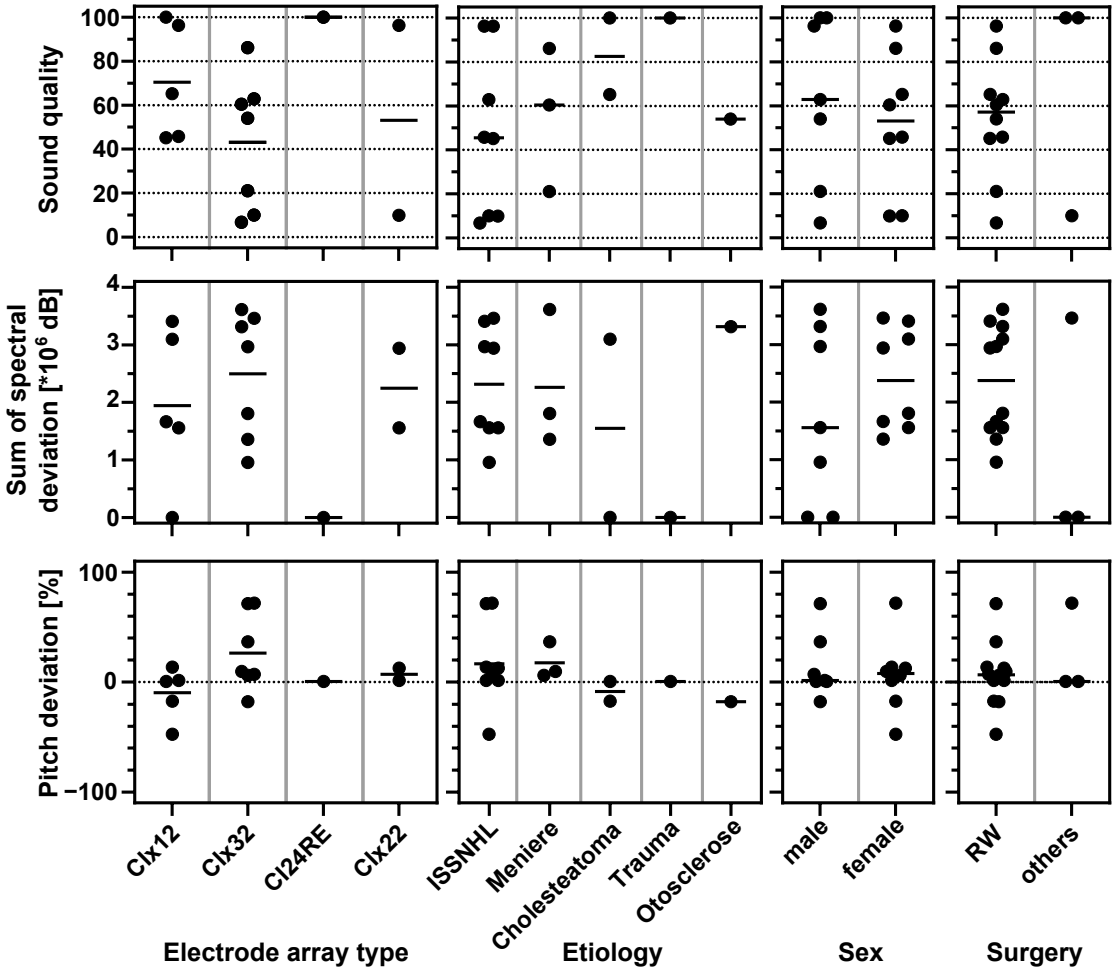

Figure A2: Relations between cochlear implant (CI) sound quality parameters (CI sound quality, pitch and spectral deviation) and electrode array type, etiology, sex and surgery technique (round window (RW) insertion or other techniques, such as cochleostomy or extended RW insertion), respectively. The horizontal lines mark the median.
ISSNHL: idiopathic sudden sensorineural hearing loss.

List of Abbreviations

3D	Three dimensional
4d-visit	Study visit 4 days after implant activation
4PTA	Four frequency pure tone average
6m-visit	Study visit approximately 6 month after implant activation
ACE	Advanced Combination Encoder
ANOVA	Analysis of variance
BP	Band-pass
BP	Bipolar
C-level	Comfortable current level
CB	Central beam
CBCT	Cone-beam computed tomography
CDL	Cochlear duct length
CI	Cochlear implant
CT	Computed tomography
DFT	Discrete Fourier transform
DoD	Duration of deafness
EEG	Electroencephalography
FFT	Fast Fourier transform
fMRT	Functional magnetic resonance imaging
GUI	graphical user interface
$HISQUI_{19}$	Hearing Implant Sound Quality Index
HL	Hearing level
HP	High-pass
ID	Identification number
IOML	Infraorbitomeatal line
ISSNHL	Idiopathic sudden sensorineural hearing loss
ITU	International Telecommunication Union
LP	Low-pass
MIP	Maximum intensity projection
MP	Monopolar
MSP	Midsagittal plane
MUSHRA	Multi-Stimulus Test with Hidden Reference and Anchor
OlKiSa	Oldenburger Kinder-Satztest ['Oldenburg children's sentence test']
PCM	Pulse-code modulation
RMS	Root mean square
SCINSEV	Stimulation-current-induced non-stimulating electrode voltage recording
SD	Standard deviation
SOE	Spread of excitation
SOL	Subtotal ossifying labyrinthitis
SPL	Sound pressure level
SSD	Single sided deafness
STFT	Short-time Fourier transform
T-level	Threshold current level
WRS_x	Word recognition score at a fixed level x

List of Figures

List of Tables

Bibliography

Abadi, M. et al. (2015). 'TensorFlow: Large-Scale Machine Learning on Heterogeneous Systems'. In: DOI: 10.5281/ZENODO.4724125. URL: https://www.tensorflow.org/ (visited on 20/05/2025).

Advanced Bionics AG (2022). 'Technical Specifications: Hires Ultra 3D Cochlear Implant'. In: URL: https://www.advancedbionics.com/content/dam/advancedbionics/Documents/Regional/en-gb/Professional/Ultra-3D-Tech-Specs-Brochure.pdf (visited on 20/05/2025).

Aebischer, P., Meyer, S., Caversaccio, M. and Wimmer, W. (2021). 'Intraoperative Impedance-Based Estimation of Cochlear Implant Electrode Array Insertion Depth'. In: *IEEE Transactions on Biomedical Engineering* 68.2, pp. 545–555. DOI: 10.1109/TBME.2020.3006934.

Akbulut, A. A., Karaman Demirel, A. and Çiprut, A. (2024). 'Music Perception and Music-Related Quality of Life in Adult Cochlear Implant Users: Exploring the Need for Music Rehabilitation'. In: *Ear and Hearing* 46.1, pp. 265–276. DOI: 10.1097/AUD.0000000000001580.

Alahmadi, A., Abdelsamad, Y., Hafez, A. and Hagr, A. (2024). 'X-ray guided anatomy-based fitting: The validity of OTOPLAN'. In: *PLOS ONE* 19.11, e0313567. DOI: 10.1371/journal.pone.0313567.

Alexiades, G., Dhanasingh, A. and Jolly, C. (2015). 'Method to estimate the complete and two-turn cochlear duct length'. In: *Otology & Neurotology* 36.5, pp. 904–907. DOI: 10.1097/MAO.0000000000000620.

Alzhrani, F. et al. (2024). 'International Consensus Statements on Intraoperative Testing for Cochlear Implantation Surgery'. In: *Ear and hearing* 45.6, pp. 1418–1426. DOI: 10.1097/AUD.0000000000001526.

Amann, E. and Anderson, I. (2014). 'Development and validation of a questionnaire for hearing implant users to self-assess their auditory abilities in everyday communication situations: the Hearing Implant Sound Quality Index (HISQUI19)'. In: *Acta Oto-Laryngologica* 134.9, pp. 915–923. DOI: 10.3109/00016489.2014.909604.

Anderson, L. B. (1994). 'Chapter 17 Paired comparisons'. In: *Handbooks in Operations Research and Management Science : Operations Research and The Public Sector*. Vol. 6. Elsevier, pp. 585–620. ISBN: 0927-0507. DOI: 10.1016/S0927-0507(05)80098-2.

Andries, E. et al. (2021). 'Systematic Review of Quality of Life Assessments after Cochlear Implantation in Older Adults'. In: *Audiology and Neurotology* 26.2, pp. 61–75. ISSN: 1421-9700. DOI: 10.1159/000508433.

Ariyasu, L., Galey, F. R., Hilsinger, R. and Byl, F. M. (1989). 'Computer-generated three-dimensional reconstruction of the cochlea'. In: *Otolaryngology–head and neck surgery* 100.2, pp. 87–91. ISSN: 0194-5998. DOI: 10.1177/019459988910000201.

Arlinger, S. (2003). 'Negative consequences of uncorrected hearing loss–a review'. In: *International Journal of Audiology* 42.sup2, pp. 17–20. DOI: 10.3109/14992020309074639.

Arndt, S. et al. (2017). 'Cochlea-Implantat-Versorgung von Patienten mit einseitiger Taubheit oder asymmetrischem Hörverlust'. In: *HNO* 65.Suppl 2, pp. 98–108. DOI: 10.1007/s00106-016-0297-5.

Baumann, U. and Nobbe, A. (2006). 'The cochlear implant electrode-pitch function'. In: *Hearing Research* 213.1-2, pp. 34–42. DOI: 10.1016/j.heares.2005.12.010.

Békésy, G. von (1963). 'Hearing Theories and Complex Sounds'. In: *The Journal of the Acoustical Society of America* 35.4, pp. 588–601. ISSN: 0001-4966. DOI: 10.1121/1.1918543.

Berenstein, C. K., Mens, L. H. M., Mulder, J. J. S. and Vanpoucke, F. J. (2008). 'Current steering and current focusing in cochlear implants: comparison of monopolar, tripolar, and virtual channel electrode configurations'. In: *Ear and hearing* 29.2, pp. 250–260. DOI: 10.1097/AUD.0b013e3181645336.

Bernhardi, R. von, Bernhardi, L. E.-v. and Eugenín, J. (2017). 'What Is Neural Plasticity?' In: *The Plastic Brain*. Vol. 1015. Cham: Springer International Publishing, pp. 1–15. ISBN: 978–3–319–62815–8.

Bessen, S. Y., Saunders, J. E., Eisen, E. A. and Magro, I. L. (2021). 'Perceptions of Sound Quality and Enjoyment After Cochlear Implantation'. In: *OTO Open* 5.3. DOI: 10.1177/2473974X211031471.

Bille, J. and Schlegel, W. (2013). *Medizinische Physik 1: Grundlagen*. Berlin: Springer Berlin. ISBN: 978-3-642-63605-9. DOI: 10.1007/978-3-642-58461-9.

Bingabr, M., Espinoza-Varas, B. and Loizou, P. C. (2008). 'Simulating the effect of spread of excitation in cochlear implants'. In: *Hearing Research* 241.1-2, pp. 73–79. DOI: 10.1016/j.heares.2008.04.012.

Blamey, P. et al. (2013). 'Factors affecting auditory performance of postlinguistically deaf adults using cochlear implants: an update with 2251 patients'. In: *Audiology and Neurotology* 18.1, pp. 36–47. DOI: 10.1159/000343189.

Blauert, J. and Jekosch, U. (1997). 'Sound-Quality Evaluation – A Multi-Layered Problem'. In: *ACUSTICA united with ACTA ACUSTICA* 83, pp. 747–753.

Boenninghaus, H.-G. and Lenarz, T. (2007). *Hals-Nasen-Ohren-Heilkunde*. 13. Aufl. Springer-Lehrbuch. Berlin, Heidelberg: Springer Medizin Verlag Heidelberg. ISBN: 9783540487227.

Brandes, R., Lang, F. and Schmidt, R. F., eds. (2020). *Physiologie des Menschen: Mit Pathophysiologie*. 32. Auflage. Springer-Lehrbuch. Berlin: Springer. ISBN: 9783662564677.

Bruschini, L. et al. (2024). 'Implantable hearing devices in clinical practice. Systematic review and consensus statements'. In: *ACTA Otorhinolaryngologica Italica* 44.1, pp. 52–67. DOI: 10.14639/0392-100X-N2651.

Brusis, T. and Mödder, U. (1984). *HNO Röntgen-Aufnahmetechnik und Normalbefunde*. Berlin, Heidelberg: Springer Berlin Heidelberg. ISBN: 978-3-642-69240-6.

Buchman, C. A. et al. (2014). 'Influence of cochlear implant insertion depth on performance: a prospective randomized trial'. In: *Otology & Neurotology* 35.10, pp. 1773–1779. DOI: 10.1097/MAO.0000000000000541.

Buzug, T. M. (2004). *Einführung in die Computertomographie*. Berlin, Heidelberg: Springer Berlin Heidelberg. ISBN: 978-3-642-62184-0.

Caldwell, M. T., Jiam, N. T. and Limb, C. J. (2017). 'Assessment and improvement of sound quality in cochlear implant users'. In: *Laryngoscope Investigative Otolaryngology* 2.3, pp. 119–124. ISSN: 2378-8038. DOI: 10.1002/lio2.71.

Canfarotta, M. W. et al. (2020). 'Frequency-to-Place Mismatch: Characterizing Variability and the Influence on Speech Perception Outcomes in Cochlear Implant Recipients'. In: *Ear and hearing* 41.5, pp. 1349–1361. DOI: 10.1097/AUD.0000000000000864.

Canfarotta, M. W. et al. (2022). 'Insertion Depth and Cochlear Implant Speech Recognition Outcomes: A Comparative Study of 28- and 31.5-mm Lateral Wall Arrays'. In: *Otology & Neurotology* 43.2, pp. 183–189. DOI: 10.1097/MAO.0000000000003416.

Cascination AG (2024). *OTOPLAN: Instructions for Use*. URL: https://www.cascination.com/en/otoplan (visited on 17/05/2025).

Chittka, L. and Brockmann, A. (2005). 'Perception space–the final frontier'. In: *PLOS Biology* 3.4, e137. DOI: 10.1371/journal.pbio.0030137.

Chung, K. and McKibben, N. (2011). 'Microphone directionality, pre-emphasis filter, and wind noise in cochlear implants'. In: *Journal of the American Academy of Audiology* 22.9, pp. 586–600. ISSN: 1050-0545. DOI: 10.3766/jaaa.22.9.4.

Chung, K., Zeng, F.-G. and Acker, K. N. (2006). 'Effects of directional microphone and adaptive multichannel noise reduction algorithm on cochlear implant performance'. In: *The Journal of the Acoustical Society of America* 120.4, pp. 2216–2227. ISSN: 0001-4966. DOI: 10.1121/1.2258500.

Cochlear Ltd. (2022a). 'Cochlear Implant Electrode Comparison'. In: FUN1142. URL: https://assets.cochlear.com/api/public/content/FUN1142-Electrode-Comparison-Sheet.pdf (visited on 05/05/2025).

Cochlear Ltd. (2020). *Custom Sound EP Software: User Guide: Version 6.0*.

Cochlear Ltd. (2022b). *Custom Sound Pro Software: Cochlear Implant Reference Guide: Version 7.0*.

Cohen, L. T., Xu, J., Xu, S. A. and Clark, G. M. (1996). 'Improved and simplified methods for specifying positions of the electrode bands of a cochlear implant array'. In: *The American Journal of Otology* 17.6, pp. 859–865.

Cosentino, S., Falk, T. H., McAlpine, D. and Marquardt, T. (2014). 'Cochlear Implant Filterbank Design and Optimization: A Simulation Study'. In: *IEEE/ACM Transactions on Audio, Speech, and Language Processing* 22.2, pp. 347–353. DOI: 10.1109/TASLP.2013.2290502.

Cucis, P.-A. et al. (2021). 'Word Recognition and Frequency Selectivity in Cochlear Implant Simulation: Effect of Channel Interaction'. In: *Journal of Clinical Medicine* 10.4. DOI: 10.3390/jcm10040679.

Cychosz, M., Winn, M. B. and Goupell, M. J. (2024). 'How to vocode: Using channel vocoders for cochlear-implant research'. In: *The Journal of the Acoustical Society of America* 155.4, pp. 2407–2437. DOI: 10.1121/10.0025274.

Dalton, D. S. et al. (2003). 'The impact of hearing loss on quality of life in older adults'. In: *The Gerontologist* 43.5, pp. 661–668. DOI: 10.1093/geront/43.5.661.

Das, S., Mitra, K. and Mandal, M. (2016). 'Sample size calculation: Basic principles'. In: *Indian Journal of Anaesthesia* 60.9, pp. 652–656. DOI: 10.4103/0019-5049.190621.

Dazert, S., Thomas, J. P., Loth, A., Zahnert, T. and Stöver, T. (2020). 'Cochlear Implantation'. In: *Deutsches Arzteblatt international* 117.41, pp. 690–700. DOI: 10.3238/arztebl.2020.0690.

Dhanasingh, A. et al. (2024). 'Cochlear implant electrode design for safe and effective treatment'. In: *Frontiers in neurology* 15, p. 1348439. DOI: 10.3389/fneur.2024.1348439.

Dhand, N. K. and Khatkar, M. S. (2014). *Statulator: An online statistical calculator: Sample Size Calculator for Estimating a Single Mean.* URL: https://www.statulator.com/SampleSize/ss1M.html (visited on 17/05/2025).

Di Maro, F., Carner, M., Sacchetto, A., Soloperto, D. and Marchioni, D. (2022). 'Frequency reallocation based on cochlear place frequencies in cochlear implants: a pilot study'. In: *European Archives of Oto-Rhino-Laryngology* 279.10, pp. 4719–4725. DOI: 10.1007/s00405-021-07245-y.

DIN EN ISO 7029 (2017). 'DIN EN ISO 7029:2017-06: Akustik- Statistische Verteilung von Hörschwellen in Bezug auf das Alter und das Geschlecht (ISO_7029:2017)'. In: German Version EN_ISO_7029:2017.

Dong, Y., Briaire, J. J., Siebrecht, M., Stronks, H. C. and Frijns, J. H. M. (2021). 'Detection of Translocation of Cochlear Implant Electrode Arrays by Intracochlear Impedance Measurements'. In: *Ear and Hearing* 42.5, pp. 1397–1404. DOI: 10.1097/AUD.0000000000001033.

Dorman, M. F., Natale, S. C., Noble, J. H. and Zeitler, D. M. (2022). 'Upward Shifts in the Internal Representation of Frequency Can Persist Over a 3-Year Period for Cochlear Implant Patients Fit With a Relatively Short Electrode Array'. In: *Frontiers in human neuroscience* 16. DOI: 10.3389/fnhum.2022.863891.

Dorman, M. F., Natale, S. C., Stohl, J. S. and Felder, J. (2024). 'Close approximations to the sound of a cochlear implant'. In: *Frontiers in Human Neuroscience* 18. DOI: 10.3389/fnhum.2024.1434786.

Dorman, M. F., Natale, S. C., Zeitler, D. M., Baxter, L. and Noble, J. H. (2019a). 'Looking for Mickey Mouse™ But Finding a Munchkin: The Perceptual Effects of Frequency Upshifts for Single-Sided Deaf, Cochlear Implant Patients'. In: *Journal of speech, language, and hearing research : JSLHR* 62.9, pp. 3493–3499. DOI: 10.1044/2019_JSLHR-H-18-0389.

Dorman, M. F., Natale, S. C., Butts, A. M., Zeitler, D. M. and Carlson, M. L. (2017). 'The Sound Quality of Cochlear Implants: Studies With Single-sided Deaf Patients'. In: *Otology & Neurotology* 38.8, e268–e273. DOI: 10.1097/MAO.0000000000001449.

Dorman, M. F. et al. (2020). 'Approximations to the Voice of a Cochlear Implant: Explorations With Single-Sided Deaf Listeners'. In: *Trends in Hearing* 24. DOI: 10.1177/2331216520920079.

Dorman, M. F. et al. (2019b). 'Cochlear Place of Stimulation Is One Determinant of Cochlear Implant Sound Quality'. In: *Audiology and Neurotology* 24.5, pp. 264–269. DOI: 10.1159/000503217.

Driedger, J. and Müller, M. (2016). 'A Review of Time-Scale Modification of Music Signals'. In: *Applied Sciences* 6.2, p. 57. DOI: 10.3390/app6020057.

Eckert, M. A., Teubner-Rhodes, S. and Vaden, K. I. (2016). 'Is Listening in Noise Worth It? The Neurobiology of Speech Recognition in Challenging Listening Conditions'. In: *Ear and Hearing* 37 Suppl 1.Suppl 1, 101S–10S. DOI: 10.1097/AUD.0000000000000300.

Eisner, F., McGettigan, C., Faulkner, A., Rosen, S. and Scott, S. K. (2010). 'Inferior frontal gyrus activation predicts individual differences in perceptual learning of cochlear-implant simulations'. In: *Journal of Neuroscience* 30.21, pp. 7179–7186. DOI: 10.1523/JNEUROSCI.4040-09.2010.

Escudé, B. et al. (2006). 'The size of the cochlea and predictions of insertion depth angles for cochlear implant electrodes'. In: *Audiology and Neurotology* 11 Suppl 1.Suppl. 1, pp. 27–33. DOI: 10.1159/000095611.

Fastl, H. (2005). 'Psycho-Acoustics and Sound Quality'. In: *Communication Acoustics*. Ed. by J. Blauert. Berlin, Heidelberg: Springer-Verlag Berlin Heidelberg, pp. 139–162. ISBN: 978-3-540-27437-7. DOI: 10.1007/3-540-27437-5_6.

Fastl, H. and Zwicker, E. (2007). *Psychoacoustics: Facts and Models*. 3rd edition. Vol. 22. Springer series in information sciences. Berlin, Heidelberg: Springer Berlin Heidelberg. ISBN: 9783540688884.

Fourier, J. B. J. and Freeman, A. (2009). *The analytical theory of heat*. New York: Cambridge University Press. ISBN: 9781108001786.

Franke-Trieger, A., Jolly, C., Darbinjan, A., Zahnert, T. and Mürbe, D. (2014). 'Insertion depth angles of cochlear implant arrays with varying length: a temporal bone study'. In: *Otology & Neurotology* 35.1, pp. 58–63. DOI: 10.1097/MAO.0000000000000211.

Franke-Trieger, A. et al. (2024). 'Voltage matrix algorithm for intraoperative detection of cochlear implant electrode misplacement'. In: *Audiology and Neurotology*, pp. 1–17. DOI: 10.1159/000543264.

Fu, Q.-J., Chinchilla, S. and Galvin, J. J. (2004). 'The role of spectral and temporal cues in voice gender discrimination by normal-hearing listeners and cochlear implant users'. In: *Journal of the Association for Research in Otolaryngology : JARO* 5.3, pp. 253–260. DOI: 10.1007/s10162-004-4046-1.

Fu, Q.-J. and Nogaki, G. (2005). 'Noise susceptibility of cochlear implant users: the role of spectral resolution and smearing'. In: *Journal of the Association for Research in Otolaryngology : JARO* 6.1, pp. 19–27. DOI: 10.1007/s10162-004-5024-3.

Fuller, C., Free, R., Maat, B. and Başkent, D. (2022). 'Self-reported music perception is related to quality of life and self-reported hearing abilities in cochlear implant users'. In: *Cochlear Implants International* 23.1, pp. 1–10. DOI: 10.1080/14670100.2021.1948716.

Gazerani, P. (2025). 'The neuroplastic brain: current breakthroughs and emerging frontiers'. In: *Brain Research* 1858, p. 149643. DOI: 10.1016/j.brainres.2025.149643.

Gfeller, K., Christ, A., Knutson, J., Witt, S. and Mehr, M. (2003). 'The effects of familiarity and complexity on appraisal of complex songs by cochlear implant recipients and normal hearing adults'. In: *Journal of Music Therapy* 40.2, pp. 78–112. DOI: 10.1093/jmt/40.2.78.

Gfeller, K. et al. (2008). 'Multivariate predictors of music perception and appraisal by adult cochlear implant users'. In: *Journal of the American Academy of Audiology* 19.2, pp. 120–134. DOI: 10.3766/jaaa.19.2.3.

GraphPad Software (2020). *GraphPad Prism*. URL: www.graphpad.com (visited on 17/05/2025).

Hahlbrock, K.-H. (1953). 'Über Sprachaudiometrie und neue Wörterteste'. In: *European Archives of Oto-Rhino-Laryngology* 162.5, pp. 394–431. DOI: 10.1007/BF02105664.

Hall, J. E., Hall, M. E. and Guyton, A. C. (2021). *Guyton and Hall textbook of medical physiology*. 14. ed. Philadelphia, PA: Elsevier. ISBN: 0323597122.

Hans, S. et al. (2021). 'Transimpedance Matrix Measurements Reliably Detect Electrode Tip Fold-over in Cochlear Implantation'. In: *Otology & Neurotology* 42.10, e1494–e1502. DOI: 10.1097/MAO.0000000000003334.

Hardy, M. (1938). 'The length of the organ of Corti in man'. In: *American Journal of Anatomy* 62.2, pp. 291–311. DOI: 10.1002/aja.1000620204.

Harris, C. R. et al. (2020). 'Array programming with NumPy'. In: *Nature* 585.7825, pp. 357–362. DOI: 10.1038/s41586-020-2649-2.

Harris, R., Pepper, C., Dennis, L., Rich, P. and Selvadurai, D. (2011). 'A practical, single-view alternative to Stenver's for plain radiographic unilateral and bilateral post-cochlear implant position check'. In: *Cochlear Implants International* 12.1, pp. 53–56. DOI: 10.1179/146701010X486408.

He, S., Teagle, H. F. B. and Buchman, C. A. (2017). 'The Electrically Evoked Compound Action Potential: From Laboratory to Clinic'. In: *Frontiers in Neuroscience* 11, p. 339. DOI: 10.3389/fnins.2017.00339.

Hochmair, I. (2021). 'Translational research around five categories of CI'. In: *Acta Oto-Laryngologica* 141.sup1, pp. 178–184. DOI: 10.1080/00016489.2021.1888516.

Hochmair, I., Hochmair, E., Nopp, P., Waller, M. and Jolly, C. (2015). 'Deep electrode insertion and sound coding in cochlear implants'. In: *Hearing Research* 322, pp. 14–23. DOI: 10.1016/j.heares.2014.10.006.

Hoppe, U., Hocke, T., Hast, A. and Iro, H. (2021). 'Cochlear Implantation in Candidates With Moderate-to-Severe Hearing Loss and Poor Speech Perception'. In: *The Laryngoscope* 131.3, E940–E945. DOI: 10.1002/lary.28771.

Hoppe, U. et al. (2022). 'Evaluation of a Transimpedance Matrix Algorithm to Detect Anomalous Cochlear Implant Electrode Position'. In: *Audiology & Neurotology* 27.5, pp. 347–355. DOI: 10.1159/000523784.

Hoth, S. and Steffens, T. (2017). In: *Medizintechnik: Verfahren - Systeme - Informationsverarbeitung*. Ed. by R. Kramme. 5., vollständig überarbeitete und erweiterte Auflage. Springer Reference Technik. Berlin: Springer. ISBN: 9783662487716. DOI: 10.1007/978-3-662-48771-6.

Hunter, J. D. (2007). 'Matplotlib: A 2D graphics environment'. In: *Computing in Science & Engineering* 9, pp. 90–95. DOI: 10.1109/MCSE.2007.55.

IBM (2021). *SPSS Inc.* Armonk, NY, USA.

Inkscape Community (2003). *Inkscape*. URL: https://inkscape.org/de/ (visited on 17/05/2025).

Ishiyama, A., Risi, F. and Boyd, P. (2020). 'Potential insertion complications with cochlear implant electrodes'. In: *Cochlear Implants International* 21.4, pp. 206–219. DOI: 10.1080/14670100.2020.1730066.

ITU-R (2015). *Method for the subjective assessment of intermediate quality level of audio systems*. URL: https://www.itu.int/rec/R-REC-BS.1534/en (visited on 17/05/2025).

Johnston, M. V. (2009). 'Plasticity in the developing brain: implications for rehabilitation'. In: *Developmental disabilities research reviews* 15.2, pp. 94–101. DOI: 10.1002/ddrr.64.

Karoui, C. et al. (2019). 'Searching for the Sound of a Cochlear Implant: Evaluation of Different Vocoder Parameters by Cochlear Implant Users With Single-Sided Deafness'. In: *Trends in hearing* 23, p. 2331216519866029. DOI: 10.1177/2331216519866029.

Kawano, A., Seldon, H. L. and Clark, G. M. (1996). 'Computer-aided three-dimensional reconstruction in human cochlear maps: measurement of the lengths of organ of Corti, outer wall, inner wall, and Rosenthal's canal'. In: *The Annals of otology, rhinology, and laryngology* 105.9, pp. 701–709. DOI: 10.1177/000348949610500906.

Kay-Rivest, E. et al. (2022). 'Predictive Value of Transimpedance Matrix Measurements to Detect Electrode Tip Foldover'. In: *Otology & Neurotology* 43.9, pp. 1027–1032. DOI: 10.1097/MAO.0000000000003667.

Kerner, H. and Wahl, W. (2013). *Mathematik für Physiker*. 3., überarb. Aufl. 2013. Springer-Lehrbuch. Berlin, Heidelberg: Springer Berlin Heidelberg, Imprint and Springer Spektrum. ISBN: 9783642376542.

Kim, H. et al. (2018). 'Cochlear Implantation in Postlingually Deaf Adults is Time-sensitive Towards Positive Outcome: Prediction using Advanced Machine Learning Techniques'. In: *Scientific Reports* 8.1, p. 18004. DOI: 10.1038/s41598-018-36404-1.

Klabbers, T. M., Huinck, W. J., Heutink, F., Verbist, B. M. and Mylanus, E. A. M. (2021). 'Transimpedance Matrix (TIM) Measurement for the Detection of Intraoperative Electrode Tip Foldover Using the Slim Modiolar Electrode: A Proof of Concept Study'. In: *Otology & Neurotology* 42.2, e124–e129. DOI: 10.1097/MAO.0000000000002875.

Knörgen, M., Brandt, S. and Kösling, S. (2012). 'Qualitätsvergleich digitaler 3D-fähiger Röntgenanlagen bei HNO-Fragestellungen am Schläfenbein und den Nasennebenhöhlen'. In: *RöFo - Fortschritte auf dem Gebiet der Röntgenstrahlen und der bildgebenden Verfahren* 184.12, pp. 1153–1160. DOI: 10.1055/s-0032-1325343.

Koch, R. W., Ladak, H. M., Elfarnawany, M. and Agrawal, S. K. (2017). 'Measuring Cochlear Duct Length - a historical analysis of methods and results'. In: *Journal of Otolaryngology - Head & Neck Surgery* 46.1, p. 19. DOI: 10.1186/s40463-017-0194-2.

Kong, W.-J., Cheng, H.-M., Ma, H., Wang, Y.-J. and Han, P. (2012). 'Evaluation of the implanted cochlear implant electrode by CT scanning with three-dimensional reconstruction'. In: *Acta Oto-Laryngologica* 132.2, pp. 116–122. DOI: 10.3109/00016489.2011.626794.

Kopsch, A. C. (2021). 'Influence of the Spread of Electric Field and Neural Excitation on Speech Recognition in Cochlear Implant Users: Transimpedance and Spread of Excitation Measurements'. Master thesis. Martin-Luther-University Halle-Wittenberg.

Kopsch, A. C., Rahne, T., Plontke, S. K. and Wagner, L. (2022). 'Influence of the spread of electric field on neural excitation in cochlear implant users: Transimpedance and spread of excitation measurements'. In: *Hearing Research* 424, p. 108591. DOI: 10.1016/j.heares.2022.108591.

Kopsch, A. C., Rahne, T., Plontke, S. K. and Wagner, L. (2024a). 'Influence of the Spread of the Electric Field on Speech Recognition in Cochlear Implant Users'. In: *Otology & Neurotology* 45.3, e221–e227. DOI: 10.1097/MAO.0000000000004086.

Kopsch, A. C., Wagner, L., Plontke, S. K. and Kösling, S. (2024b). 'A Case Series Suggests Peaking Transimpedance as a Possible Marker for Scalar Dislocations in Cochlear Implantation'. In: *Audiology and Neurotology*, pp. 1–10. DOI: 10.1159/000541954.

Kral, A., Aplin, F. and Maier, H. (2021). *Prostheses for the brain: Principles and applications of neuroprostheses*. Elsevier Academic Press. ISBN: 9780128188934.

Kral, A., Kronenberger, W. G., Pisoni, D. B. and O'Donoghue, G. M. (2016). 'Neurocognitive factors in sensory restoration of early deafness: a connectome model'. In: *The Lancet. Neurology* 15.6, pp. 610–621. DOI: 10.1016/S1474-4422(16)00034-X.

Kurz, A. et al. (2025). 'Anatomy-based fitting improves speech perception in noise for cochlear implant recipients with single-sided deafness'. In: *European Archives of Oto-Rhino-Laryngology* 282.1, pp. 467–479. DOI: 10.1007/s00405-024-08984-4.

Landsberger, D. M. and Srinivasan, A. G. (2009). 'Virtual channel discrimination is improved by current focusing in cochlear implant recipients'. In: *Hearing Research* 254.1-2, pp. 34–41. DOI: 10.1016/j.heares.2009.04.007.

Landsberger, D. M., Svrakic, M., Roland, J. T. and Svirsky, M. (2015). 'The Relationship Between Insertion Angles, Default Frequency Allocations, and Spiral Ganglion Place Pitch in Cochlear Implants'. In: *Ear and hearing* 36.5, e207–13. DOI: 10.1097/AUD.0000000000000163.

Lazard, D. S. et al. (2012). 'Pre-, per- and postoperative factors affecting performance of postlinguistically deaf adults using cochlear implants: a new conceptual model over time'. In: *PLOS ONE* 7.11, e48739. DOI: 10.1371/journal.pone.0048739.

Lee, J. S. et al. (2003). 'PET evidence of neuroplasticity in adult auditory cortex of postlingual deafness'. In: *Journal of nuclear medicine : official publication, Society of Nuclear Medicine* 44.9, pp. 1435–1439. ISSN: 0161-5505. URL: https://jnm.snmjournals.org/content/44/9/1435 (visited on 17/05/2025).

Lehnhardt, E. and Laszig, R. (2009). *Praxis der Audiometrie*. Stuttgart: Georg Thieme Verlag. ISBN: 9783133690096.

Li, H. et al. (2021). 'Three-dimensional tonotopic mapping of the human cochlea based on synchrotron radiation phase-contrast imaging'. In: *Scientific Reports* 11.1, p. 4437. DOI: 10.1038/s41598-021-83225-w.

Li, N. P. and Kanazawa, S. (2016). 'Country roads, take me home... to my friends: How intelligence, population density, and friendship affect modern happiness'. In: *British Journal of Psychology* 107.4, pp. 675–697. DOI: 10.1111/bjop.12181.

Livingston, G. et al. (2024). 'Dementia prevention, intervention, and care: 2024 report of the Lancet standing Commission'. In: *Lancet (London, England)* 404.10452, pp. 572–628. DOI: 10.1016/S0140-6736(24)01296-0.

Lundh, F. (1999). *An introduction to tkinter*. URL: https://wiki.python.org/moin/TkInter (visited on 17/05/2025).

Ma, C. et al. (2023). 'Longitudinal Speech Recognition Changes After Cochlear Implant: Systematic Review and Meta-analysis'. In: *The Laryngoscope* 133.5, pp. 1014–1024. DOI: 10.1002/lary.30354.

Ma, K. W., Mak, C. M. and Wong, H. M. (2020). 'Acoustical measurements and prediction of psychoacoustic metrics with spatial variation'. In: *Applied Acoustics* 168, p. 107450. DOI: 10.1016/j.apacoust.2020.107450.

Marsh, M. A. et al. (1993). 'Radiologic evaluation of multichannel intracochlear implant insertion depth'. In: *Am J Otol* 14, pp. 386–391. URL: https://pubmed.ncbi.nlm.nih.gov/8238277/ (visited on 17/05/2025).

Maurits, N. M. and Curcic-Blake, B. (2024). *Math for Scientists: Refreshing the Essentials*. Second edition. Cham, Switzerland: Springer Nature Switzerland AG. ISBN: 9783031441400.

McDermott, H., Sucher, C. and Simpson, A. (2009). 'Electro-acoustic stimulation. Acoustic and electric pitch comparisons'. In: *Audiology and Neurotology* 14 Suppl 1.Suppl. 1, pp. 2–7. DOI: 10.1159/000206489.

McFee, B., Stoeter, F.-R. and Sarfati, M. (2015). *PyRubberband*. URL: https://pyrubberband.readthedocs.io/en/stable/index.html (visited on 01/01/2025).

McFee, B. et al. (2022). 'librosa/librosa: 0.9.1'. In: DOI: 10.5281/ZENODO.6097378. URL: https://librosa.org.

McKay, C. M. (2018). 'Brain Plasticity and Rehabilitation with a Cochlear Implant.' In: *Advances in oto-rhino-laryngology* 81, pp. 57–65. DOI: 10.1159/000485586.

Med-El (2012). *MED-EL Electrode Arrays. Designed for Atraumatic Implantation Providing Superior Hearing Performance*. URL: https://cochlearimplanthelp.com/wp-content/uploads/2012/11/med-el_12mkt_22767r3_electrode-comparison-brochure.pdf (visited on 17/05/2025).

Mehta, A. H. and Oxenham, A. J. (2017). 'Vocoder Simulations Explain Complex Pitch Perception Limitations Experienced by Cochlear Implant Users'. In: *Journal of the Association for Research in Otolaryngology : JARO* 18.6, pp. 789–802. DOI: 10.1007/s10162-017-0632-x.

Mertens, G., van Rompaey, V., van de Heyning, P., Gorris, E. and Topsakal, V. (2020). 'Prediction of the Cochlear Implant Electrode Insertion Depth: Clinical Applicability of two Analytical Cochlear Models'. In: *Scientific Reports* 10.1, p. 3340. DOI: 10.1038/s41598-020-58648-6.

Mertens, G., Kleine Punte, A., Bodt, M. de and van de Heyning, P. (2015). 'Sound quality in adult cochlear implant recipients using the HISQUI19'. In: *Acta Oto-Laryngologica* 135.11, pp. 1138–1145. DOI: 10.3109/00016489.2015.1066934.

Mesnildrey, Q., Hilkhuysen, G. and Macherey, O. (2016). 'Pulse-spreading harmonic complex as an alternative carrier for vocoder simulations of cochlear implants'. In: *The Journal of the Acoustical Society of America* 139.2, pp. 986–991. DOI: 10.1121/1.4941451.

Mewes, A. (2024). 'Estimation of cochlear implant electrode insertion depth for speech processor fitting'. In: *Zeitschrift für Audiologie* 63 (1), pp. 24–27. URL: https://www.z-audiol.de (visited on 03/12/2024).

Meyer, M. (2021). *Signalverarbeitung: Analoge und digitale Signale, Systeme und Filter*. 9th ed. 2021. Springer eBook Collection. Wiesbaden: Springer Fachmedien Wiesbaden and Springer Vieweg. ISBN: 9783658328016.

Microsoft Corporation (2016). *Microsoft Excel*. URL: https://office.microsoft.com/excel (visited on 01/01/2025).

Micuda, A., Li, H., Rask-Andersen, H., Ladak, H. M. and Agrawal, S. K. (2024). 'Morphologic Analysis of the Scala Tympani Using Synchrotron: Implications for

Cochlear Implantation'. In: *The Laryngoscope* 134.6, pp. 2889–2897. DOI: 10.1002/lary.31263.

Morise, M. and Watanabe, Y. (2018). 'Sound quality comparison among high-quality vocoders by using re-synthesized speech'. In: *Acoustical Science and Technology* 39.3, pp. 263–265. DOI: 10.1250/ast.39.263.

Möser, M. (2015). *Technische Akustik*. 10. Aufl. 2015. VDI-Buch. Berlin, Heidelberg: Springer Berlin Heidelberg. ISBN: 9783662477045.

Müller-Graff, F.-T. et al. (2024). 'Umfassender Literaturüberblick über die Anwendung der otologisch-chirurgischen Planungssoftware OTOPLAN® bei der Cochleaimplantation. Englische Version'. In: *HNO* 72.Suppl 2, pp. 89–100. DOI: 10.1007/s00106-023-01417-4.

Nadir, J., Ein, A. A. and Alqadi, Z. (2016). 'A technique to encrypt-decrypt stereo wave file'. In: *International Journal of Computer and Information Technology* 05.

Nogueira, W., Büchner, A., Lenarz, T. and Edler, B. (2005). 'A Psychoacoustic "NofM"-Type Speech Coding Strategy for Cochlear Implants'. In: *EURASIP Journal on Advances in Signal Processing* 2005.18, pp. 1–16. DOI: 10.1155/ASP.2005.3044.

Nyquist, H. (1928). 'Certain Topics in Telegraph Transmission Theory'. In: *Transactions of the American Institute of Electrical Engineers* 47.2, pp. 617–644. DOI: 10.1109/T-AIEE.1928.5055024.

OpenStax (2016). 'Anatomy and Physiology'. In: URL: https://cnx.org/contents/FPtK1zmh@8.25:fEI3C8Ot@10/Preface (visited on 05/05/2025).

Orfanidis, S. J. (1996). *Introduction to signal processing*. Prentice Hall signal processing series. Upper Saddle River, NJ: Prentice Hall. ISBN: 013240334X.

Paouris, D., Kunzo, S. and Goljerová, I. (2023). 'Validation of Automatic Cochlear Measurements Using OTOPLAN® Software'. In: *Journal of Personalized Medicine* 13.5, p. 805. DOI: 10.3390/jpm13050805.

Peters, J. P. M. et al. (2018). 'The Sound of a Cochlear Implant Investigated in Patients With Single-Sided Deafness and a Cochlear Implant'. In: *Otology & Neurotology* 39.6, pp. 707–714. DOI: 10.1097/MAO.0000000000001821.

Photinos, P. (2021). *The Physics of Sound Waves (Second Edition): Music, Instruments, and Sound Equipment*. 2nd ed. IOP Ebooks Series. Bristol: Institute of Physics Publishing. ISBN: 9780750335393.

Präsidium der DGHNO-KHC (2021). *Weißbuch: Cochlea-Implantat(CI)-Versorgung*. URL: https://cdn.hno.org/media/2021/ci-weissbuch-20-inkl-anlagen-datenblocke-und-zeitpunkte-datenerhebung-mit-logo-05-05-21.pdf (visited on 05/05/2025).

Python Software Foundation (2016). *winsound — Sound-playing interface for Windows*. URL: https://docs.python.org/3/library/winsound.html#module-winsound (visited on 05/05/2025).

Rader, T., Döge, J., Adel, Y., Weissgerber, T. and Baumann, U. (2016a). 'Place dependent stimulation rates improve pitch perception in cochlear implantees with single-sided deafness'. In: *Hearing Research* 339, pp. 94–103. DOI: 10.1016/j.heares.2016.06.013.

Rader, T. et al. (2024). 'Comparison of speech perception in bimodal cochlear implant patients with respect to the cochlear coverage'. In: *HNO* 72.Suppl 1, pp. 17–24. DOI: 10.1007/s00106-023-01327-5.

Rader, T. et al. (2016b). 'Management of Cochlear Implant Electrode Migration'. In: *Otology & Neurotology* 37.9, e341–8. DOI: 10.1097/MAO.0000000000001065.

Rasband, W. (1997). *ImageJ*. URL: https://ij.imjoy.io/ (visited on 05/05/2025).

Raybaut, P. (2009). *Spyder - documentation*. URL: https://www.spyder-ide.org/ (visited on 05/05/2025).

Reiss, L. A. J., Turner, C. W., Erenberg, S. R. and Gantz, B. J. (2007). 'Changes in pitch with a cochlear implant over time'. In: *Journal of the Association for Research in Otolaryngology : JARO* 8.2, pp. 241–257. DOI: 10.1007/s10162-007-0077-8.

Riegel, J., Mayer, W. and van Havre, Y. (2001). *FreeCAD*. URL: http://www.freecadweb.org (visited on 05/05/2025).

Rijk, S. R. de, Tam, Y. C., Carlyon, R. P. and Bance, M. L. (2020). 'Detection of Extracochlear Electrodes in Cochlear Implants with Electric Field Imaging/Transimpedance Measurements: A Human Cadaver Study'. In: *Ear and Hearing* 41.5, pp. 1196–1207. DOI: 10.1097/AUD.0000000000000837.

Rijk, S. R. de et al. (2022). 'Detection of Extracochlear Electrodes Using Stimulation-Current- Induced Non-Stimulating Electrode Voltage Recordings With Different Electrode Designs'. In: *Otology & Neurotology* 43.5, e548–e557. DOI: 10.1097/MAO.0000000000003512.

Rosen, S., Zhang, Y. and Speers, K. (2015). 'Spectral density affects the intelligibility of tone-vocoded speech: Implications for cochlear implant simulations'. In: *The Journal of the Acoustical Society of America* 138.3, EL318–23. DOI: 10.1121/1.4929618.

Roy, A. T., Carver, C., Jiradejvong, P. and Limb, C. J. (2015). 'Musical Sound Quality in Cochlear Implant Users: A Comparison in Bass Frequency Perception Between Fine Structure Processing and High-Definition Continuous Interleaved Sampling Strategies'. In: *Ear and Hearing* 36.5, pp. 582–590. DOI: 10.1097/AUD.0000000000000170.

Roy, A. T., Jiradejvong, P., Carver, C. and Limb, C. J. (2012a). 'Assessment of sound quality perception in cochlear implant users during music listening'. In: *Otology & Neurotology* 33.3, pp. 319–327. DOI: 10.1097/MAO.0b013e31824296a9.

Roy, A. T., Jiradejvong, P., Carver, C. and Limb, C. J. (2012b). 'Musical sound quality impairments in cochlear implant (CI) users as a function of limited high-frequency perception'. In: *Trends in Amplification* 16.4, pp. 191–200. DOI: 10.1177/1084713812465493.

Saki, N. et al. (2023). 'The Impact of Cochlear Implantation on Sound Quality and Quality of Life in Postlingually Deaf Adults: A Prospective Study'. In: *Egyptian Journal of Ear, Nose, Throat and Allied Sciences* 24.24, pp. 1–6. DOI: 10.21608/ejentas.2023.220379.1651.

Schell-Majoor, L., Rennies, J., Ewert, S. D. and Kollmeier, B. (2016). 'Validierung einer Methode zur gleichzeitigen Bewertung von Rauigkeit, SchÃrfe, Tonhaltigkeit, Lautheit und Lästigkeit'. In: *DAGA*. URL: https://pub.dega-akustik.de/DAGA_2016/data/articles/000034.pdf (visited on 05/05/2025).

Schnupp, J., Nelken, I. and King, A. (2012). *Auditory neuroscience: Making sense of sound*. Cambridge, Massachusetts and London, England: The MIT Press. ISBN: 9780262113182.

Schraivogel, S., Aebischer, P., Weder, S., Caversaccio, M. and Wimmer, W. (2023a). 'Cochlear implant electrode impedance subcomponents as biomarker for residual

hearing'. In: *Frontiers in Neurology* 14, p. 1183116. DOI: 10.3389/fneur.2023.1183116.

Schraivogel, S., Weder, S., Mantokoudis, G., Caversaccio, M. and Wimmer, W. (2024). 'Predictive Models for Radiation-Free Localization of Cochlear Implants' Most Basal Electrode using Impedance Telemetry'. In: *IEEE Transactions on Biomedical Engineering*, pp. 1–12. DOI: 10.1109/TBME.2024.3509527.

Schraivogel, S. et al. (2023b). 'Postoperative Impedance-Based Estimation of Cochlear Implant Electrode Insertion Depth'. In: *Ear and Hearing* 44.6, pp. 1379–1388. DOI: 10.1097/AUD.0000000000001379.

Schvartz-Leyzac, K. C., Colesa, D. J., Swiderski, D. L., Raphael, Y. and Pfingst, B. E. (2023). 'Cochlear Health and Cochlear-implant Function'. In: *Journal of the Association for Research in Otolaryngology* 24, pp. 5–29. DOI: 10.1007/s10162-022-00882-y.

Sehlmeyer, M. et al. (2024). 'How Cochlear Implant Position and Perilymph Composition Affect Stimulation Electrode Impedance'. In: *2024 IEEE International Symposium on Medical Measurements and Applications (MeMeA)*. IEEE, pp. 1–5. ISBN: 979-8-3503-0799-3. DOI: 10.1109/MeMeA60663.2024.10596900.

Shannon, R. V., Zeng, F. G., Kamath, V., Wygonski, J. and Ekelid, M. (1995). 'Speech recognition with primarily temporal cues'. In: *Science (New York, N.Y.)* 270.5234, pp. 303–304. DOI: 10.1126/science.270.5234.303.

Shannon, R. V., Fu, Q.-J. and Galvin, J. (2004). 'The number of spectral channels required for speech recognition depends on the difficulty of the listening situation'. In: *Acta oto-laryngologica. Supplementum* 552, pp. 50–54. DOI: 10.1080/03655230410017562.

Shaul, C. et al. (2019). 'Electrical Impedance as a Biomarker for Inner Ear Pathology Following Lateral Wall and Peri-modiolar Cochlear Implantation'. In: *Otology & Neurotology* 40.5, e518–e526. DOI: 10.1097/MAO.0000000000002227.

Siniša Tomić and Dalibor Drljača (2023). 'Digitalization of Sound Using Pulse Code Modulation (PCM)'. In: *JITA - APEIRON* 25.1, pp. 42–47. DOI: 10.7251/JIT2301042T.

Smith, Z. M., Delgutte, B. and Oxenham, A. J. (2002). 'Chimaeric sounds reveal dichotomies in auditory perception'. In: *Nature* 416.6876, pp. 87–90. DOI: 10.1038/416087a.

Söderqvist, S., Sivonen, V., Koivisto, J., Aarnisalo, A. and Sinkkonen, S. T. (2023). 'Spread of the intracochlear electrical field: Implications for assessing electrode array location in cochlear implantation'. In: *Hearing Research* 434, p. 108790. DOI: 10.1016/j.heares.2023.108790.

Söderqvist, S. et al. (2021). 'Intraoperative transimpedance and spread of excitation profile correlations with a lateral-wall cochlear implant electrode array'. In: *Hearing Research* 405, p. 108235. DOI: 10.1016/j.heares.2021.108235.

Spahn, B. et al. (2025). 'Pre- and Postoperative Imaging of Cochlear Implantation in Cadaveric Specimens Using Low-Dose Photon-Counting Detector CT'. In: *American Journal of Neuroradiology* 46.2, pp. 362–371. DOI: 10.3174/ajnr.A8533.

Stakhovskaya, O., Sridhar, D., Bonham, B. H. and Leake, P. A. (2007). 'Frequency map for the human cochlear spiral ganglion: implications for cochlear implants'. In: *Journal of the Association for Research in Otolaryngology : JARO* 8.2, pp. 220–233. DOI: 10.1007/s10162-007-0076-9.

Steinhauer, C., Sønderbo, T. and Paisa, R. (2023). 'A Real-Time Cochlear Implant Simulator - Design and Evaluation: Zenodo'. In: *Proceedings of the Sound and Music Computing Conference*. DOI: 10.5281/ZENODO.10063009.

Sun, X. (2000). 'Voice quality conversion in TD-PSOLA speech synthesis'. In: *IEEE*, pp. II953–II956. DOI: 10.1109/ICASSP.2000.859119.

Svrakic, M. et al. (2015). 'Measurement of Cochlear Implant Electrode Position From Intraoperative Post-insertion Skull Radiographs: A Validation Study'. In: *Otology & Neurotology* 36.9, pp. 1486–1491. DOI: 10.1097/MAO.0000000000000852.

Tan, C.-T., Martin, B. and Svirsky, M. A. (2017). 'Pitch Matching between Electrical Stimulation of a Cochlear Implant and Acoustic Stimuli Presented to a Contralateral Ear with Residual Hearing'. In: *Journal of the American Academy of Audiology* 28.3, pp. 187–199. DOI: 10.3766/jaaa.15063.

Tang, Q., Benítez, R. and Zeng, F.-G. (2011). 'Spatial channel interactions in cochlear implants'. In: *Journal of neural engineering* 8.4, p. 046029. DOI: 10.1088/1741-2560/8/4/046029.

Távora-Vieira, D. et al. (2023). 'Evaluation of the Performance of OTOPLAN-Based Cochlear Implant Electrode Array Selection: A Retrospective Study'. In: *Journal of Personalized Medicine* 13.8, p. 1276. DOI: 10.3390/jpm13081276.

The Slicer Community (2025). *3D Slicer*. URL: https://www.slicer.org/ (visited on 05/05/2025).

Thomson, R. S., Auduong, P., Miller, A. T. and Gurgel, R. K. (2017). 'Hearing loss as a risk factor for dementia: A systematic review'. In: *Laryngoscope Investigative Otolaryngology* 2.2, pp. 69–79. DOI: 10.1002/lio2.65.

Trudel, M. et al. (2018). 'Comparative Impacts of Scala Vestibuli Versus Scala Tympani Cochlear Implantation on Auditory Performances and Programming Parameters in Partially Ossified Cochleae'. In: *Otology & Neurotology* 39.6, pp. 700–706. DOI: 10.1097/MAO.0000000000001816.

Tzvi-Minker, E. and Keck, A. (2023). 'How Can We Compare Cochlear Implant Systems across Manufacturers? A Scoping Review of Recent Literature'. In: *Audiology Research* 13.5, pp. 753–766. DOI: 10.3390/audiolres13050067.

van de Heyning, P. et al. (2008). 'Incapacitating unilateral tinnitus in single-sided deafness treated by cochlear implantation'. In: *The Annals of otology, rhinology, and laryngology* 117.9, pp. 645–652. DOI: 10.1177/000348940811700903.

van den Honert, C. and Stypulkowski, P. H. (1987). 'Single fiber mapping of spatial excitation patterns in the electrically stimulated auditory nerve'. In: *Hearing Research* 29.2-3, pp. 195–206. DOI: 10.1016/0378-5955(87)90167-5.

van Rossum, G. (1991). *Python*. URL: https://docs.python.org/2/reference/ (visited on 03/04/2025).

van Veen, t. c. (2012). 'How to Wreck a Nice Beach: The Vocoder from World War II to Hip-Hop, the Machine Speaks (Dave Tompkins)'. In: *Dancecult* 4.2, pp. 67–70. DOI: 10.12801/1947-5403.2012.04.02.04.

Vandali, A. E., Whitford, L. A., Plant, K. L. and Clark, G. M. (2000). 'Speech perception as a function of electrical stimulation rate: using the Nucleus 24 cochlear implant system'. In: *Ear and hearing* 21.6, pp. 608–624. DOI: 10.1097/00003446-200012000-00008.

Virtanen, P. et al. (2020). 'SciPy 1.0: fundamental algorithms for scientific computing in Python'. In: *Nature Methods* 17.3, pp. 261–272. DOI: 10.1038/s41592-019-0686-2.

Vogl, T. J. et al. (2015). 'Pre-, Intra- and Post-Operative Imaging of Cochlear Implants'. In: *RöFo - Fortschritte auf dem Gebiet der Röntgenstrahlen und der bildgebenden Verfahren* 187.11, pp. 980–989. DOI: 10.1055/s-0035-1553413.

Völker, C., Bisitz, T., Huber, R. and Ernst, S. M. A. (2015). 'Adaptions for the MUlti Stimulus test with Hidden Reference and Anchor (MUSHRA) for elder and technical unexperienced participants'. In: *DAGA*.

Wagener, K. and Kollmeier, B. (2005). 'Evaluation des Oldenburger Satztests mit Kindern und Oldenburger Kinder-Satztest'. In: *Zeitschrift für Audiologie* 44(3), pp. 134–143.

Waggener, B. and Waggener, W. N. (1995). *Pulse Code Modulation Techniques*. Springer Science & Business Media. ISBN: 9780442014360.

Wagner, L., Plontke, S. K. and Rahne, T. (2023). 'An analysis of the spread of electric field within the cochlea for different devices including custom-made electrodes for subtotal cochleoectomy'. In: *PLOS ONE* 18.9, e0287216. DOI: 10.1371/journal.pone.0287216.

Wagner, L., Plontke, S. K., Rahne, T. and Kopsch, A. C. (2025). 'Time course of transimpedances is affected by cochlea implant surgical technique'. In: *Zeitschrift fur medizinische Physik*. DOI: 10.1016/j.zemedi.2025.04.006.

Wang, Z. et al. (2019). 'Deep Learning Based Metal Artifacts Reduction in Post-operative Cochlear Implant CT Imaging'. In: Springer, Cham, pp. 121–129. DOI: 10.1007/978-3-030-32226-7_14.

Whibley, S., Day, M., May, P. and Pennock, M. (2015). *WAV Format Preservation Assessment*. Ed. by British Library Digital Preservation Team. URL: https://wiki.dpconline.org/images/4/46/WAV_Assessment_v1.0.pdf (visited on 05/05/2025).

Wissenschaftliche Dienste des Deutschen Bundestages (2022). 'Aktuelle statistische Daten zu Cochlea-Implantaten'. In: Deutscher Bundestag. URL: https://www.bundestag.de/resource/blob/909018/7a57be6e6721ed9c032d73839a698213/WD-9-046-22-pdf.pdf (visited on 05/05/2025).

World Health Organization (2021). *World report on hearing*. 1st ed. Geneva. ISBN: 9789240020481. URL: https://www.who.int/publications/i/item/9789240020481 (visited on 05/05/2025).

Wouters, J., McDermott, H. J. and Francart, T. (2015). 'Sound Coding in Cochlear Implants: From electric pulses to hearing'. In: *IEEE Signal Processing Magazine* 32.2, pp. 67–80. DOI: 10.1109/MSP.2014.2371671.

Wright, R. and Uchanski, R. M. (2012). 'Music perception and appraisal: cochlear implant users and simulated cochlear implant listening'. In: *Journal of the American Academy of Audiology* 23.5, 350–65, quiz 379. DOI: 10.3766/jaaa.23.5.6.

Xu, J., Xu, S. A., Cohen, L. T. and Clark, G. M. (2000). 'Cochlear view: postoperative radiography for cochlear implantation'. In: *The American journal of otology* 21.1, pp. 49–56.

Xu, L. and Pfingst, B. E. (2003). 'Relative importance of temporal envelope and fine structure in lexical-tone perception'. In: *The Journal of the Acoustical Society of America* 114.6 Pt 1, pp. 3024–3027. DOI: 10.1121/1.1623786.

Zahnert, T. (2011). 'The differential diagnosis of hearing loss'. In: *Deutsches Arzteblatt International* 108.25, 433–43, quiz 444. DOI: 10.3238/arztebl.2011.0433.

Zeng, F.-G., Rebscher, S., Harrison, W., Sun, X. and Feng, H. (2008). 'Cochlear Implants: System Design, Integration, and Evaluation'. In: *IEEE Reviews in Biomedical Engineering* 1, pp. 115–142. DOI: 10.1109/RBME.2008.2008250.

Zeng, F.-G., Tang, Q. and Lu, T. (2014). 'Abnormal pitch perception produced by cochlear implant stimulation'. In: *PLOS ONE* 9.2, e88662. DOI: 10.1371/journal.pone.0088662.

Zhang, J. et al. (2019). 'Sound quality evaluation and prediction for the emitted noise of axial piston pumps'. In: *Applied Acoustics* 145, pp. 27–40. DOI: 10.1016/j.apacoust.2018.09.015.

Zhang, L. et al. (2024). 'Transimpedance Matrix Can Be Used to Estimate Electrode Positions Intraoperatively and to Monitor Their Positional Changes Postoperatively in Cochlear Implant Patients'. In: *Otology & Neurotology* 45.4, e289–e296. DOI: 10.1097/MAO.0000000000004145.

Zhou, Q.-Y., Park, J. and Koltun, V. (2018). *Open3D: A Modern Library for 3D Data Processing*. URL: http://arxiv.org/pdf/1801.09847v1 (visited on 05/05/2025).

Zuniga, M. G. et al. (2017). 'Tip Fold-over in Cochlear Implantation: Case Series'. In: *Otology & neurotology : official publication of the American Otological Society, American Neurotology Society [and] European Academy of Otology and Neurotology* 38.2, pp. 199–206. DOI: 10.1097/MAO.0000000000001283.

Zwicker, E. and Fastl, H. (2007). *Psychoacoustics: Facts and Models*. 1st ed. Vol. v.22. Springer Series in Information Sciences Ser. Cham: Springer International Publishing and Springer Nature. ISBN: 9783662095621.

Zwolan, T. A., Collins, L. M. and Wakefield, G. H. (1997). 'Electrode discrimination and speech recognition in postlingually deafened adult cochlear implant subjects'. In: *The Journal of the Acoustical Society of America* 102.6, pp. 3673–3685. DOI: 10.1121/1.420401.

Curriculum Vitae

Personal Details

Name: Anna Christina Kopsch

Academic degree: Master of Science (MSc)

Education

Since 2022	**University hospital Halle, Department of Otorhinolaryngology, Head and Neck Surgery** Scientific Officer/Doctoral Student, Clinical Audiologist
2019 – 2021	**Martin-Luther-University Halle-Wittenberg** Discipline: Medical Physics, Master of Science
2016 – 2020	**Martin-Luther-University Halle-Wittenberg** Discipline: Medical Physics, Bachelor of Science
2008 – 2016	**Märkisches Gymnasium Bochum** A-Level

Halle (Saale), June 27th, 2025

Anna Christina Kopsch

List of Publications

Comment

Parts of this thesis have been publicized as oral presentations at national conferences or as scientific papers.

Journal Articles

Kopsch, A. C. (2022). 'Einfluss der elektrischen Feldausbreitung auf die neurale Erregungsausbreitung und auf das Sprachverstehen in Cochlea-Implantat-Trägern'. In: *Zeitschrift für Audiologie* 61.2.

Kopsch, A. C., Rahne, T., Plontke, S. K. and Wagner, L. (2022). 'Influence of the spread of electric field on neural excitation in cochlear implant users: Transimpedance and spread of excitation measurements'. In: *Hearing Research* 424, p. 108591. DOI: 10.1016/j.heares.2022.108591.

Kopsch, A. C., Wagner, L., Plontke, S. K. and Kösling, S. (2024a). 'A case series suggests peaking transimpedance as a possible marker for scalar dislocations in cochlear implantation'. In: *Audiology & Neuro-otology*, pp. 1–15. DOI: 10.1159/000541954.

Kopsch, A. C., Plontke, S. K. and Rahne, T. (2024b). 'Simulations indicate that the sound of a cochlear implant may adapt to that of a normnal hearing'. In: *submitted, Scientific Reports*.

Kopsch, A. C., Rahne, T., Plontke, S. K. and Wagner, L. (2024c). 'Influence of the spread of the electric field on speech recognition in cochlear implant users'. In: *Otology & Neurotology* 45.3, e221–e227. DOI: 10.1097/MAO.0000000000004086.

Rahne, T., Wagner, T. M., Kopsch, A. C., Plontke, S. K. and Wagner, L. (2023). 'Influence of age on speech recognition in noise and hearing effort in listeners with age-related hearing loss'. In: *Journal of Clinical Medicine* 12.19, p. 6133. ISSN: 2077-0383. DOI: 10.3390/jcm12196133.

Wagner, L., Plontke, S. K., Rahne, T. and Kopsch, A. C. (2025). 'Time course of transimpedances is affected by cochlea implant surgical technique'. In: *Zeitschrift fur medizinische Physik*. DOI: 10.1016/j.zemedi.2025.04.006.

Conference Proceedings

Kopsch, A. C., Plontke, S. K. and Rahne, T. (2024). 'Klangqualität von Simulationen des Klangeindrucks von Cochlea-Implantat-Tragenden in Abhängigkeit von der Trage-Erfahrung: German Medical Science GMS Publishing House'. In: *26. Jahrestagung der Deutschen Gesellschaft für Audiologie*. DOI: 10.3205/24DGA035.

Kopsch, A. C., Schramm, D. and Rahne, T. (2025). 'Fehlerabschätzung des Insertionswinkels von Cochlea-Implantat-Elektrodenträgern in Abhängigkeit des Röntgenaufnahmewinkels: German Medical Science GMS Publishing House'. In: *27. Jahrestagung der Deutschen Gesellschaft für Audiologie und Arbeitstagung der Arbeitsgemeinschaft Deutschsprachiger Audiologen, Neurootologen und Otologen*. DOI: 10.3205/25DGA111.

Kopsch, A. C., Wagner, L., Plontke, S. K. and Rahne, T. (2023). 'Klang eines Cochlea-Implantats in Abhängigkeit der Hörerfahrung: erste Hörbeispiele: German Medical Science GMS Publishing House'. In: *25. Jahrestagung der Deutschen Gesellschaft für Audiologie*. DOI: 10.3205/23DGA034.

Kopsch, A. C., Rahne, T., Plontke, S. K. and Wagner, L. (2022). 'Einfluss der elektrischen Feldausbreitung auf das Sprachverstehen in Cochlea-Implantat-Trägern: Transimpedanzmessungen: German Medical Science GMS Publishing House'. In: *24. Jahrestagung der Deutschen Gesellschaft für Audiologie*. DOI: 10.3205/22DGA161.

Kurz, S. R., Rahne, T., Plontke, S. and Kopsch, A. C. (2025). 'Simulationsmodelle zur Erfassung der Klangwahrnehmung von CI-Tragenden mit einem 12-Elektroden-Cochleaimplantat-System: German Medical Science GMS Publishing House'. In: *27. Jahrestagung der Deutschen Gesellschaft für Audiologie und Arbeitstagung der Arbeitsgemeinschaft Deutschsprachiger Audiologen, Neurootologen und Otologen*. DOI: 10.3205/25DGA205.

Leingärtner-Goth, E., Rahne, T., Wagner, L. and Kopsch, A. C. (2024). 'Sprachverstehen nach Cochleaimplantation in Abhängigkeit von der cochleären Abdeckung: German Medical Science GMS Publishing House'. In: *26. Jahrestagung der Deutschen Gesellschaft für Audiologie*. DOI: 10.3205/24DGA135.

Plontke, S. K. et al. (2025). 'Schwannome des Innenohres: Symptome, Befunde und Funktions-Erhalt oder -Rehabilitation nach chirurgischer Tumorentfernung – eine monozentrische Fallserie mit 126 Patienten: German Medical Science GMS Publishing House'. In: *27. Jahrestagung der Deutschen Gesellschaft für Audiologie und Arbeitstagung der Arbeitsgemeinschaft Deutschsprachiger Audiologen, Neurootologen und Otologen*. DOI: 10.3205/25dga090.

Wagner, L., Kopsch, A. C., Plontke, S. K. and Rahne, T. (2023). 'Transimpedanzen im Zeitverlauf bei PatientInnen nach subtotaler Cochleoektomie: German Medical Science GMS Publishing House'. In: *25. Jahrestagung der Deutschen Gesellschaft für Audiologie*. DOI: 10.3205/23DGA111.

Wagner, L., Kopsch, A. C., Rahne, T. and Plontke, S. K. (2024). 'Programmierung und elektrophysiologische Messungen mit Cochlea-Implantaten bei Patienten nach Entfernung intracochleärer Schwannome: German Medical Science GMS Publishing House'. In: *26. Jahrestagung der Deutschen Gesellschaft für Audiologie*. DOI: 10.3205/24DGA032.

Wagner, L., Rahne, T., Plontke, S. and Kopsch, A. C. (2025). 'Veränderungen der Transimpedanzen nach Rundfensterinsertion und Cochleoektomie im Zeitverlauf: German Medical Science GMS Publishing House'. In: *27. Jahrestagung der Deutschen Gesellschaft für Audiologie und Arbeitstagung der Arbeitsgemeinschaft Deutschsprachiger Audiologen, Neurootologen und Otologen*. DOI: 10.3205/25DGA067.

Eidesstattliche Erklärung

Hiermit erkläre ich, dass ich die vorliegende Doktorarbeit selbständig und ohne unzulässige Hilfe Dritter verfasst habe. Für die Erstellung dieser Arbeit wurden folgende KI-gestützte Hilfsmittel verwendet: DeepL[1], Rubriq[2], ChatGPT[3]. Die genannten Hilfsmittel wurden zur Überprüfung von Rechtschreibung, Grammatik und Zeichensetzung, und zur Überarbeitung des Ausdrucks genutzt. Nach der Verwendung dieser Hilfsmittel habe ich den Inhalt überprüft und übernehme die Verantwortung dieser Inhalt vollumfänglich. Ich versichere, dass ich alle verwendeten Quellen und Hilfsmittel aufgeführt habe. Die aus fremden Werken wörtlich oder inhaltlich entnommenen Gedanken und Daten sind als solche kenntlich gemacht. Diese Arbeit wurde bisher keiner anderen Prüfungskommission vorgelegt.

Außerdem versichere ich, dass gegen mich derzeit kein Ermittlungsverfahren eingeleitet wurde und dass ich nicht vorbestraft bin.

Halle (Saale), 27. Juni 2025

Anna Christina Kopsch

[1]DeepL, www.deepl.com, Zugriff am: 10.06.2025
[2]Rubriq, www.rubriq.com, Zugriff am: 10.06.2025
[3]ChatGPT, www.chatgpt.com, Zugriff am: 10.06.2025

Danksagung

An dieser Stelle möchte ich mich bei all jenen bedanken, die mich auf dem Weg zu dieser Dissertation begleitet und unterstützt haben. Diese Arbeit wurde durch die Hilfe und Ermutigung meiner Betreuer, Kollegen, Freunde und Familie in entscheidender Weise geprägt.

Mein besonderer Dank gilt meinem Betreuer Prof. Torsten Rahne, der mich stets mit großem Engagement und sachlicher Kompetenz unterstützte. Sein stets offenes Ohr, die vielen produktiven Diskussionen, seine ehrliche Meinung und die hilfreichen Ratschläge waren für den Fortschritt dieser Arbeit von unschätzbarem Wert.

Ich danke auch meinem Betreuer Prof. Reichert, der sich bereit erklärt hat, diese Arbeit zu begleiten. Für die Möglichkeit, mein Forschungsthema frei zu entwickeln, sowie für die spürbare Unterstützung während des gesamten Prozesses bin ich ihm dankbar.

Prof. Plontke danke ich für die Möglichkeit, meine Dissertation in der Klinik für Hals-, Nasen-, Ohrenheilkunde, Kopf- und Hals-Chirurgie der Universitätsmedizin zu schreiben. Ich habe den interdisziplinären Austausch sehr geschätzt und mich durch sein großes Interesse an wissenschaftlicher Arbeit stets inspiriert und unterstützt gefühlt.

Ein großer Dank geht an das gesamte interdisziplinäre Team des Halleschen Implant-Centrums. Die tägliche Zusammenarbeit war nicht nur fachlich bereichernd, sondern auch menschlich wertvoll. Besonders danken möchte ich meinen Bürokolleginnen Dr. Luise Wagner, Ulrike Pohle und Anika Morgenstern für den stetigen Austausch – ob während unserer Forschungstreffen oder im Arbeitsalltag zwischendurch. Unsere Forschungstreffen, deren inhaltliche Vorbereitung und die gemeinsamen Diskussionen haben mich immer wieder zum Nachdenken angeregt und meine Arbeit inhaltlich vorangebracht.

Mein Dank geht an alle, die mir ermöglicht haben, den Klinikalltag mitzugestalten und an wissenschaftlichen Tagungen teilzunehmen. Diese Erfahrungen haben nicht nur meine fachliche Perspektive erweitert, sondern auch zu meiner persönlichen Weiterentwicklung beigetragen.

Abschließend möchte ich meinen Eltern, meinen Brüdern, meinen Schwiegereltern, meinen Freunden und meinem Partner für ihre Liebe, ihre Geduld und ihr Vertrauen herzlich danken.

Anna Christina Kopsch